R.L. (2)

Second Quarter
1993

AFRRI Reports

REPORT DOCUMENTATION PAGE

Form Approved
OMB No. 0704-0188

1. AGENCY USE ONLY *(Leave blank)*	2. REPORT DATE	3. REPORT TYPE AND DATES COVERED
	August 1993	Reprints/Technical

4. TITLE AND SUBTITLE

AFRRI Reports, Second Quarter 1993

5. FUNDING NUMBERS

PE: NWED QAXM

6. AUTHOR(S)

7. PERFORMING ORGANIZATION NAME(S) AND ADDRESS(ES)

Armed Forces Radiobiology Research Institute
8901 Wisconsin Avenue
Bethesda, MD 20889-5603

8. PERFORMING ORGANIZATION REPORT NUMBER

SR93-13 - SR93-19

9. SPONSORING/MONITORING AGENCY NAME(S) AND ADDRESS(ES)

Defense Nuclear Agency
6801 Telegraph Road
Alexandria, VA 22310-3398

10. SPONSORING/MONITORING AGENCY REPORT NUMBER

11. SUPPLEMENTARY NOTES

12a. DISTRIBUTION/AVAILABILITY STATEMENT

Approved for public release; distribution unlimited.

12b. DISTRIBUTION CODE

13. ABSTRACT *(Maximum 200 words)*

This volume contains AFRRI Scientific Reports SR93-13 through SR93-19 for April-June 1993.

14. SUBJECT TERMS

15. NUMBER OF PAGES
67

16. PRICE CODE

17. SECURITY CLASSIFICATION OF REPORT	18. SECURITY CLASSIFICATION OF THIS PAGE	19. SECURITY CLASSIFICATION OF ABSTRACT	20. LIMITATION OF ABSTRACT
UNCLASSIFIED	UNCLASSIFIED	UNCLASSIFIED	UL

CLASSIFIED BY:

DECLASSIFY ON:

CONTENTS

Scientific Reports

Experimental Hematology 21:303–310 (1993)

Experimental Hematology

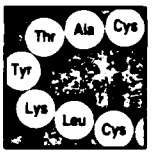

Hematopoietic growth factors and glucocorticoids synergize to mimic the effects of IL-1 on granulocyte differentiation and IL-1 receptor induction on bone marrow cells in vivo

Claire M. Dubois,[1] Ruth Neta,[2] Jonathan R. Keller,[3] Sten E.W. Jacobsen,[1] Joost J. Oppenheim,[1] Francis Ruscetti[1]

[1]The Laboratory of Immunoregulation, NCI-Frederick Cancer Research & Development Center, Frederick, MD; [2]Department of Experimental Hematology, Armed Forces Radiological Research Institute, Bethesda, MD; [3]Biological Carcinogenesis and Development Program, Program Resources/DynCorp Inc., NCI-Frederick Cancer Research & Development Center, Frederick, MD

Offprint requests to: Dr. Francis W. Ruscetti, Laboratory of Molecular Immunoregulation, Bldg. 560, Rm. 21-89A, Frederick Cancer Research & Development Center, Frederick, MD 21702-1201

(Received 18 December 1991; in revised form 23 June 1992; accepted 31 August 1992)

Abstract. The mechanisms by which interleukin-1 (IL-1) stimulates hematopoiesis are not clear. We have previously shown that in vivo administration of IL-1 indirectly increases IL-1 receptor (IL-1R) expression on both immature and mature bone marrow (BM) cells, partly due to IL-1-induced hematopoietic growth factor (HGF) production. Because IL-1 also stimulates the hypothalamic pituitary-adrenal axis resulting in the production of glucocorticoids (GC), we assessed whether in vivo treatment with HGF and glucocorticoids upregulates IL-1R. Administration of IL-1 to adrenalectomized mice reduces by 53% IL-specific binding on light density bone marrow (LDBM) cells compared to sham-operated mice. The administration of dexamethasone (dex) alone induced only a slight increase in IL-1R expression but synergized with granulocyte colony-stimulating factor (G-CSF), granulocyte-macrophage CSF (GM-CSF), IL-3 and IL-6 to upregulate IL-1R expression. Flow cytometry analysis using the RB6-8C5 antibody, which is differentially expressed on myeloid cells, indicated that combined G-CSF and dex treatment acts to promote increased numbers of differentiated myeloid progenitors in the bone marrow. Autoradiographic analysis confirmed that while G-CSF and dex increased IL-1R expression on all myeloid cells, it was particularly pronounced for myelocytes, promyelocytes and metamyelocytes. These results suggest that the ability of IL-1 to enhance granulocyte differentiation in vivo is partly due to its ability to induce a cascade of cytokines and steroids which in turn regulate IL-1 receptor expression.

Key words: IL-1 receptor—CSFs—Glucocorticoids—Myelopoiesis

Introduction. Interleukin-1 (IL-1) is a pleiotropic cytokine affecting the immune, inflammatory, neuroendocrine and hematopoietic systems [1,2]. Much of this diversity is based on the ability of IL-1 to induce production of other biologic mediators such as corticotropin releasing factor, corticosteroids, adrenocorticotropic hormone (ACTH), insulin and hematopoietic growth factors (G-CSF, GM-CSF, IL-6, IL-8, transforming growth factor beta [TGF-ß] and tumor necrosis factor alpha [TNF-α]) from multiple cell types.

The ability of IL-1 to synergize with HGFs to promote the growth and differentiation of primitive progenitor cells in vitro [3-5] suggests that IL-1 also plays an important role in the regulation of hematopoiesis [6]. In vivo administration of IL-1 induces an initial rapid mobilization of neutrophils from the bone marrow, followed by cycling of hematopoietic progenitor cells resulting in the expansion of the granulocytic compartment [7-11]. These effects presumably contribute to the ability of IL-1 to accelerate the recovery of hematopoietic stem cells and blood neutrophils following myelosuppression by chemotherapeutic drugs or exposure to lethal radiation [12-16].

In order to better understand the mechanism of action of IL-1 in vivo, we demonstrated that the IL-1 mediated upregulation of IL-1 receptors on bone marrow cells after in vivo administration of IL-1 occurs by an indirect mechanism [17]. In contrast, several hematopoietic growth factors, such as GM-CSF, G-CSF, IL-3 and IL-6 but not IL-1, act in vitro to upregulate IL-1R on both progenitor cells [18] and mature myeloid cells [18,19]. In vivo administration of HGFs, however, only partially mimic the ability of IL-1 to upregulate IL-1R expression [17]. It is, therefore, likely that other factors also contribute to the in vivo upregulation of IL-1 on hematopoietic progenitor cells. Since the in vivo administration of IL-1 also results in an elevation of corticosteroids in plasma [20] and glucocorticoids enhance in culture the expression of IL-1R on monocytes, B lymphocytes and fibroblasts [21,22], GCs might participate in the upregulation of IL-1R on bone marrow cells observed in response to IL-1. In this study, evidence is presented for a role for GCs as well as HGFs in IL-1R regulation.

Materials and methods

Mice. CD2F1 male mice were purchased from the Animal Genetics and Production Branch, National Cancer Institute, NIH (Frederick, MD). Animals were handled as previously described [23]. Animal care was provided in accordance with the procedures outlined in the *Guide for Care and Use of Laboratory Animals* (NIH Publication #86-23, 1985).

Reagents. Human recombinant IL-1α was supplied by Hoffmann-La Roche (Nutley, NJ). Human recombinant G-CSF was supplied by Amgen Corp. (Thousand Oaks, CA). Human recombinant IL-6 (5×10^6 U/mL) in pyrogen-free solution was kindly provided by Dr. Menachem Rubinstein (Interpharm

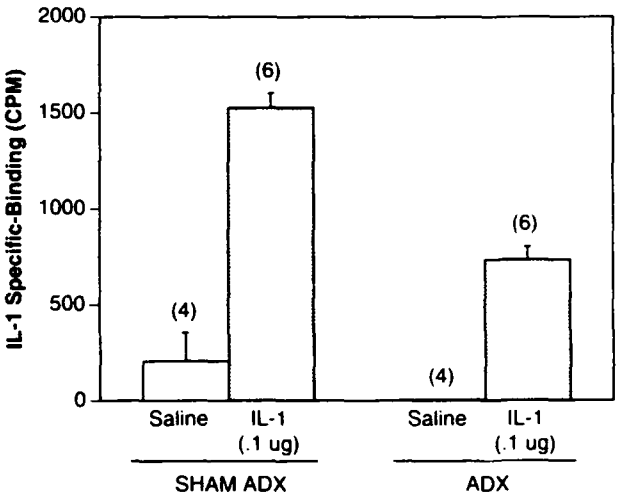

Fig. 1. Comparative effect of in vivo IL-1 on IL-1R expression on BM cells from adrenalectomized (removal of adrenal gland) mice vs. sham-adrenalectomized (similar surgical procedure without removal of the adrenal gland) mice. Mice were adrenalectomized 14 days before injection of 100 ng IL-1. Sixteen to 18 hours after IL-1 administration, BM cells were harvested and tested for the expression of IL-1R as described in Materials and methods. Each bar represents the mean ± SE of 2 experiments from which the level of background binding (280 ± 41) was subtracted. The numbers in parentheses represent the number of mice receiving each treatment.

Laboratory, Ness-Ziona, Israel). Murine IFN-γ was kindly provided by Genentech (San Francisco, CA). Murine recombinant IL-3 and GM-CSF were generously provided by Dr. Steven Gillis (Immunex Corp., Seattle, WA). Human recombinant TGF-ß was generously provided by Dr. Tony Purchio (Bristol-Myers/Squibb Pharmaceuticals, Seattle, WA). Dexamethasone sodium phosphate was purchased from LymphoMed Inc. (Rosemont, IL).

In vivo procedures. Cytokines and dexamethasone were diluted in pyrogen-free saline on day of injection. Predetermined optimal doses of cytokines [17,23,24] were given intraperitoneally (i.p.) at the same time as dex administered at 50 µg/mouse or at the dose indicated in the text. Bone marrow cells were tested for the expression of IL-1R 16 to 18 hours after treatment. Adrenalectomy was performed under anesthesia 14 days before the experiment. Adrenalectomized mice were given 1.0% (wt/vol) NaCl in drinking water.

Measurement of CSF activity in serum. CSF titer in serum was measured as follows. Briefly, mice were bled 2 to 3 hours after IL-1 injection and serum was collected by centrifugation after clot formation. CSF activity was determined using bone marrow colony assay for CSF activity as previously described [20]. Briefly, BM cells were suspended in 1.0 mL IMDM, 10% FCS, in 0.3% Seaplaque agarose (Rockland, ME) in the presence or absence of serum (serial 2-fold dilutions). The cells were plated in 35 mm Lux petri dishes (Miles Laboratories Inc., Naperville, IL) and incubated at 37°C in 5.0% CO_2 and scored for colonies (>50 cells) growth after 7 days of incubation. CSF activity was expressed as colony-forming units per millimeter, based on the colony count at 50% of maximum response (Ed50).

Preparation of bone marrow cells. Murine bone marrow cells were aspirated from femurs and low-density mononuclear cells were isolated by separation on Lymphocyte Separation Medium (Organon Teknika Corp., Durham, NC).

Flow cytometry analysis of bone marrow cells. BM cells from saline-, dex- and/or cytokine-treated mice were labeled with either monoclonal antibody (MAB) RB6-8C5, Thy-1, L3T4, F480 or control IgG in an indirect immunofluorescence assay. Briefly, 10^6 BM cells were resuspended in RPMI with 10% fetal calf serum and incubated for 30 minutes at 4°C with 1.0 µg of the appropriate MAB. The cells were washed and then incubated with fluorescein-labeled goat antirat antibody for 30 minutes at 4°C. The cells were then washed 2 times with PBS alone, fixed with 1.0% paraformaldehyde in PBS and analyzed using Coulter Profile II.

Preparation of iodinated IL-1. Human rIL-1α was labeled with ^{125}I using chloramine-T reagent as described previously [25]. The radiolabeled IL-1α had a specific activity that ranged from 1 to $3x10^{15}$ cpm/mmol. There was no significant loss of biological activity of radiolabeled IL-1α as determined by the thymocyte comitogenic activity assay.

Receptor binding assay. Fractionated bone marrow cell suspensions were washed once with cold medium and cell pellets were treated for 1 minute on ice with 50 mm glycine-HCl (pH 3.0) to remove potentially bound cytokines. Subsequently, the cells were washed twice with binding medium (RPMI 1.0% BSA supplemented with 0.1% sodium azide and 10 mm Hepes) and incubated at 4°C with 500 pm ^{125}I-labeled IL-1α in a final volume of 0.2 mL. After 1 to 2 hours of incubation, cell-bound radioactivity was separated from unbound ^{125}I-IL-1α by centrifugation of the sample through a mixture of 1.5:1 (vol/vol) dibutyl phthalate/bis(2-ethylhexyl)-phthalate (Eastman Kodak Co., Rochester, NY). Nonspecific binding was determined by incubating bone marrow cells with labeled IL-1α in the presence of 50-fold excess of unlabeled ligand.

Autoradiography. LDBM cells from mice treated 16 to 18 hours with IL-1, G-CSF and/or dex were prepared as described for receptor binding assay and incubated at 4°C with 1.0 nm ^{125}I-IL-1α. After 1 hour of incubation, cell-bound radioactivity was separated from unbound IL-1 by centrifugation of the sample through a layer of cold FBS. The autoradiography was performed using a modification of a previously described technique [26]. Briefly, $2x10^5$ cells were centrifuged onto microscope slides coated with 0.5% gelatin, fixed in methanol for 10 minutes, coated with Kodak NTB2 photographic emulsion and exposed at 4°C for 4 weeks. Slides were developed with Kodak D-19 developer, fixed with Kodak fixer, stained with Jenner-Giemsa. The number of grains was determined for over 50 cells per slide for 2 slides.

Results

Endogenous corticosteroid production is involved in the upregula-

Table 1. IL-1-stimulated CSF production in adrenalectomized and sham-adrenalectomized mice

Mice[a]	IL-1 injection (ug/mice)[b]	CSF titer (U/mL)[c]
Sham-ADX	None	< 20
Sham-ADX	0.1	590
Sham-ADX	1.0	705
ADX	None	< 20
ADX	0.1	750
ADX	1.0	853

[a]Mice were either adrenalectomized or sham-adrenalectomized as described [23].
[b]Mice were bled 2 to 3 hours after IL-1 injection as described in Materials and methods.
[c]Serum was assayed for CSF activity as described in Materials and methods. The data represent CSF titers of pooled serum from 3 mice.

tion of IL-1R. To examine the role of endogenous corticosteroids in the upregulation of IL-1R on bone marrow cells after IL-1 injection, mice were adrenalectomized. The highest dose of IL-1 (100 ng/mouse) that adrenalectomized mice could tolerate was given i.p. 14 days after surgery. As already demonstrated in normal animals [17], the administration of 100 ng of IL-1 to sham-adrenalectomized mice resulted in a 15-fold increase in IL-1-specific binding compared to saline-treated sham-adrenalectomized mice at 16 hours after injection of IL-1 (Fig. 1). This time was chosen based on our previous studies showing maximal IL-1R expression at 16 to 18 hours [17]. The specific binding of IL-1 on BM cells from IL-1-treated adrenalectomized mice was reduced by 53% compared with IL-1-treated sham-adrenalectomized mice. No specific IL-1 binding was detectable on bone marrow cells from adrenalectomized mice. These data suggest that endogenous corticosteroids participate in the constitutive and IL-1-induced expression of IL-1R.

Since it has been established that IL-1-induces HGF production [2,23], we studied whether adrenalectomy influences IL-stimulated HGF production. For this, adrenalectomized and control (sham-adrenalectomized) mice were bled 2 to 3 hours after IL-1 injection. IL-1 induced similar levels of CSF production in all mice tested (Table 1), indicating that adrenalectomy does not impair IL-stimulated HGF production. We next examined the ability of exogenous addition of dex to synergize with IL-1 in the regulation of IL-1R expression. The injection of optimal concentrations of dex (50 μg) [27] in the presence of optimal amounts of IL-1 (1.0 μg) [17] did not increase IL-1R expression (Fig. 2). At concentrations of 0.1 and 0.3 μg of IL-1 per mouse, however, dex increased IL-1R expression 2-fold. The magnitude of IL-1 upregulation in these cases, however, did not equal the magnitude seen with optimal IL-1 concentrations.

Dexamethasone synergizes with HGFs in the upregulation of IL-1R. Since we have recently determined that increased IL-1R expression after IL-1 administration to mice was mediated, in part, through endogenous HGF production [17], we examined the effect of dexamethasone in combination with HGFs on IL-1R expression on BM cells. Mice were injected with equivalent doses of hematopoietic growth factors such as G-CSF, GM-CSF, IL-3 and IL-6 as well as TGF-ß, a negative regulator of hematopoiesis. Among the cytokines tested, G-CSF, GM-CSF, IL-3 or IL-6 treatment in combination with dex (50 μg) results in a synergistic effect on IL-1R expression on bone marrow cells (Fig. 3). At equivalent doses, rG-CSF was slightly more potent than GM-CSF, followed by IL-6 and IL-3 (Fig. 3). G-CSF plus dex and GM-CSF plus dex were equal to or better than IL-1. TGF-ß alone did not increase IL-1R expression and did not synergize with dexamethasone.

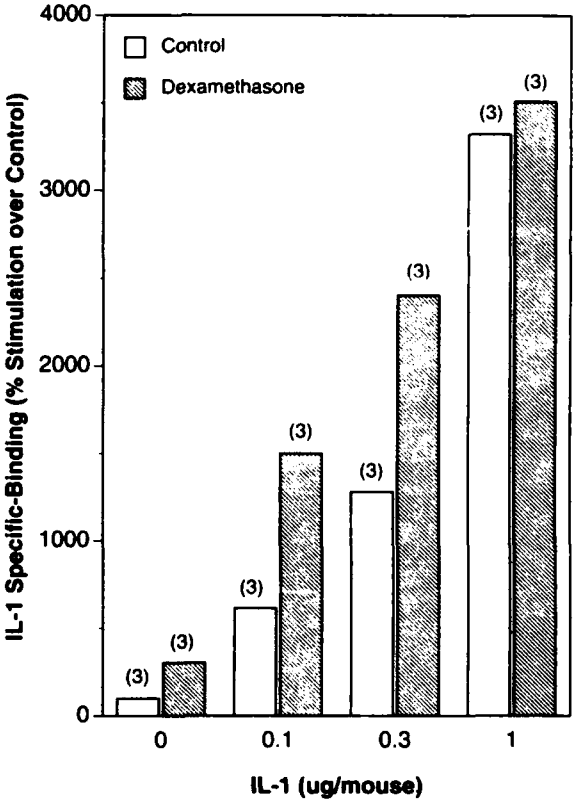

Fig. 2. Dose-dependent interaction between dex and IL-1 administration for increase in IL-1R expression
Mice were injected i.p. with either saline, the indicated doses of IL-1 and maximal dose (50 μg) of dex. Sixteen to 18 hours after treatment radioreceptor assays for the expression of IL-1R on BM cells were done as described in Materials and methods. The data represent the mean ± SE of duplicate determinations using pooled cells from 3 animals. Background was 259 ± 34, which was subtracted from the data shown.

Using G-CSF, the dose-dependence of the synergistic interaction between dex and HGFs was studied. The administration of a previously determined [17] optimal dose of G-CSF significantly increased the expression of IL-1R on BM cells (4.3-fold) (Fig. 4). The administration of dex alone induced a 2-fold increase in IL-1R expression but synergized with G-CSF to upregulate IL-1R in vivo in a dose-dependent fashion (Fig. 4). In all experiments performed (n=7), the administration of G-CSF (5.0 μg) and dex (50 μg) upregulated IL-1R expression to a greater extent than seen with an optimal dose (1.0 μg) of IL-1 alone (Fig. 4). This synergy with G-CSF in increasing IL-1R expression was dose-dependent on dex (Fig. 4).

To determine if G-CSF and dex can act on isolated hematopoietic cells in vitro, normal BM cells were incubated in vitro with G-CSF and/or different concentrations of dex. G-

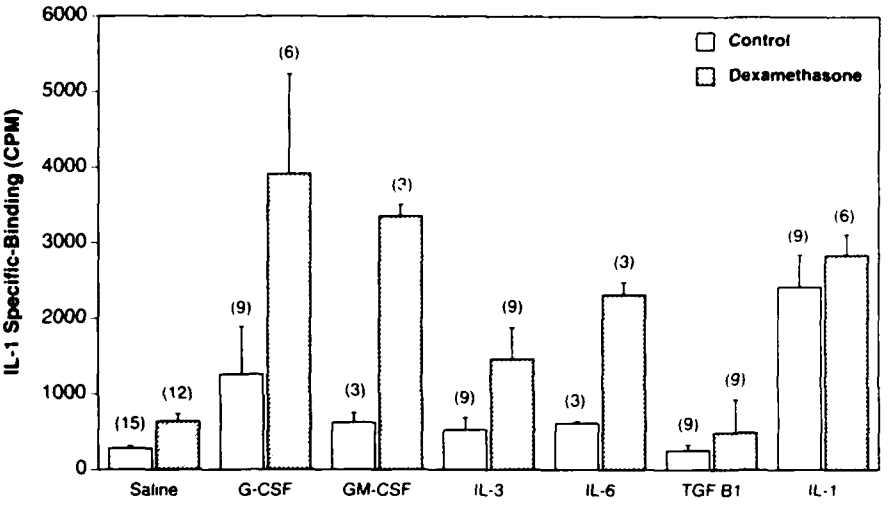

Fig. 3. Hematopoietic growth factors synergize with dexamethasone to upregulate IL-1R expression
Mice were injected i.p. with either saline, IL-1 (1.0 μg), G-CSF (5.0 μg), GM-CSF (5.0 μg), IL-3 (5.0 μg), IL-6 (5.0 μg), TGF-ß (5.0 μg) and/or dex (50 μg). Sixteen to 18 hours after treatment, BM cells were harvested and tested for the expression of IL-1R using radioreceptor assay. The data represent the mean ± SE of determinations using 3 to 15 mice as indicated in parentheses, 2 to 4 experiments for each cytokine. The level of background binding was 315 ± 52, which was subtracted from the data shown here.

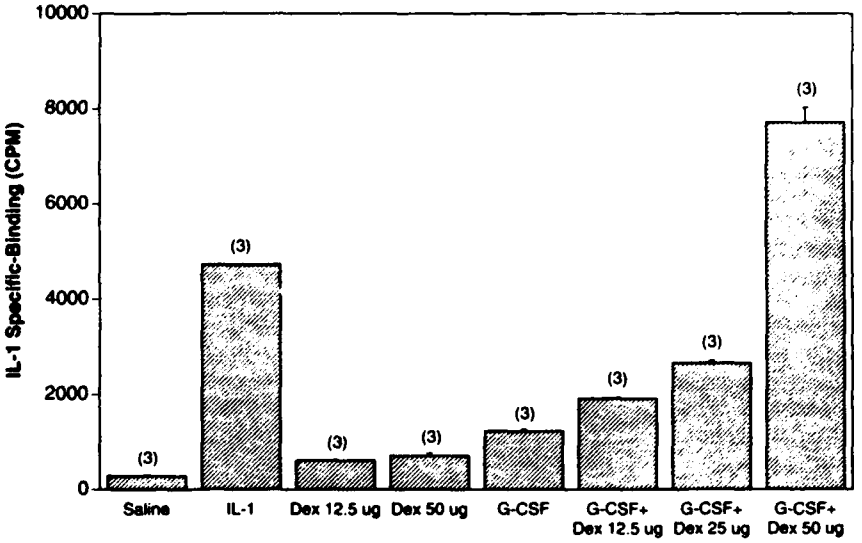

Fig. 4. Dose-dependent synergistic interaction between dexamethasone and G-CSF administration for the increase in IL-1R expression
Mice were injected i.p. with either saline, maximal dose of IL-1 (1.0 μg), maximal dose of G-CSF (5.0 μg) and/or increasing doses of dex. Sixteen to 18 hours after the treatments, radioreceptor assay for the expression of IL-1R on BM cells was performed as described in Materials and methods. The data represent the mean ± SE of duplicate determinations of at least 2 experiments using pooled cells from 3 animals. The level of background binding was 259 ± 34, which was subtracted from the data shown here.

CSF and dex also synergize in vitro to increase IL-1-specific binding (Table 2), whereas IL-1 by itself had no effect.

Distribution of IL-1R on bone marrow cells from G-CSF- and dex-treated mice. We next evaluated whether the in vivo administration of G-CSF and GC increased expression of IL-1R on a specific population or subpopulation of BM cells. Mice received a single injection of saline or a combination of G-CSF and dex. IL-1 binding to BM cells was determined by autoradiography, 16 to 18 hours after injection. Autoradiographic analysis of cells from saline-treated animals showed that most of the labeled cells belonged to the granulocytic series (Table 3, Fig. 5). Seven percent of the undifferentiated blast/early cells were labeled with 8 grains per cell. After treatment with G-CSF and dex, these cells were 19% positive with 28 grains per cell. Promyelocytes and myelocytes (43% positive with 19 grains per cell) were the most heavily labeled cells after G-CSF and dex treatment (87% positive with 57 grains per cell). Thirteen and 16% of eosinophilic and monocytic cells exhibited a similar pattern of labeling with 7 to 8 specific grain per cell. More monocytic cells were labeled after G-CSF and dex treatment (31%) with a small increase in the number of grains per cell (8 to 17). This treatment had no effect on eosinophilic cells. No specific IL-1 labeling was observed on erythroid cells. These results clearly demonstrate that G-CSF and dex treatment results in an increase in IL-1R expression along the myelocytic series and is particularly pronounced for myelocytes followed by metamyelocytes and segmented neutrophils.

G-CSF and dexamethasone promote granulopoiesis. Because the administration of IL-1 induces an initial rapid mobilization of neutrophils from the bone marrow followed by increased cycling of hematopoietic progenitor cells, resulting in the expansion of granulocytes in the marrow [7-11], we examined whether the combination of G-CSF and dex also promoted an expansion of myeloid cells. Bone marrow cells were analyzed by fluorescence-activated cell sorting accordingly to the differential expression of RB6-8C5 antigen on myeloid cells [28].

Table 2. In vitro interaction between G-CSF and dexamethasone in the upregulation of IL-1R on bone marrow cells

Factor added[a]	IL-1-specific binding (CPM)[b]
None	798 ± 56
DEX 10^{-9}M	1341 ±30
G-CSF	4195 ± 273
G-CSF + DEX 10^{-10}M	5985 ± 409
G-CSF + DEX 10^{-9}M	8685 ± 22
IL-1	747 ± 220

[a]LDBM cells obtained from normal mice by Ficoll separation were incubated 24 hours in the presence or absence of the 20 ng/mL of IL-1 or G-CSF and the indicated concentrations of dex.
[b]Bone marrow cells were treated for IL-1 binding as described in Materials and methods. The data represent the mean ± SEM of duplicate determination of a representative experiment of 2 experiments. The level of background binding was 402 ± 168 cpm which was subtracted from the total cpm to give the data shown here.

Table 3. Distribution of IL-1R on BM cells from G-CSF plus dexamethasone–treated mice

	Specific IL-1 binding			
	% labeled		mean grain count	
Cell type	saline	G-CSF + Dex	saline	G-CSF + Dex
Blasts/ early cells	7	19	8	28
Promyelocytes/ myelocytes	43	87	19	57
Metamyelocytes	29	72	11	30
Later neutrophils	23	39	7	23
Eosinophils	13	13	7	8
Monocyte	16	31	8	17
Nucleated erythroid	0	0	0	0

Data represent background-subtracted grain count over more than 20 cells of each type. The level of background binding of >5 grains was subtracted from the total grain count to give the data shown here.

The RB6-8C5^{hi} cells are enriched for the end stage (segmented) neutrophils (>75%) while the RB6-8C5^{lo} cells are enriched for myeloblasts, promyelocytes and myelocytes (>80%). The RB6-8C5^{lo} population represents 19 to 24% of total bone marrow and contains 50% of CFU-GM progenitors [28]. As previously demonstrated [28], the administration of IL-1 to mice results in a 206% increase in the RB6-8C5^{lo} population and a concomitant 41% loss of RB6-8C5^{hi} (Fig. 6, Table 4). Treatment of mice with G-CSF and dex induced a 406% increase in the RB6-8C5^{lo} immature myeloid population and no reduction in the RB6-8C5^{hi} population. In comparison, dex and G-CSF promoted a 206% and 218% increase in RB6-8C5^{lo} population, respectively, and a 137% increase and a 45% reduction in the RB68C5^{hi} population, respectively.

Discussion

We have previously demonstrated that injection of mice with IL-1 results in considerable upregulation of type II IL-1R on myeloid-enriched progenitors [17]. By the administration of antibody against type I IL-1R not present on bone marrow progenitors, we have clearly demonstrated that this upregulation occurs through an indirect mechanism. Administration of IL-1 in vivo stimulates the hypothalamic-pituitary-adrenal axis, resulting in the production of GC [20] as well as HGF production by type 1 IL-1R expressing accessory cells [29-32]. Both GC and HGF are elevated rapidly, with maximal levels reached within 2 hours after IL-1 administration [20,29]. GC have been previously shown to upregulate IL-1R on human monocytes and B cells in vitro [21,22].

In this report, evidence is presented that IL-1-induced endogenous GC synergize with HGF to mediate IL-1 responsiveness on bone marrow cells. The injection of IL-1 to adrenalectomized mice reduced the upregulation of IL-1R by 53% compared with sham-adrenalectomized mice. This effect, which is associated with diminished GC production, is not due to impaired IL-1-induced HGF production in adrenalectomized animals (Table 1). The concomitant administration of GC and HGF such as G-CSF, GM-CSF, IL-3 and IL-6, to normal mice synergistically increased functional IL-1R on bone marrow cells. In addition, this synergy between GC and HGF was also seen in vitro. The observations concerning glucocorticoid modulation of IL-1R in vivo using adrenalectomized mice and the synergy between G-CSF and dex are in agreement with a recent observation from Shieh et al. [19]. While the data indicate a role for GC in IL-1 receptor regulation, other mechanisms cannot be excluded.

In addition, we found that GM-CSF and G-CSF were equally potent in synergizing with dex while IL-6 and IL-3 were approximately 50% as potent. Unlike IL-1, HGF and GCs can stimulate IL-1R expression on hematopoietic cells in vitro [33, 34]. Whether this is a direct effect must await the results of technically difficult binding and antibody-blocking assays on single cells.

Because administration of IL-1 rapidly induces an initial mobilization of neutrophils from the bone marrow followed by increased cycling of hematopoietic progenitor cells, resulting in the expansion of granulocytic compartment in the bone marrow [20,23], we examined whether G-CSF and dex have the same effect. Bone marrow cells were analyzed by fluorescence-activated cell sorting according to the differential expression of RB6-8C5 antigen on myeloid cells [28]. We had previously shown that RB68C5^{hi} cells are enriched for the end stage (segmented) neutrophils (>75%) while the RB6-8C5^{lo} cells are enriched for myeloblasts, promyelocytes and myelocytes (>80%). While the administration of IL-1 to mice results in an 206% increase in the RB6-8C5^{lo} population and a concomitant 41% loss of RB6-8C5^{hi}, treatment of mice with G-CSF and dex induced a 406% increase in the RB6-8C5^{lo} immature myeloid population and no reduction in the RB6-8C5^{hi} population. In addition, autoradiographic analysis of IL-1 binding on bone marrow cells after G-CSF and dex treatment showed that while cells in all stages of granulocytic development had increased IL-1 binding, the most dramatic increase in terms of number of cells positive and grains per cell were the myelocytes, promyelocytes and metamyelocytes.

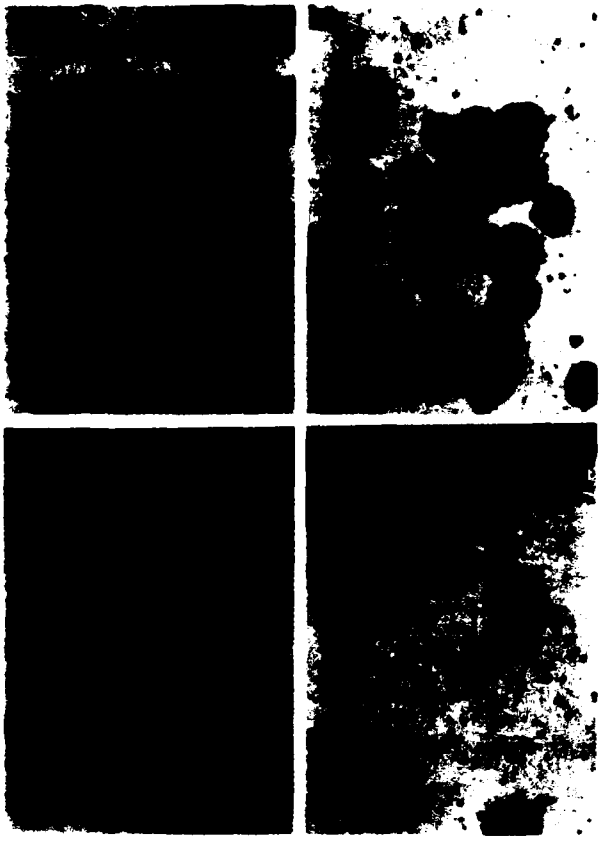

Fig. 5. Autoradiography of ^{125}I-IL-1-labeled LDBM cells from control and G-CSF plus dex-treated mice
Mice received a single i.p. injection of G-CSF (5.0 μg) and dex (50 μg). After 16 hours, bone marrow cells were harvested and radioautography of BMC labeled with ^{125}I-IL-1. Emulsion films were developed after 4 weeks. Panels **A, C** and **D** without cold IL-1; panel **B** with an excess of cold IL-1.

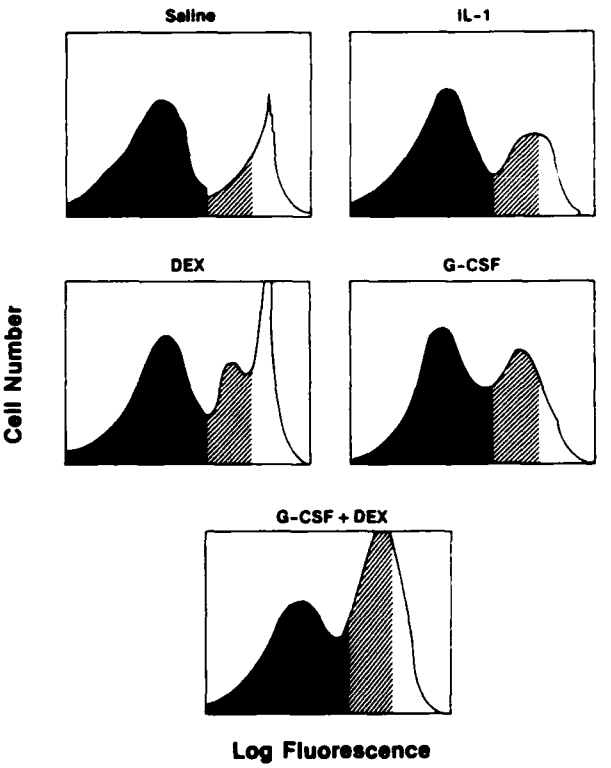

Fig. 6. Differential expression of RB6-8C5 antigen on BM cells from mice treated with G-CSF and/or dexamethasone
Mice were injected i.p. with either saline, *IL-1 (1.0 μg)*, G-CSF (5.0 μg) and/or dex (50 μg). Sixteen to 18 hours after treatment, BM cells were labeled in indirect immunofluorescence assay by using the MAB RB6-8C5 as outlined in Materials and methods. The cells were gated according to fluorescent intensity into 8C5^{neg} (solid region) showing fluorescence between channels 0 and 60, 8C5^{lo} (hatched region) between 60 and 175 and 8C5^{hi} (open region) between 175 and 250. The background staining of the isotype-matched control antibody was less than 3.5% for each treatment.

Whether the increased IL-1R binding leads to increased IL-1 responsiveness is being studied. Thus, it is shown that G-CSF and dex in combination in vivo mimic the effects of IL-1 in granulocyte differentiation.

In addition, we have previously shown that an antibody against type I IL-1R not expressed on neutrophils blocked most of the initial mobilization of neutrophils together with HGF production by type I–expressing stromal cells [17,23]. This confirms that chemotactic response of neutrophils to IL-1 is indirect, probably mediated through IL-1-induced potent chemotactic cytokines such as IL-8 [35,36]. In this report, we show that G-CSF alone can mimic the extent of the initial mobilization of bone marrow neutrophils due to IL-1 (Fig 6, Table 4). Unlike IL-1, G-CSF is directly chemotactic for neutrophils in vitro [37]. It is therefore likely that G-CSF participates with other cytokines induced by IL-1 in the mobilization of neutrophils observed after IL-1 administration.

In general, the amplitude of the response to IL-1 correlates with cell surface receptor expression. For example, positive regulators such as PDGF increased the number of IL-1R together with the capacity of the cell to respond to IL-1 [38]. In addition, treatment of hematopoietic progenitor cells with negative regulators such as TGF-ß blocked the ability of IL-1 to promote high proliferative potential (HPP) colony formation as well as greatly reduced the expression of IL-1R expression [39]. Clinically, increased IL-1R expression has been noted in sepsis, organ failure and acute disseminated inflammation [40]. In this report, concomitant injection of HGF and GC increased IL-1R expression on myeloid cells in the bone marrow with the most increase seen on the myelocyte and promyelocytes followed by metamyelocytes and segmented neutrophils. Such an increase in IL-1R on a premitotic population would serve to promote cellular differentiation and/or cell division, resulting in an amplification of granulocyte differentiation. Therefore, the ability of IL-1 to enhance granulopoiesis in normal [7-11] as well as in myelosuppressed [12-16] mice may be partly due to the unique ability of IL-1 to induce a complex cascade of cytokines and steroids, which can then act to regulate IL-1 receptor expression.

In conclusion, these results provide new insights into the mechanism of IL-1 restorative effects in the marrow. IL-1 stimulates production of HGF and GC which in turn upregulate the expression of IL-1R and render the cells more responsive to IL-1. This accounts for the initial burst of granu-

Table 4. Flow cytometric analysis of BM cells from dex- and G-CSF-treated mice using RB6-8C5 antibody

Treatments[a]	Populations[b] RB6-8C5^{lo}	RB6-8C5^{hi}
Saline	7.7 ± 2.4 (100)	15.8 ± 1.1 (100)
IL-1	16.3 ± 4.6 (210)	9.8 ± 1.3 (62)
Dex	15.4 ± 5.6 (200)	23.3 ± 0.9 (147)
G-CSF	23.6 ± 2.2 (306)	11.8 ± 1.6 (74)
G-CSF + Dex	31.3 ± 7.4 (406)	18.0 ± 601 (114)

[a]Mice were injected i.p. with either saline, maximal doses of IL-1 (1 ug), G-CSF (5 ug) and/or dex (50 ug). Sixteen to 18 hours after treatment, 10^6 BM cells were labeled in an indirect immunofluorescence assay by using the MAB RB6-8C5 as outlined in Materials and methods. Background staining of the isotype-matched control antibody was >3.5% for each treatment. Data represent mean ± SEM for 2 experiments using pooled cells from 3 mice.
[b]The numbers in parentheses represent the percent of stimulation and inhibition of controls (saline-treated). Using an established protocol (28), 8C5^{neg} showed fluorescence between channels 0 and 60, 8C5^{lo} between 60 and 175 and 8C5^{hi} between 175 and 250.

lopoiesis seen after administration of even nanogram amounts of IL-1.

Acknowledgments

This project was funded in part by federal funds from the Department of Human Health and Services under contract #NO1-CO-74102. The content of this publication does not necessarily reflect the views or policies of the Department of Health and Human Services, nor does mention of trade names, commercial products or organizations imply endorsement by the U.S. government. In addition, the work was supported by the Armed Forces Radiobiology Research Institute, Defense Nuclear Agency, under work unit 00129. No endorsement by the Defense Nuclear Agency or the Department of Defense has been given or should be inferred. Claire M. Dubois is a recipient of a research fellowship from the Fonds de la Recherche en Santé du Quebec.

We thank Dr. Dan L. Longo for helpful discussions and review of this manuscript.

References

1. Oppenheim JJ, Kovacs EJ, Matsushima K, Durum SK (1986) There is more than one interleukin-1. Immunol Today 7:45
2. Dinarello CA (1991) Interleukin-1 and interleukin-1 antagonism. Blood 77:1627
3. Stanley ER, Bartocci A, Patinkin D, Rosendall M, Bradley TR (1986) Regulation of very primitive, multipotent, hemopoietic cells by hemopoietin-1. Cell 4:669
4. Mochizuki DY, Eisenman JR, Conlon PJ, Larsen AD, Tushinski RJ (1987) Interleukin-1 regulates hematopoietic activity, a role previously ascribed to hemopoietin-1. Proc Natl Acad Sci USA 84:5267
5. Zsebo KM, Wypych J, Yuschenkoff VN, Lu H, Hunt P, Dukes PP, Langley KE (1988) Effects of hematopoietin-1 and interleukin-1 activities on early hematopoietic cells of the bone marrow. Blood 71:962
6. Moore MAS (1989) Role of interleukin-1 in hematopoiesis. Immunol Res 8:165
7. Kampschmidt RF, Upchurch HF (1977) Possible involvement of leukocytic endogenous mediator in granulopoiesis. Proc Soc Exp Biol Med 155:89
8. Stork LC, Peterson VM, Rundus CH, Robinson WA (1988) Interleukin-1 enhances murine granulopoiesis in vivo. Exp Hematol 16:163
9. Neta R, Sztein MB, Oppenheim JJ, Gillis S, Douches SD (1987) The in vivo effect of interleukin-1. I. Bone marrow cells are induced to cycle after administration of interleukin-1. J Immunol 139:1861
10. Johnson CJ, Douglas JK, Topper MI, Braunschweiger PG, Furmanski P (1989) In vivo hematopoietic effects of recombinant interleukin-1α in mice: Stimulation of granulocytic, monocytic, megakaryocytic, and early erythroid progenitors, suppression of late-stage erythropoiesis, and reversal of erythroid suppression with erythropoietin. Blood 73:678
11. Newton RC, Sandlin G, Pezzella K, Huang J, McKearn J (1989) Flow cytometric analysis of the effect of interleukin-1 administration on bone marrow populations in mice. J Biol Response Mod 8:155
12. Moore MAS, Warren DJ (1987) Synergy of interleukin-1 and granulocyte colony-stimulating factor: in vivo stimulation of stem-cell recovery and hematopoietic regeneration following 5-fluorouracil treatment of mice. Proc Natl Acad Sci USA 84:7134
13. Benjamin WR, Tare NS, Hayes TJ, Becker JM, Anderson TD (1989) Regulation of hemopoiesis in myelosuppressed mice by human recombinant IL-1α. J Immunol 142:792
14. Moreb J, Zucali JR, Gross MA, Weiner RS (1989) Protective effects of IL-1 on human hematopoietic progenitor cells treated in vitro with 4-hydroperoxycyclophosphamide. J Immunol 142:1937
15. Futami H, Jansen R, MacPhee MJ, Keller J, McCormick K, Longo DL, Oppenheim JJ, Ruscetti FW, Wiltrout RH (1990) Chemoprotective effects of rHIL-1α in cyclophosphamide-treated normal and tumor-bearing mice: protection from acute toxicity, hematological effects, development of late mortality and enhanced therapeutic efficacy. J Immunol 145:4121
16. Neta R, Douches S, Oppenheim JJ (1986) Interleukin-1 is a radioprotector. J Immunol 136:2483
17. Dubois CM, Ruscetti FW, Keller JR, Oppenheim JJ, Hestdal K, Chizzonite R, Neta R (1991) In vivo IL-1 administration indirectly promotes type II IL-1R expression on hematopoietic bone marrow cells: novel mechanism for the hematopoietic effects of IL-1. Blood 78:2841
18. Dubois CM, Ruscetti FW, Oppenheim JJ, Keller JR (1990) Induction of interleukin-1 receptor (IL-1R) on normal hematopoietic progenitor cells by colony-stimulating factor. Exp Hematol 18:615 (abstr)
19. Shieh J-H, Peterson RHF, Moore MAS (1991) IL-1 modulation of cytokine receptors on bone marrow cells. J Immunol 147:1273
20. Besedovski H, Adriana DR, Sorkin E, Dinarello C (1986) Immunoregulatory feedback between interleukin-1 and glucocord hormones. Science 233:652
21. Akahoshi T, Oppenheim JJ, Matsushima K (1988) Interleukin-1 stimulates its own receptor on human fibroblasts through the endogenous production of prostaglandins. J Clin Invest 82:1219
22. Akahoshi T, Oppenheim JJ, Matsushima K (1988)

Induction of high affinity interleukin-1 receptor on human peripheral blood lymphocytes by glucocorticoid hormones. J Exp Med 167:924

23. Neta R, Vogel SN, Plocinski JM, Tare NS, Benjamin W, Chizzonite R, Pilcher M (1990) In vivo modulation with anti-interleukin-1 (IL-1) receptor (p80) antibody 35F5 of the response to IL-1: the relationship of radioprotection, colony-stimulating factor, and IL-6. Blood 76:57
24. Neta R, Vogel SN, Sipe JD, Wong GG, Nordan RP (1987) Comparison of in vivo effects of human recombinant IL-1 and human recombinant IL-6 in mice. Lymphokine Res 7:403
25. Palaszynski EW, Ihle JN (1984) Evidence for specific receptors for interleukin-3 on lymphokine-dependent cell lines established from long-term bone marrow cultures. J Immunol 132:1872
26. Nicola NA, Metcalf D (1985) Binding of ^{125}I-labeled granulocyte colony-stimulating factor to normal murine hematopoietic cells. J Cell Physiol 124:313
27. Gustavson LE, Benet LZ (1985) Pharmacokinetics of natural and synthetic glucocorticoids. In: Anderson DC, Winder JSD (eds) The adrenal cortex. Butterworth, NY: Wiley-Liss, 321
28. Hestdal K, Ruscetti FW, Ihle N, Jacobsen SEW, Dubois CM, Kopp WC, Longo DL, Keller JR (1991) Characterization and regulation of RB6-8C5 antigen expression on murine bone marrow cells. J Immunol 147:22
29. Vogel SN, Douches SD, Kaufman EN, Neta R (1987) Induction of colony-stimulating factor in vivo by recombinant interleukin-1α and recombinant tumor necrosis factor. J Immunol 138:2143
30. Zucali JR, Dinarello CA, Oblon DJ, Gross MA, Anderson L, Weiner RS (1986) Interleukin-1 stimulates fibroblasts to produce granulocyte-macrophage colony-stimulating activity and prostaglandin E2. J Clin Invest 77:1857
31. Bagby GC, Dinarello CA, Wallace P, Wagner C, Hefeneider S, McCall E (1986) Interleukin-1 stimulates granulocyte-macrophage colony-stimulating activity release by vascular endothelial cells. J Clin Invest 78:1316
32. Fibbe WE, Van Damme J, Billiau A, Voogt PJ, Duinkerken N, Kluck PMC, Falkenburg JHF (1986) Interleukin-1 (22 K factor) induces release of granulocyte-macrophage colony-stimulating activity from human mononuclear phagocytes. Blood 68:1316
33. Shieh J-H, Peterson RHF, Moore MAS (1991) Granulocyte colony-stimulating factor modulation of cytokine receptors on bone marrow cells. J Immunol 147:2984
34. Dubois CM, Neta R, Ruscetti FW, Jacobsen SEW, Oppenheim JJ, Keller JK (1990) Upregulation of p65 IL-1 receptor (IL-1R) on bone marrow cells by G-CSF and glucocorticoids. J Cell Biochem suppl 15F:109 (abstr)
35. Yoshimura T, Matsushima K, Oppenheim JJ, Leonard EJ (1987) Neutrophil chemotactic factor produced by lipopolysaccharide (LPS)-stimulated human blood mononuclear leukocytes: partial characterization and separation from interleukin-1 (IL-1). J Immunol 139:788
36. Matsushima K, Oppenheim JJ (1989) Interleukin-8 and MCAF: novel inflammatory cytokines inducible by IL-1 and TNF. Cytokine 1:2
37. Wang JM, Chen ZG, Colella S, Bonilla MA, Welte K, Bordigon C, Mantovani A (1988) Chemotactic activity of recombinant human granulocyte colony-stimulating factor. Blood 72:1456
38. Bonin PD, Sings JP (1988) Modulation of interleukin-1 receptor expression and interleukin-1 response in fibroblasts by platelet-derived growth factor. J Biol Chem 263:11052
39. Dubois CM, Ruscetti FR, Palaszynski EW, Falk LA, Oppenheim JJ, Keller JR (1990) Transforming growth factor ß is a potent inhibitor of interleukin-1 (IL-1) receptor expression: proposed mechanism of inhibition of IL-1 action. J Exp Med 172:737
40. Fasano MB, Cousart S, Neal S, McCall C (1991) Increased Expression of the interleukin-1 receptor on blood neutrophils with the sepsis syndrome. J Clin Invest 88:1452

HIGH RESOLUTION GEL ELECTROPHORESIS METHODS FOR STUDYING SEQUENCE-DEPENDENCE OF RADIATION DAMAGE AND EFFECTS OF RADIOPROTECTANTS IN DEOXYOLIGONUCLEOTIDES

B. Mao*, C.E. Swenberg**, Y. Vaishnav** and N.E. Geacintov*

*Chemistry Department, New York University
New York, N.Y., 10003, U.S.A.

**Radiation Biochemistry Department, Armed Forces Radiobiology Research Institute, Bethesda, MD 20889, U.S.A.

INTRODUCTION

Ionizing radiation is known to produce both single and double-strand breaks in DNA (von Sonntag et al., 1981; Hutchinson, 1985; Ward, 1988). In aqueous DNA solutions, radiolysis of water produces OH· radicals which react with DNA bases and sugar residues; hydrogen atom abstraction from the sugar moieties produces radicals which ultimately give rise to strand scission. In the case of low LET radiation (e.g. γ-irradiation), DNA damage caused by OH· radicals generated in the bulk of the aqueous solution is called the "indirect effect" (see for example, Skov, 1984; Achey and Durea, 1974; van Rijn et al., 1985; Roots et al., 1985; Siddiqi and Bothe, 1987; Schulte-Frohlinde, 1989). In the case of high LET radiation, e.g. charged heavy particles, a direct deposition of energy within the DNA molecules is dominant in producing DNA damage by the "direct effect" (see Holley et al., 1990, for example). The formation of DNA strand breaks, in particular double-strand breaks, are rather strongly correlated with ionizing radiation-induced cell killing (Coquerelle, 1978; Elkind, 1985). Other harmful effects of ionizing radiation (Beebe, 1982), including mutations (Waters et al., 1991; Jaberaboansari et al., 1991; Raha and Hutchinson, 1991; Geacintov and Swenberg, 1992) have been well documented.

High resolution electrophoretic gels (Maxam and Gilbert, 1980) are ideal for monitoring the occurrence of DNA strand breaks (Tullius, 1987). However, there are only a few reports on the use of these techniques in studies of radiation damage in DNA (Henner et al., 1982, 1983). In this work we have further explored the utility of these electrophoresis methods to study the formation of strand breaks induced in short deoxyoligonucleotides (11-base pairs) in the single and double-stranded forms in the presence and absence of the known radioprotectant molecule cysteamine (van der Shans, 1970; Roots and Okada, 1972; Bird, 1980; Ward, 1983; Held et al., 1984; Smoluk et al., 1988; Zheng et al., 1988).

EXPERIMENTAL METHODS

The deoxyribooligonucleotides 5'-d(CACATGTACAC) (**X**) and its complement 5'-d(GTGTACATGTG) (**Y**)were synthesized by the phosphoramidite method using a Biosearch Cyclone automated DNA synthesizer (Milligen-Biosearch Corp., San Rafael, CA). The oligonucleotides were purified by oligonucleotide purification columns (Applied Biosystems,

Biological Effects and Physics of Solar and Galactic Cosmic Radiation, Part A, Edited by C.E. Swenberg *et al.*, Plenum Press, New York, 1993

Foster City, CA), and by HPLC using a Rainin Dynamax C_4 column (Rainin Instrument Co., Woburn, MA) using 0.1 M triethylamine-acetate/acetonitrile solvent mixtures. The oligonucleotide **X** was labeled at the 5'-end with [γ^{32}P]ATP purchased from New England Nuclear Corporation (Boston, MA) and employing a T_4 polynucleotide kinase 5'-terminus labeling system (Bethesda Research Laboratories, Gaithersburg, MD). Prior to irradiation, the oligonucleotide was further purified using a 20% polyacrylamide denaturing (7 M urea) gel electrophoresis system , which was also used in all subsequent experiments with DNA exposed to ionizing radiation.

The duplexes **X:Y** (d(CACATGTACAC)· d(GTGTACATGTG)) were formed by annealing the two individual oligonucleotides following standard procedures which involved heating a stoichiometric solution (20 mM sodium phosphate buffer, pH 7) of **X** and **Y** to 85 °C and slow (overnight) cooling to 4 °C. The formation of **X:Y** duplexes was ascertained by electrophoresis on native 20 % polyacrylamide gels (without urea) at 4 °C; the duplex samples were characterized by bands which migrated significantly slower than the single-stranded oligonucleotides.

All irradiations were carried out at 4 °C in air-saturated 20 mM sodium phosphate buffer solutions at pH 7.0. The single- or double-strand concentrations were 0.25 and 0.5 μM (expressed in terms of strand molarities), respectively. The samples were irradiated with either ^{60}Co γ-radiation or neutrons at the Armed Forces Radiobiology Research Institute at Bethesda, MD as described elsewhere in these proceedings (Swenberg et al., 1992).

RESULTS

γ-Irradiation

Typical densitometer tracings of Maxam-Gilbert gels are shown in Fig. 1 for the single-strand **X** (2.5 μM nucleotide concentration) for the case of the unirradiated control, and **X** exposed to 100 and to 200 Gy. Analogous results for the double-stranded **X:Y** oligonucleotides (5 μM) are shown in Fig. 2. Characteristic double-maxima due to frank strand breaks are observed in both the single- and double-stranded oligonucleotides, but are best defined in the case of the irradiated duplex **X:Y**, particularly at the higher dosage of 200 Gy. Besides the intense band due to the original 11-mer (lowest mobility broad band on the

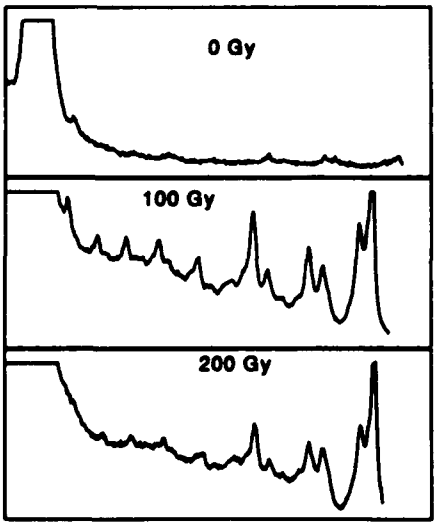

Figure 1. Densitometer tracings of an electrophoresis gel of the single-strand **X** exposed to γ-irradiation.

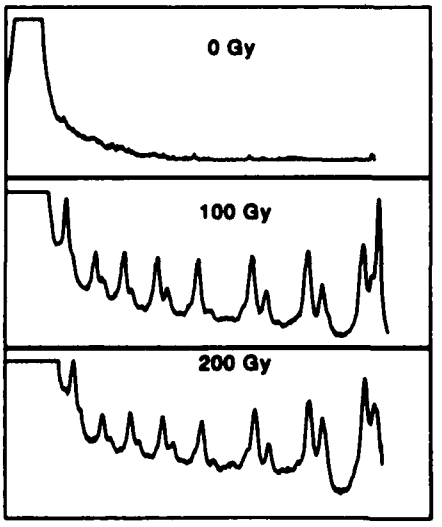

Figure 2. Densitometer tracings of an electrophoresis gel of the duplex **X:Y** exposed to γ-irradiation.

left), eight other types of fragments, corresponding to 10-, 9-, 8-, 7-, 6-, 5-, 4-, and 3-mers are distinguishable. The bands due to the nucleotide monomer and dimer fragments are missing, because the mobilities of these fragments are so high that they are located beyond the scale shown in Figs. 1-6.

Each type of fragment (the different fragments differ from one another by the number of nucleotides) is characterized by double bands in the electrophoretic gels. The occurrence of double-bands for each type of 5'-end-labeled fragment has been previously observed by Henner et al. (1983) and attributed to the occurrence of two types of 3'-termini; the slower migrating fragment contains a 3'-phosphoryl group, while the faster moving fragment contains a glycolate moiety attached to the 3'-phosphoryl group via the 2"-OH group of glycolic acid.

In the case of the irradiated single-stranded oligonucleotide **X**, the maxima due to the shorter fragments are superimposed on a background whose amplitude increases with increasing size of the electrophoresed fragments. In the case of the γ-irradiated double-stranded **X:Y** this background appears to be less pronounced, and the amplitudes of the bands due to strand breaks appear to be greater (Fig. 2) than in the single-stranded case (Fig. 1).

Neutron-irradiation

In the case of the single-strand oligonucleotide **X**, double-bands can be recognized only in the case of the 3-mer, 4-mer, and 5-mer (Fig. 3). At the higher dosage, the higher molecular weight bands tend to disappear. In the case of the duplex (Fig. 4), bands due to all eight fragments, together with the faster moving phosphate glycolate bands, are recognizable.

Estimation of fractions of damaged oligonucleotides

The fraction of damaged oligonucleotides was estimated by comparing the radioactivities in the 11-mer band, and in all of the shorter fragment bands (including the monomer and dimer bands not shown in Figs. 1-6). This was accomplished by integrating the areas under the densitometer tracings and comparing the areas under the 11-mer band, and summing the areas under the tracings corresponding to all lower mobility fragments (including the background). The area under the intense 11-mer band was estimated by a serial

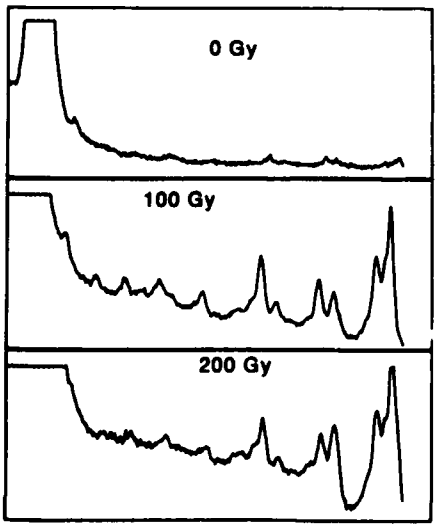

Figure 3. Densitometer tracings of an electrophoresis gel of the single-strand **X** exposed to fission neutron-irradiation.

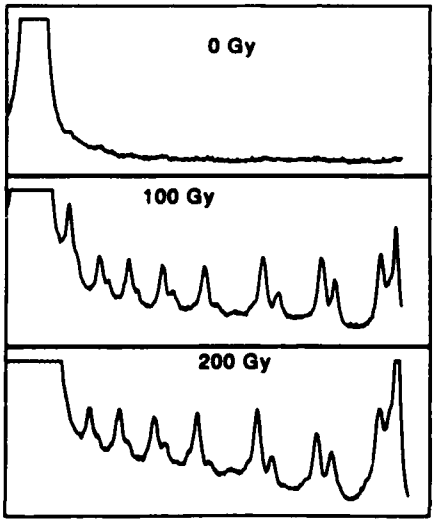

Figure 4. Densitometer tracings of an electrophoresis gel of the duplex **X:Y** exposed to fission neutron-irradiation.

dilution procedure, thus producing bands of sufficiently low amplitudes for densitometric analysis. In all cases, the fraction of damaged oligonucleotides estimated in this manner varied from 4 - 5 %.

Effects of the radioprotectant cysteamine

In the presence of 10 mM cysteamine, there is a large reduction in strand break formation in the γ-irradiated duplex **X:Y** (Fig. 5) even at the relatively high dosage of 400 Gy. In the case of neutron irradiation (also at a dosage of 400 Gy), a protective effect is also observed, although it appears to be less pronounced than in the case of γ-irradiation (Fig. 6).

The protection factors (PF) = $(PF_0)/(PF_{cyst})$, defined here as the ratio of areas under the densitometric traces due to damaged fragments (including the background) in the absence (PF_0) and presence of cysteamine (PF_{cyst}), were evaluated for both types of irradiation. For γ-irradiation, $(PF)_\gamma \approx 16$, while in the case of neutron irradiation this factor was significantly smaller with $(PF)_n \approx 2.3$.

DISCUSSION

Single strand breaks and base/sugar damage

Two kinds of radiation damage can be observed and distinguished with the high resolution denaturing polyacrylamide gels: (1) strand breaks which are characterized by rather sharp bands due to fragments with different numbers of nucleotides, and (2) unspecified, probably multiply damaged oligonucleotide fragments which give rise to pronounced backgrounds in the autoradiograms, and the continuous background levels in the densitometer tracings. We presume that this background, whose contribution rises with increasing dosage, is due to modification of the bases and to damaged sugar residues at the 3'-ends of the oligonucleotides. The formation of multiply damaged DNA fragments at the dosages employed in this work is consistent with quantitative estimates made previously by Ward and Kuo (1978). Multiple damage per oligonucleotide fragment is expected to give rise to a heterogeneity of molecular weights and thus to a broadening of each individual fragment band; ultimately, as the level of damage is increased, the broadening should lead to an

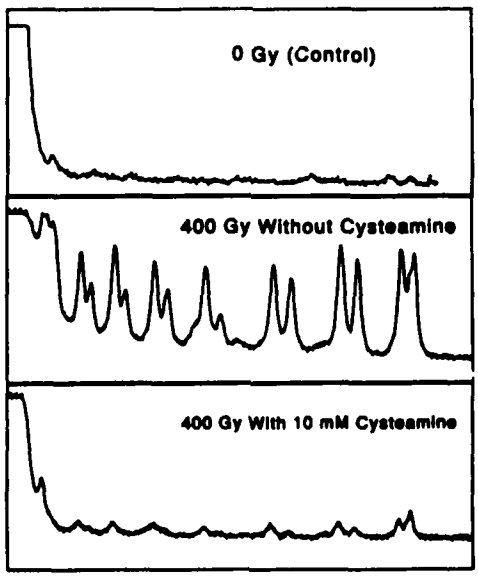

Figure 5. Densitometer tracings of an electrophoresis gel of the duplex X:Y exposed to γ-irradiation with and without cysteamine (10 mM).

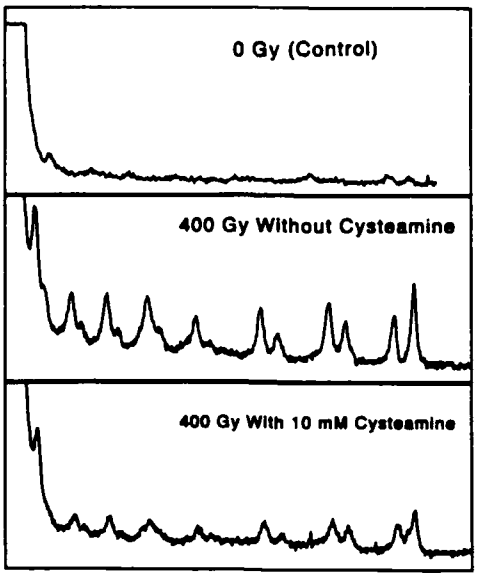

Figure 6. Densitometer tracings of an electrophoresis gel of the duplex X:Y exposed to fission neutron-irradiation with and without cysteamine (10 mM).

overlapping of the individual bands and eventually their ultimate disappearance into the background.

It is evident from Figs. 1-4 that the amplitudes of the shorter molecular weight fragments (e.g. the 3-mer, 4-mer, and 5-mer), after subtraction of the background, are larger than those of the higher molecular weight fragments. It thus appears that there are more frank strand breaks closer to the 5'-end of X than to the 3'-end. However, Henner et al. (1982) reported that strand scission events in various DNA fragments 12-150 nucleotides long occur uniformly at all nucleotide sites. The apparent preference for strand scission near the 5'-end observed here may involve factors other than intrinsic differences in the efficiencies of strand scission, as noted below.

The mechanisms of DNA strand scission induced by ionizing radiation involves mainly hydrogen abstraction from the sugar residues by OH· and other radicals, especially in the case of γ-irradiation where the indirect effect dominates (Achey and Durea, 1974; von Sonntag et al., 1981; Skov, 1984; van Rijn et al., 1985; Siddiqi and Bothe, 1987; Ward, 1988; Schulte-Frohlinde, 1989). Since the irradiations were performed in the presence of atmospheric oxygen, hydrogen abstraction from the sugar moieties, followed by the formation and decomposition of peroxyl radicals, results in strand breaks (von Sonntag, 1981; Liphard et al., 1990). Each fragment formed may have suffered earlier base damage, or may undergo further modification under the action of ionizing radiation. At the relatively high dosages of 100-200 Gy, the higher the molecular weight of a fragment, the greater the probability of multiply damaged sites on a given fragment. Thus, the number and distribution of damaged sites per fragment should be greater the larger the fragment. In other words, the heterogeneity of multiply damaged fragments should increase with increasing molecular weight. Therefore, the gel bands associated with higher molecular weight fragments (e.g. the 6-mer, 7-mer, 8-mer, 9-mer and 10-mer bands in Fig. 1 and Fig. 3) tend to be less well defined than the three smaller 3-, 4-, and 5-mer fragments. Also, with increasing dose and in the case of the single stranded X, the bands due to the higher molecular weight fragments appear to merge into the background, an effect which is consistent with the model proposed here.

Patterns of damage in single- and double-stranded DNA fragments

There is a significant difference in the gel electrophoresis patterns of the single-stranded and double-stranded DNA subjected to γ-irradiation. In the single-stranded case, the background due to modified DNA is significantly more pronounced than in the case of the duplex. However, the occurrence of well defined bands due to fragments differing from one another by one nucleotide, appears to be greater for irradiated duplexes than for irradiated single strands. These observations are consistent with the notion that bases are more susceptible to attack by OH· radicals in the single- rather than in the double-stranded forms (Ward and Kuo, 1978). In single-stranded DNA, the number of OH· radicals reacting with the bases is 7-10 greater than the number reacting with the sugars (as measured by strand scission), whereas in double-stranded DNA this ratio of base damage/sugar damage is between 2.8 and 4 (Ward, 1988). As discussed above, base damage is expected to significantly contribute to the observed heterogeneous distributions of molecular weights, and thus to the background in the densitometer traces. Since damage to the sugar moieties leads to strand scission, and such damage is more pronounced in duplexes than in single-stranded DNA (Ward and Kuo, 1978), the bands due to strand scission are more prominent in the electrophoretic gels of γ-irradiated duplex DNA than for single-stranded DNA.

Effects of γ- and neutron irradiation

For low LET γ-irradiation, DNA damage occurs primarily via the indirect effect. In the case of fission neutrons, damage primarily results from high energy recoil protons (Watt, 1988). Strand scission in the indirect mechanism is more likely in duplex DNA than in single-stranded DNA, whereas for the direct mechanism, strand scission in single-stranded and double-stranded DNA is expected to be comparable. Recently, Spotheim-Morizot et al. (1990) have suggested that single-strand breaks induced in supercoiled DNA irradiated with fission neutrons are caused primarily by OH· radicals. Our results are consistent with this view as there are no discernible differences in the electrophoresis patterns of either single- or double-stranded DNA exposed to either γ- or neutron irradiation (Figs. 1-4) and the fractions of damaged oligonucleotides (4 - 5%) are similar in both cases.

Effects of the radioprotective agent cysteamine

Cysteamine, has an electrical charge of +1 at pH 7.0, and binds to the negatively charged DNA polyion, thus providing a significant degree of protection against damage produced by OH· radicals and strand scission (Roots and Okada, 1972; Smoluk et al., 1988; Zheng et al., 1988; Spotheim-Morizot et al., 1991). The diffusion length of OH· radicals is about 60 Å (Roots and Okada, 1975) and thus radical scavenging by thiols in the bulk solution constitutes an important radioprotection mechanism (Swenberg, 1988); in addition, thiols can interact directly with radicals on the DNA molecules by proton transfer, thus further reducing DNA damage. In aerated solutions, the protective effect of the endogeneous thiol, glutathione (GSH), results predominantly from the scavenging of radicals; strand breaks are caused by the decay of DNA peroxyl radicals and these apparently do not significantly react with GSH (Liphard et al., 1990).

Cysteamine causes a dramatic reduction of strand scission in the duplex **X:Y** exposed to γ-irradiation (Fig. 5); at a 10 mM cysteamine concentration, the protection factor $(PF)_{\gamma} \approx 16$. Similar effects were observed in the case of plasmid DNA by Roots and Okada (1972) and by Spotheim-Morizot et al. (1991). These results are in accord with the dominance of the indirect effect and the role of OH· radicals in causing DNA damage by the low LET γ-irradiation. For fission neutron irradiation, there is also a marked reduction in DNA damage in the presence of cysteamine (Fig. 6), although the protection factor $(PF)_n$ is only 2.3, considerably smaller than in the case of γ-irradiation. These observations suggest that a fraction of strand breaks induced by neutron irradiation are produced by mechanisms different from those operative for low LET irradiation. These mechanisms probably involve the direct formation of DNA radicals by recoil protons, α-particles, etc. (Spotheim-Morizot et al., 1991).

SUMMARY AND CONCLUSION

The polyacrylamide high resolution gel system is suitable for quantitatively determining the occurrence of strand breaks in oligonucleotides. The apparent base-sequence effects observed here in oligonucleotides exposed to γ- and fission neutron irradiation seems to be related to the lengths of the fragments generated by strand scission, rather than to different probabilities of breaks occurring at different sites within the oligonucleotide. The heterogeneous distributions of molecular weight of the degradation products (fragments of reduced chain length) is attributed to multiple base-damage. High resolution gel methods allow for quantitative estimates of radioprotection factors. These techniques can also be used for evaluating the sequence-dependence of strand-breaks in DNA with unusual tertiary structures, or with DNA complexed with proteins.

ACKNOWLEDGEMENTS

The portion of the work carried out at New York University was supported by the Office of Health and Environmental Research of the U.S. Department of Energy, Grant DE-FGO2-86ER60405.

REFERENCES

Achey, P. and Duryea, H., 1974. Production of DNA strand breaks by hydroxyl radicals. Int. J. Radiat. Biol. 25: 595-601.

Beebe, G.W., 1982. Ionizing radiation and health. Am. Scientist 70: 35-44.

Bird, R.P., 1980. Cysteamine as a protective agent with high LET radiations. Radiat. Res. 82: 290-296.

Coquerelle, T, Hagen, U., Köhnlein, W. and Crump, W. , 1978. Radiation effects on the biological function of DNA, in "Effects of Ionizing Radiation on DNA", Bertinchamps, A.J., Hütterman, J., Köhnlein, W. and Téoule, R., Eds., Springer-Verlag, Berlin, New York, pp. 261-302.

Elkind, M.M., 1985. DNA damage and cell killing, Cancer 56: 2351-2363.

Geacintov, N.E. and Swenberg, C.E., 1992. Chemical, molecular biology, and genetic techniques for correlating DNA base damage induced by ionizing radiation with biological end-points, in: "Physical and chemical Mechanisms in Molecular Radiation Biology", Varma, M.N. and Glass, W.A., Eds., Plenum Press, New York, pp. 452-474.

Held, K.D., Harrop, H.A. and Michael, B.D. , 1984. Effects of oxygen and sulphydril-containing compounds on irradiated transforming DNA. II. Glutathione, cysteine and cysteamine. Int. J. Radiat. Biol. 45: 615-626.

Henner, W.D., Grunberg, S.M. and Haseltine, W.A., 1982. Sites and structure of γ radiation-induced DNA strand breaks. J. Biol. Chem. 257: 11750-11754.

Henner, W.D., Rodriguez, L.O., Hecht, S.M. and Haseltine, W.A., 1983. γ Ray induced deoxyribonucleic acid strand breaks. J. Biol. Chem. 258: 711-713.

Holley, W.R., Chatterjee, A. and Magee, J.L., 1990. Production of DNA strand breaks by direct effects of heavy charged particles. Radiat. Res. 121: 161-168.

Hutchinson, F., 1985. Chemical changes induced in DNA by ionizing radiation. Progr. Nucleic Acid Res. Mol. Biol. 32: 115-154.

Jaberaboansari, A., Dunn, W.C., Preston, R.J., Mitra, S. and Waters, L.C., 1991. Mutations induced by ionizing radiation in plasmid replicated in human cells. II. Sequence analysis of α-particle-induced mutations. Radiat. Res. 127: 202-210.

Liphard, M., Bothe, E. and Schulte-Frohlinde, D. , 1990. The influence of glutathione on single-strand breakage in single-stranded DNA irradiated in aqueous solution in the absence and presence of oxygen. Int. J. Radiat. Biol. 58: 589-602.

Maxam, A.M. and Gilbert, W., 1980. Sequencing end-labeled DNA with base-specific chemical cleavage. Methods. Enzymol. 65: 499-560.

Raha, M. and Hutchinson, F., 1991. Deletions induced by gamma rays in the genome of Escherichia coli. J. Mol. Biol. 220: 193-198.

Roots, R. and Okada, S., 1972. Protection of DNA molecules of cultured mammalian cells from radiation-induced single-strand scissions by various alcohols and SH compounds. Int. J. Radiat. Biol. 21: 329-342.

Roots, R. and Okada, S., 1975. Estimation of lifetimes and diffusion distances of radicals involved in X-ray-induced DNA strand breaks or killing of mammalian cells. Radiat. Res. 64: 306-320.

Roots, R., Chatterjee, A., Chang, P., Lommel, L. and Blakely, E.A., 1985. Characterization of hydroxyl radical-induced damage after sparsely and densely ionizing radiation, Int. J. Radiat. Biol. 47: 157-166.

Schulte-Frohlinde, D., 1989. Studies of radiation effects on DNA in aqueous solution. The L.H. Gray Lecture. ICRU News, December issue, 4-15.

Siddiqi, M.A. and Bothe, E., 1987. Single- and double-strand break formation in DNA irradiated in aqueous solution: dependence on dose and OH radical scavenger concentration. Radiat. Res. 112: 449-463.

Skov, K.A., 1984. The contribution of hydroxyl radicals to radiosensitization: a study of DNA damage. Radiat. Res. 99: 502-510.

Smoluk, G.D., Fahey, R.C. and Ward, J.F., 1988. Interaction of glutathione and other low-molecular weight thiols with DNA: evidence for counterion condensation and coion depletion near DNA. Radiat. Res. 114: 3-10.

Spotheim-Morizot, M., Charlier, M. and Sabattier, R., 1990. DNA radiolysis by fast neutrons. Int. J. Radiat. Biol. 57: 301-313.

Spotheim-Morizot, M., Franchet, J., Sabattier, R. and Charlier, M., 1991. DNA radiolysis by fast neutrons. II. Oxygen, thiols and ionic strength effects, Int. J. Radiat. Biol. 59: 131-1324.

Swenberg, C.E., 1988. DNA and radioprotection, in: "Terrestrial Space Radiation and its Biological Effects", NATO ASI Series A: Life Sciences Vol. 154, McCormack, P.D., Swenberg, C.E. and Bücker, eds., Plenum Press, New York, pp. 675-695.

Swenberg, C.E., Speicher, J.M. and Miller, J.H., 1992. Does the topology of closed supercoiled DNA effect its radiation sensitivity? These Proceedings.

Tullius, T.D., 1987. Chemical "snapshots" of DNA: using the hydroxyl radical to study the structure of DNA and DNA-protein complexes. Trends Biochem. Sci. 12: 297-301.

van der Schans, G.P. and Blok, J., 1970. The influence of oxygen and sulphhydryl compounds on the production of breaks in bacteriophage DNA by gamma-rays. Int. J. Radiat. Biol. 17: 25-38.

van Rijn, K., Mayer, T., Blok, J., Verberne, J.B. and Loman, H., 1985. Reaction rate of OH radicals with ϕX174 DNA: influence of salt and scavenger. Int. J. Radiat. Biol. 47: 309-317.

von Sonntag, C., Hagen, U., Schön-Bopp and Schulte-Frohlinde, D., 1981. Radiation-induced strand breaks in DNA: chemical and enzymatic analysis of end groups and mechanistic aspects. Adv. Radiat. Biol. 9: 109-142.

Ward, J.F. and Kuo, I., 1978. Radiation damage to DNA in aqueous solution: a comparison of the response of the single-stranded form with that of the double-stranded form. Radiat. Res. 75: 278-285.

Ward, J.F., 1983. Chemical aspects of DNA radioprotection, in: "Radioprotectors and Anticarcinogens", Nygaard, O.F. and Simic, M.G., eds., Academic Press, New York, pp. 73-85.

Ward, J.F., 1988. DNA damage produced by ionizing radiation in mammalian cells: identities, mechanisms of formation, and repairability. Progr. Nucleic Acid Res. Mol. Biol. 35: 95-125.

Waters, L.C., Skipi, M.O., Julian Preston, R., Mitra, S. and Jaberaboansari , 1991. Mutations induced by ionizing radiation in plasmid replicated in human cells. I. Similar, nonrandom distribution of mutations in unirradiated and X-irradiated DNA. Radiat. Res. 127: 190-201.

Watt, D.E., 1988. Absolute biological effectiveness of neutrons and photons. Radiation Protection Dosimetry 23: 63-67.

Zheng, S., Newton, G.L., Gonick, G., Fahey, R.C. and Ward, J.F., 1988. Radioprotection of DNA by thiols: relationship between the net charge on a thiol and its ability to protect DNA. Radiat. Res. 114: 11-27.

FREE-RADICAL YIELDS IN PROTON IRRADIATION OF ORIENTED DNA: RELATIONSHIP TO ENERGY TRANSFER ALONG DNA CHAINS

J.H. Miller*, D.L. Frasco*, M. Ye*, C.E. Swenberg**, L.S. Myers, Jr., and A. Rupprecht***

*Pacific Northwest Laboratory, Richland, WA 99352
**Armed Forces Radiobiology Research Institute, Bethesda, MD 20814
***University of Stockholm, S-106 91 Stockholm, Sweden

ABSTRACT

Spatial patterns of energy deposition on the nanometer scale are currently believed to be a major factor in determining the biological effectiveness of ionizing radiation. If the most common precursors of biologically significant lesions are clusters of ionization in or near DNA, then intramolecular energy and charge transfer along DNA chains could be very important in lesion development. This paper describes investigations of these phenomena through model calculations and measurements of radical yields in oriented DNA exposed to proton irradiation.

INTRODUCTION

The idea that the critical lesions in radiation biology result from clustering of ionizations on a nanometer scale can be traced to the early work of Lea (1947), Howard-Flanders (1958), and Barendsen (1964). More recent support for this model of the biological effects of ionizing radiation comes from the analysis of cell killing by radiations with different linear-energy-transfer (LET) based on computer simulations of track structure in water (Goodhead, 1987). Although these biophysical models ignore the complexity of the cellular medium and the macromolecular structures that regulate its function, their basic conclusion can be rationalized by the high scavenging capacity of the chemical environment of DNA (Roots and Okada, 1975) and the efficiency of repair of minor perturbations of DNA structure (Doetsch and Cunningham, 1990).

From arguments of this type, one concludes that the most common precursor of cytotoxic and mutagenic effects from radiation exposure is a cluster of ionization in or, at least, very near to the DNA molecule. The involvement of macromolecules in the early stages of lesion production opens the possibility of intramolecular energy and charge transfer following excitation or ionization by the radiation field. These processes acting in the presence of traps for energy and charge provide a mechanism for concentrating energy deposited in macromolecular systems that is independent of stochastic processes in the slowing down of charged particles. Conversely, energy and charge transfer along DNA chains may dissipate clusters of excitation and ionization before biologically significant lesions are formed. In general, the existence of energy and charge migration in macromolecules tends to decouple lesion production from the stochastics of energy deposition

Biological Effects and Physics of Solar and Galactic Cosmic Radiation, Part A, Edited by C.E. Swenberg *et al.*, Plenum Press, New York, 1993

just as ordinary diffusion tends to decouple radiation chemistry on a long time scale from track effects in the radiolysis of homogeneous solutions of small molecules.

Recent findings at several laboratories have raised questions about the assumption that radiation-induced DNA damage remains localized on the nanometer scale during lesion formation. Observations by Arroyo et al. (1986) that the yield of neutron-induced free radicals in oriented DNA fibers was dependent on the orientation of the sample relative to the neutron flux were attributed to energy transfer between stacked DNA bases. Al-Kazwini et al. (1990) presented evidence that electrons can move along DNA chains for distances up to about 100 base pairs. Data obtained by van Lith et al. (1986) on microwave conductivity in pulsed radiolysis suggest that excess electrons in frozen DNA solutions can migrate for distances of the order of 100 nm in the structured water layers around macromolecular chains.

Simultaneous with these experimental results, there has been a renewed interest in nonlinear modes of vibrational excitation in DNA called solitons (Baverstock and Cundall, 1988). Several models for solitary waves in DNA have been proposed (Englander et al., 1980; Yomosa, 1984; Takeno and Homma, 1987; Zhang, 1987, Muto et al., 1988). In Yomosa's model, about 0.4 eV of vibrational energy is transported along DNA at a rate of about 100 nm/ns as a disruption of hydrogen bonds between complementary bases. The broad spectrum of excitation associated with the absorption of energy from ionizing radiation in biological systems (Bednár, 1985) should provide ample opportunity to overcome the energy threshold required to initiate nonlinear phenomena like solitons (van Zandt, 1989).

The first section of this paper discusses models for the effects of energy and charge transfer on free-radical yields in oriented DNA samples exposed to direct proton-beam irradiation. Experiments designed to detect an orientation dependence of radical yields from proton irradiation of oriented DNA are described in the second section. Our conclusions are presented in the final section.

MODELING RADICAL YIELDS IN PROTON IRRADIATION OF ORIENTED DNA

We have investigated (Miller et al., 1988; Miller and Swenberg, 1990) mechanisms for the observation by Arroyo et al. (1986) that DNA base radicals induced by neutrons are dependent on the orientation of DNA fibers relative to the neutron flux. Monte Carlo codes developed by Wilson and Paretzke (1981) and scoring algorithms contributed by Charlton (1985) were used to model energy deposition in oriented DNA under direct proton-beam irradiation. Table I summarizes our results for a 1 MeV proton flux incident on an oriented DNA sample either parallel or perpendicular to the fiber direction. Although the average amount of energy deposited in the parallel case is 5 times greater than in the perpendicular case, the average separation between the excitations or ionizations in the same DNA chain is about 100 times greater in the parallel case. The pattern of deposition in the parallel case is also more sensitive to uncertainty in the fiber orientation relative to the proton beam.

If the pattern of energy deposition events along a DNA chain in the parallel case is as diffuse as these model calculations suggests, then only long-range modes of intramolecular energy or charge transfer could couple the excitations and ionization in the molecule in ways

Table 1. Energy Deposition in Oriented DNA by 1 MeV Protons

Orientation	Energy Deposited (eV)	Event Separation (nm)
0°	293	224
0° ± 10°	150	47
90°	62	2
90° ± 10°	62	2

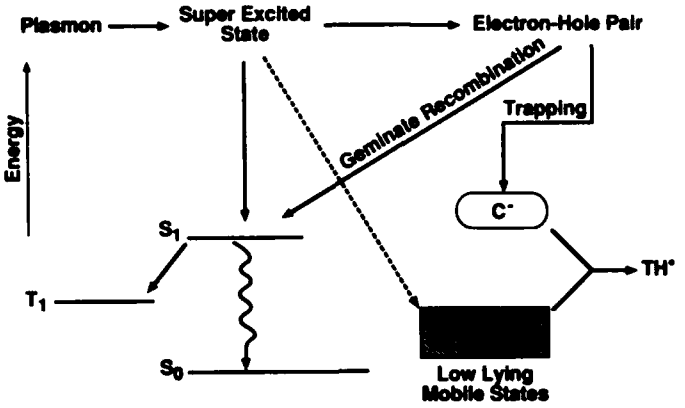

Figure 1. Decay Modes of Energy Absorbed in Solid DNA Samples

that would make the yield of free radicals orientation dependent. For example, recent work by Georghiou (1990) indicates that singlet excitations of bases in calf thymus DNA at room temperature move only 1 or 2 base pairs before they are irreversible trapped. Clearly, this type of excitation has a low probability of interacting with other energy deposition events in same DNA chain and should have equivalent effects in both irradiation geometries.

Energy absorbed from ionizing radiation in oriented DNA fibers should produce modes of excitation that are considerably more mobile than singlet excitons (Al-Kazwini et al., 1990; van Lith et al., 1986; Yomosa, 1984). Figure 1 illustrates a mechanism by which solitons might influence free-radical yields when DNA at 77° K is exposed to a proton beam parallel to the molecular orientation. The interaction of DNA with protons and secondary electrons produces highly excited electronic states that decay primarily through formation of electron-hole pairs. Usually this decay is accompanied by some conversion of electronic to vibrational energy. Sufficiently large vibrational excitations in DNA can be self cohering (van Zandt, 1989). Recent work by Bernhard (1989) suggests that excess electrons are trapped on cytosine by reversible proton transfer from guanine. If many super-excited states are produced in the same DNA chain by a proton flux that is parallel to the molecular orientation, then the probability of interaction between trapped electrons and solitons increases. This interaction may induce electron transfer to thymine where TH· is formed by irreversible protonation at C6.

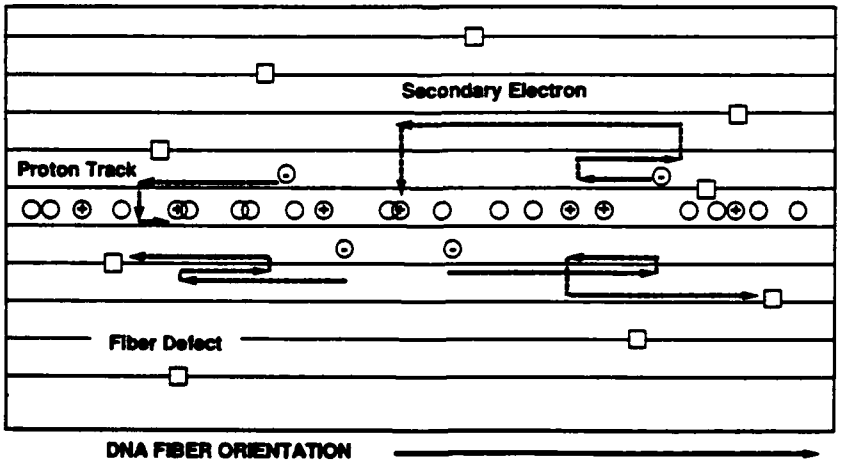

Figure 2. Schematic of Electron-hole Recombination in Oriented DNA Exposed to a Proton Flux that is Parallel to the DNA Fibers.

The model illustrated in figure 1 neglects the mobility of electrons ejected in the decay of super-excited states by ion-pair formation. The high mobility and long lifetime of excess electrons in the hydration layers of DNA (van Lith et al., 1986) could also contribute to orientation effects in DNA damage by proton irradiation. This mechanism is illustrated in figure 2, where the dashed lines represent trajectories of ejected electrons that move primarily in hydration layers around DNA but occasionally are scattered between DNA chains. The squares represent fiber defects that mainly determine the mean free path of excess electrons when the sample is exposed to low LET radiation or protons perpendicular to the fiber orientation. However, when proton tracks are parallel to the fiber direction, many positive ions lie in the high-mobility path of excess electrons. This increases the probability of electron-hole recombination and could reduce the yield of primary radical anions and cation in the parallel case.

EXPERIMENTS WITH PROTON IRRADIATION OF ORIENTED DNA

Preparation of oriented DNA samples (Rupprecht, 1966) to look for effects like those illustrated in figures 1 and 2 involves wet spinning of high molecular weight DNA into fibers that are wound on a spool to form a thin sheet of oriented DNA. Samples for perpendicular

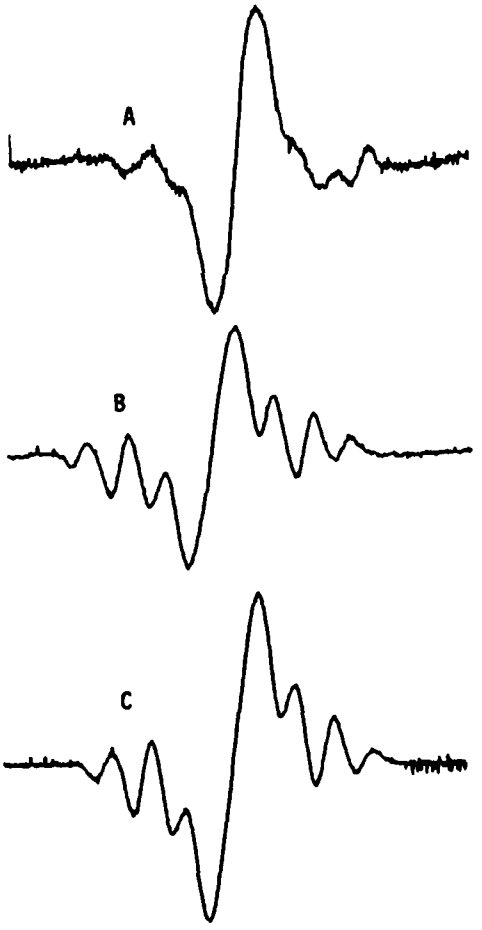

Figure 3. EPR Spectra of Oriented DNA Exposed to γ-rays (A) and Protons Perpendicular (B) or Parallel (C) to the DNA Fibers.

irradiation were made by pressing together a sufficient number of sheets to give a thickness greater than the range of a 4 MeV proton, which is about 0.5 mm. Samples for parallel irradiation were sliced from a block of oriented DNA that had a thickness slightly less than the 3 mm inside diameter of quartz tubes used to transfer irradiated samples to the electron paramagnetic resonance (EPR) spectrometer. All samples were approximately 1 cm long and weighed about 15 mg.

For irradiation, the samples were placed on a copper block in contact with a reservoir of liquid nitrogen and held in place by a thin polyester film. After cooling to 77° K, the sample was placed in a vacuum chamber attached to the beam line of the accelerator. Samples were exposed to graded doses of 4 MeV protons in the range of 20 to 60 kGy. The dose rate of 2.5 kGy/min was less than the value of 10 kGy/min recommended by Henriksen and Snipes (1970) to avoid sample heating. After irradiation, the samples were removed from the vacuum chamber and transferred to a precooled EPR tube. During this transfer, the sample lost contact with liquid-nitrogen cooled surfaces for less than one second as it fell through a funnel into the EPR tube. Several samples were exposed to γ-rays for comparison with published data (Gräslund et al., 1971) and the results of proton irradiation. In this case the sample could be sealed into an EPR tube before irradiation due to the penetrating power of the radiation.

The EPR spectra shown in figures 3A-3C were observed after 4 kGy of γ-rays, 56 kGy of protons incident perpendicular to the fiber orientation, and 48 kGy of protons parallel to the DNA chains, respectively. All three spectra are composed of a central line that we associate with primary radical anion and cation species with varying amounts of modulation in the wings resulting from TH· production. The greater amount of TH· observed with proton irradiation is not likely to be due to sample warming during the transfer from the proton beam line to the EPR spectrometer because the irradiated samples were kept in contact with liquid nitrogen cooled surfaces and the magnitude of the central line relative to the structure in the wings did not change as a function of proton dose. The greater proportion of TH· with proton irradiation may be due to the higher dose required to detect radicals since the total radical yield per unit of dose was more than an order of magnitude lower for protons than for γ-rays; however, the shape of the EPR spectrum did not change significantly with proton dose in the range investigated. The recommendation of Henriksen and Snipes (1970) regarding the dose rate was based on their experience with 6.5 MeV electrons which may not apply to proton irradiation; hence, the higher yield of TH· that we observed with protons may have resulted from sample heating due to a dose rate that was too large.

Unlike the results reported for neutrons (Arroyo et al., 1986), EPR spectra of radicals produced by direct proton irradiation of oriented DNA in parallel and perpendicular geometries were not significantly different. Figure 4 shows that, within experimental error, total radical yields were also independent of the orientation of DNA fibers relative to the proton flux. To obtain these results, differential EPR spectra were recorded digitally and

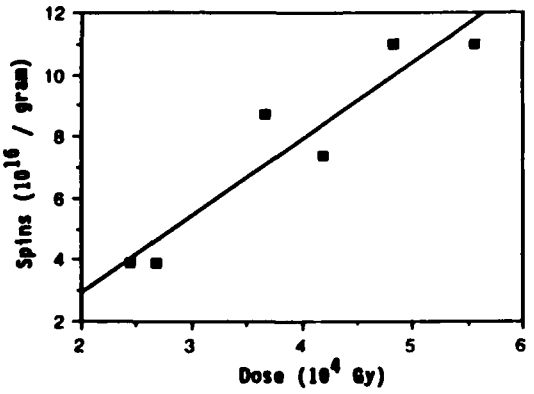

Figure 4. Total Radical Yields in Parallel (●) and Perpendicular (□) Proton Irradiation of Oriented DNA at 77° K.

double integrated to give the area under the absorption lines. This area was converted to number of spins by comparison with a standard sample of 2,2 diphenyl-1-picrylhydrazyl (DPPH) dissolved in paraffin.

CONCLUSIONS

We did not find any evidence for long-range energy or charge transfer in DNA from experiments in which oriented DNA was exposed to direct proton-beam irradiation. This may be due to the high doses and dose rates used in our experiments. The dose and dose rate could be reduced by redesigning the sample holder and transfer system to avoid the limitations on sample size imposed by the present system. Experiments with larger samples, higher proton energies for greater penetration, and improved EPR detection sensitivity might reveal orientation effects that are not present in our data due to sample heating or other processes that destroy free radicals at high exposure levels (Bernhard, 1981).

ACKNOWLEDGEMENTS

The authors gratefully acknowledge support for this work by the Office of Health and Environmental Research of the U.S. Department of Energy under contract DE-AC06-76RLO 1830, the Armed Forces Radiobiology Research Institute, and the Swedish Medical Science Research Council.

REFERENCES

Arroyo, C.M., A.J. Carmichael, C.E. Swenberg, and L.S. Myers, Jr., 1986, "Neutron-induced free radicals in oriented DNA." Int. J. Radiat. Biol. 50: 789-793.

Al-Kazwini, A.T., P. O'Neill, G.E. Adams, and E.M. Fielden, 1990, "Radiation-induced energy migration within solid DNA: The role of misonidazole as an electron trap." Radiat. Res. 121: 149-153.

Barendsen, G.W., 1964, "Impairment of the proliferative capacity of human cells in culture by α-particles with differing linear-energy transfer." Int. J. Radiat. Biol. 8: 453-466.

Baverstock, K.F. and R.B. Cundall, 1988, "Long range energy transfer in DNA." Radiat. Phys. Chem. 32: 553-556.

Bednár, J., 1985, "Electronic excitations in condensed biological matter." .Int. J. Radiat. Biol. 48: 147-166.

Bernhard, W.A., 1981, "Solid-state radiation chemistry of DNA: The bases." Adv. Radiat. Biol. 9: 199-280.

Bernhard, W.A., 1989, "Sites of electron trapping in DNA as determined by ESR of one-electron-reduced oligonucleotides." J. Phys. Chem. 93: 2187-2189.

Charlton, D.E., D.T. Goodhead, W.E. Wilson, and H.G. Paretzke, 1985, "The deposition of energy in small cylindrical targets by high LET radiations." Radiat. Prot. Dosim. 13: 123-125.

Doetsch, P.W. and R.P. Cunningham, 1990, "The enzymology of apurinic/apyrimidinic endonucleases." Mutat. Res. 236: 173-201.

Englander, S.W., N.R. Kallenbach, A.J. Heeger, J.A. Krumhansl, and S. Litwin, 1980, "Nature of the open state in long polynucleotide double helices: Possibility of soliton excitation." Proc. Natl. Acad. Sci. 77: 7222-7226.

Georghiou, S., S. Zhu, R. Weidner, C.-R. Huang and G. Ge, 1990, "Singlet-singlet energy transfer along the helix of a double-stranded nucleic acid at room temperature" J. Biomol. Struct. Dyn. 8: 657-674.

Goodhead, D.T., 1987, "Physical basis for biological effect." Nuclear and Atomic Data for Radiotherapy and Related Radiobiology (International Atomic Energy Agency, Vienna), pp. 37-53.

Gräslund, A., A. Ehrenberg, A. Rupprecht, and G. Ström, 1971, "Ionic base radicals in γ-irradiated DNA." Biochim. Biophys. Acta 254: 172-186.

Henriksen, T. and W. Snipes, 1970, "Radiation-induced radicals in thymine: ESR studies of single crystals." Radiat. Res. 42: 255-269.

Howard-Flanders, P., 1958, "Physical and chemical mechanisms in the injury of cells by ionizing radiation." Adv. Biol. Med. Phys. 6: 553-603.

Lea, D.E., 1947, "The induction of chromosome structural changes by radiation: detailed quantitative interpretation." British Journal of Radiology, Supplement 1: 75-83.

Miller, J.H., W.E. Wilson, C.E. Swenberg, L.S. Myers, Jr. and D.E. Charlton, 1988, "Stochastic model of free radical yields in oriented DNA exposed to densely ionizing radiation at 77K." Int. J. Radiat. Biol. 53: 901-907.

Miller, J.H. and C.E. Swenberg, 1990, "Free-radical yields in DNA exposed to ionizing radiation: Role of energy and charge transfer." Can. J. Phys. 68: 962-966.

Muto, V., J. Halding, P.L. Christiansen and A.C. Scott, 1988, "Solitons in DNA." J. Biomol. Struct. Dyn. 4: 873-894.

Roots, R. and S. Okada, 1975, "Estimation of life times and diffusion distances of radicals in x-ray-induced DNA strand breaks or killing of mammalian cells." Radiat. Res. 64: 306-320.

Rupprecht, A., 1966, "Preparation of oriented DNA by wet spinning." Acta Chem. Scand. 20: 494-504.

Takeno, S. and S. Homma, 1987, "Kinks and breathers associated with collective sugar puckering in DNA." Progress of Theoretical Physics 77: 548-562.

van Lith, D., J.M. Warman, M.P. de Haas, and A. Hummel, 1986, "Electron migration in hydrated DNA and collagen at low temperatures." J. Chem. Soc., Faraday Trans. 1 82: 2933-2943.

van Zandt, L.L., 1989, "DNA solitons with realistic parameter values." Phys. Rev. A 40: 6134-6137.

Wilson, W.E. and H.G. Paretzke, 1981, "Calculations of distribution of energy imparted and ionization by fast protons in nanometer sites." Radiat. Res. 87: 521-537.

Yomosa S., 1984, "Solitary excitations in deoxyribonucleic acid (DNA) double helices." Phys. Rev. A 30: 474-480.

Zhang, C.-T., 1987, "Soliton excitations in deoxyribonucleic acid (DNA) double helices." Phys. Rev. A 35: 886-891.

Effects of S-2-(3-Methylaminopropylamino)ethyl Phosphorothioic Acid (WR-3689), Alone or Combined with Caffeine, On Catecholamine Content of Mouse Hypothalamus (43603)

D. L. PALAZZOLO[1] AND K. S. KUMAR

Department of Radiation Biochemistry, Armed Forces Radiobiology Research Institute, Bethesda, Maryland 20889-5603

Abstract. **S-2-(3-Methylaminopropylamino)ethylphosphorothioic acid (WR-3689) is a radioprotective agent that is behaviorally toxic at radioprotective doses. It was recently reported that the combination of WR-3689 and caffeine ameliorated behavioral toxicity (determined by locomotor activity in mice) compared with WR-3689 alone. Since catecholamines can modulate locomotor activity, we determined norepinephrine (NE) and dopamine (DA) content (using high-performance liquid chromatography) in the hypothalamus of mice after treatment with WR-3689, caffeine, and the combination of the two drugs. CD2F1 male mice were injected intraperitoneally with saline (control), WR-3689 (100 and 200 mg/kg), caffeine (20 and 40 mg/kg), or the combination of WR-3689 (200 mg/kg) and caffeine (40 mg/kg). Control values for NE and DA ranged between 200 and 220 pg/mg and 69 and 94 pg/mg of hypothalamic tissue, respectively. WR-3689 had no effect on the content of NE and DA. In contrast, NE increased to (mean ± SE) 324 ± 27 pg/mg and 377 ± 61 pg/mg ($P < 0.05$) 4 hr after injections of 20 and 40 mg/kg of caffeine, respectively. Similarly, DA increased to 142 ± 13 pg/mg ($P < 0.05$) 4 hr after injection of 40 mg/kg of caffeine. The combination of WR-3689 and caffeine had no effect on NE and DA contents when compared with control values. These results suggest that WR-3689 can affect catecholamine metabolism in the mouse hypothalamus, but the mode of action is not clear.** [P.S.E.B.M. 1993, Vol 203]

Phosphorothioates are effective radioprotectors (1). When these drugs are administered to laboratory rodents, the $LD_{50/30}$ of γ-irradiation is increased considerably. When given in doses that are efficacious against radiation, these drugs are also behaviorally toxic. One such compound, *S*-2-(3-aminopropylamino)ethylphosphorothioic acid (WR-2721), is known to affect behavior in a number of species, including mice, rats, monkeys, and humans (2). When mice are treated with WR-2721, a significant decrement in locomotor activity is observed (3). WR-2721 impairs the ability of rats to maintain balance on an accelerod (4) and of monkeys to visually discriminate between tasks (5). In humans, common side effects of WR-2721 include nausea and vomiting, hypotension, hypocalcemia, and mild somnolence (6–8). Due to the nature of these toxic effects, there is reason to suspect that phosphorothioate-induced behavioral toxicity is derived from an imbalance in the central nervous system (CNS).

In clinical applications, the toxic side effects of phosphorothioates can be controlled. If these radioprotectants are to be used during space explorations, nuclear accidents, or when individuals must venture into radiologically hazardous environments, the toxic side effects of these drugs, particularly performance decrement, cannot be tolerated. If the side effects of phosphorothioates are eliminated without compromising radioprotection, these compounds could be used effec-

[1] To whom requests for reprints should be addressed at Radiation Biochemistry Department, Armed Forces Radiobiology Research Institute, 8901 Wisconsin Avenue Bethesda, MD 20889-5603.

Received October 26, 1992. [P.S.E.B.M. 1993, Vol 203]
Accepted March 4, 1993.

0037-9727/93/2033-0304$3.00/0

tively against the damaging effects of radiation in these scenarios (9).

Several analogs of WR-2721 have been synthesized and tested for radioprotection (10). Among these analogs, *S*-2-(3-methylaminopropylamino)ethylphosphorothioic acid (WR-3689), a methylated derivative of WR-2721, proved to be less toxic and clearly superior in some respects than WR-2721 (11). Studies reported in this paper were done using WR-3689.

In a recent study (12), the methylxanthine caffeine was administered to mice in combination with WR-3689 in an attempt to reduce its behavioral toxicity. The study indicated that the combination of WR-3689 and caffeine abolishes the decrement in locomotor activity normally observed in mice when WR-3689 is given alone. In addition, caffeine does not appear to alter the radioprotective efficacy of WR-3689 (13). Although the locomotor activity test is a better indicator of the tendency to perform, rather than the capacity to perform, it is still possible that the locomotor decrement produced by WR-3689 is a result of adverse alterations in the metabolism of neurotransmitters in the CNS. The catecholamines, in particular norepinephrine (NE) and dopamine (DA), are important neurotransmitters involved in the modulation of locomotor activity (14). Investigating the effects of phosphorothioates on catecholamines in the brain may provide a neurochemical basis for the phosphorothioate-induced decrement in locomotor activity.

The methylxanthines are potent stimulators of the CNS (15) and are known to affect catecholaminergic activity, but the mechanisms behind these effects are controversial and complicated. In the past, investigators have reported no changes (16–21), increases (17, 22, 23), and decreases (16) in absolute catecholamine levels in the brain after treatment with caffeine. Catecholamine turnover studies reveal similar ambiguities. There are reports indicating no changes (21), increases (17, 24–26), and decreases (17) in turnover in the brain.

The aim of the present study was to determine the effects of phosphorothioates and methylxanthines on the catecholaminergic system within the CNS. The content of NE and DA was assayed in mouse hypothalamus after treatment with WR-3689, caffeine, and the combination of the two drugs. The results of this study will help elucidate mechanisms involved in WR-3689- and/or caffeine-induced alterations of catecholamine metabolism as well as mechanisms involved in WR-3689-induced behavioral toxicity.

Materials and Methods

Animals. Male CD2F1 mice, 8–10 weeks old, were purchased from Charles River Laboratories (Boston, MA) and were housed five per cage in an air-conditioned (21 ± 1°C and 50 ± 10% relative humidity), light-controlled (lights on from 0600 to 1800 hr) American Association for Accreditation of Laboratory Animal Care-accredited facility. The mice were provided with food and water *ad libitum* and were maintained for at least 2 weeks before use in the experiments.

Drugs. WR-3689 was obtained from the Drug Synthesis and Chemistry Branch, Division of Cancer Treatment, National Cancer Institute (Bethesda, MD) and anhydrous caffeine was obtained from Sigma Chemical Co. (St. Louis, MO).

Experimental Procedure. On the eve of experimentation, six groups of mice (five mice/group) were transferred to a nearby room to acclimatize them to new surroundings. At 0830 hr the following morning, intraperitoneal injections of neutralized saline (control; Group 1), WR-3689 (100 and 200 mg/kg; Groups 2 and 3), caffeine (20 and 40 mg/kg; Groups 4 and 5), and the combination of WR-3689 (200 mg/kg) and caffeine (40 mg/kg) (Group 6) were administered. One mouse from each group was sacrificed by quick cervical dislocation at the time of injection and the other four mice from each group were sacrificed at 1, 2, 4, and 8 hr after injection. Immediately after sacrifice, the hypothalamus was removed, weighed, and placed in 200 μl of 0.05 *M* $HClO_4$. The tissue was then sonicated (30 sec) and centrifuged in an Eppendorf microcentrifuge (3 min). The supernatant was stored at −80°C until the time of catecholamine analysis. The experiment was repeated eight times ($n = 8$ for each time point within each treatment group).

Analysis. Catecholamine concentrations were determined using high-performance liquid chromatography with electrochemical detection (Bioanalytical Systems, West Lafayette, IN) (27, 28). The high-performance liquid chromatography system incorporated an LC-4B electrochemical detector; a 10-cm, phase II, 3-μm octadecasilane reversed-phase column; and a glassy carbon working electrode. The mobile phase (pH 3.1) was made with degassed pyrogen-free water filtered through a Milli-Q purification system (Milipore Co., Bedford, MA) and included monochloroacetic acid (14.15 g/liter), sodium hydroxide (4.675 g/liter), disodium EDTA (150 mg/liter), octanesulfonic acid (300 mg/liter) as the ion-pairing agent, and 3.5% acetonitrile. The mobile phase was pumped through the system by a Beckman (Fullerton, CA) 112 solvent delivery module at a flow rate of 1.7 ml/min. The sensitivity of the detector was 2 nA full scale. The potential of the working electrode was 0.80 V with respect to a Ag/AgCl reference electrode. Standard and sample injections were made by a Rheodyne (Cotati, CA) 7125 syringe-loading injection valve. Standards for the catecholamine assays contained 600 pg of NE, DA, and isoproterenol per 50 μl of 0.05 *M* $HClO_4$. Isoproterenol served as the internal standard. Samples for the catecholamine assay contained 20 μl of homogenate and 30 μl of 0.05 *M* $HClO_4$ containing 600 pg of isoproter-

enol. Injection volume was 25 μl for both standards and samples.

Statistics. Data were collected with the use of a Shimadzu CR-4A Chromatopac (Columbia, MD). Mean values (±SE) are expressed as pg/mg wet wt of hypothalamic tissue. Comparisons between treatment groups at each time point were made using Student's t test, where $P < 0.05$ indicates statistical significance.

Results

Effects of WR-3689 and Caffeine Administered Individually on Hypothalamic Catecholamine Content. The effects of WR-3689 on the hypothalamic content of NE and DA are shown in Figure 1. Control values of NE and DA ranged between 200 and 220 pg/mg and 69 and 94 pg/mg of hypothalamic tissue, respectively. Administration of WR-3689 (100 and 200 mg/kg) had no effect on the content of NE or DA (Fig. 1). Figure 2 shows the effects of caffeine on the hypothalamic contents of NE and DA. NE content (Fig. 2) significantly increased ($P < 0.05$) above control values at 2 and 4 hr after administration of 20 mg/kg of caffeine and at all time points after administration of 40 mg/kg caffeine. The highest NE concentrations occurred 4 hr after caffeine treatment and were 324 ± 27 and 377 ± 61 pg/mg after the 20 mg/kg and 40 mg/kg injections, respectively. Compared with control values, DA (Fig. 2) was unaffected after treatment with 20 mg/kg of caffeine, but was significantly increased ($P < 0.05$) at 1 and 2 hr after administration of 40 mg/kg of caffeine. The highest DA concentration, 142 ± 14 pg/mg, occurred 2 hr after the 40-mg/kg injection of caffeine.

Effects of WR-3689 and Caffeine Administered Simultaneously on Hypothalamic Catecholamine Content. In Figure 3, the contents of NE and DA in the hypothalamus of mice treated with the combination of WR-3689 and caffeine are compared with the individual treatments of WR-3689 (200 mg/kg) and caffeine (40 mg/kg) alone. Catecholamine levels in the combined treatment group (200 mg/kg of WR-3689 and 40 mg/kg of caffeine) were not significantly different from the levels in the control group (data not shown), indicating that WR-3689 attenuates the caffeine-induced increase in catecholamines in mouse hypothalamus. NE and DA contents in the caffeine-treated group were significantly higher ($P < 0.05$) than in the WR-3689 treatment group at 2, 4, and 8 hr after

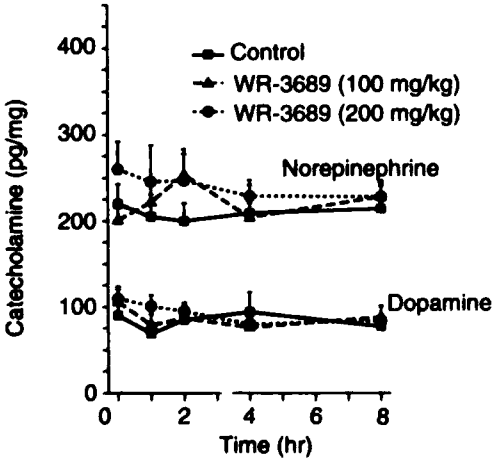

Figure 1. Effects of WR-3689 (100 and 200 mg/kg) on NE and DA content in the mouse hypothalamus. Control values are represented by the solid lines while 100-mg/kg and 200-mg/kg WR-3689-treated mice are represented by dotted and dashed lines, respectively.

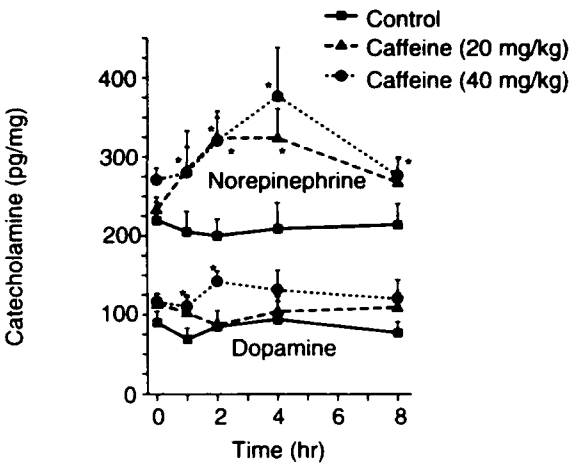

Figure 2. Effects of caffeine (20 and 40 mg/kg) on NE and DA content in the mouse hypothalamus. Control values are represented by the solid lines while 20-mg/kg and 40-mg/kg caffeine-treated mice are represented by dotted and dashed lines, respectively. *Significance ($P < 0.05$) between the control and caffeine treatment groups.

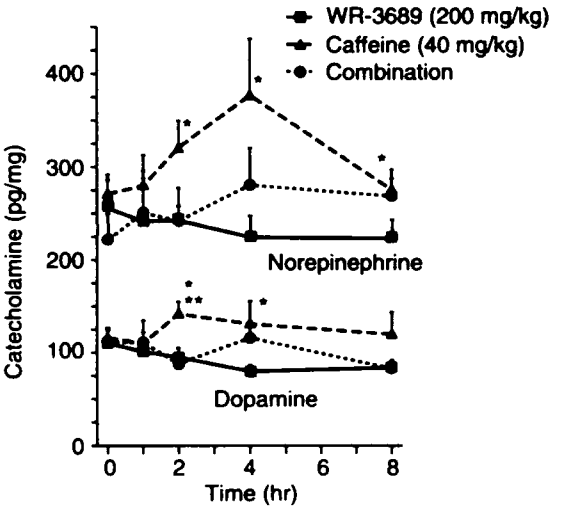

Figure 3. Effects of WR-3689 (200 mg/kg), caffeine (40 mg/kg), and the combination of the two agents at doses of 200 mg/kg and 40 mg/kg, respectively, on NE and DA content in the mouse hypothalamus. The WR-3689 treatment is represented by the solid line, the caffeine treatment is represented by the dotted line, and the combined treatment is represented by the dashed line. *Significance ($P < 0.05$) between the caffeine and WR-3689 treatment groups. **Significance ($P < 0.05$) between the caffeine and combined treatment group.

drug administration (Fig. 3). DA content in the caffeine-treated group was also significantly higher ($P < 0.05$) than in the combined treatment group 2 hr after drug administration. Although NE and DA contents in the combined treatment group were higher than the WR-3689-treated group and lower than the caffeine-treated group at 4 hr after injections, these differences were not statistically significant.

Discussion

The results of this study indicate that WR-3689 has no apparent effect on the hypothalamic content of NE and DA. This is consistent with prevailing thought that WR compounds do not readily cross the blood-brain barrier (BBB) (29, 30). Biodistribution studies indicate that only 0.1–0.2% of the total ^{35}S-radiolabeled WR-2721 (29) and WR-3689 (30) is accumulated in the brain 15–30 min after systemic injections. Since there were no differences in catecholamines between the controls and WR-3689-treated mice, it would seem that the small amount of WR-3689 taken up by the brain may not be sufficient to cause derangements in neuroendocrine processes. Alternatively, it is possible that WR-3689 could act centrally to affect synthesis and release of catecholamines in such a way that steady state levels of catecholamines remain unaltered. Dobric *et al.* (31) showed that WR-2721 (300 mg/kg, ip) antagonizes the effects of 9-gray γ-irradiation on the brain content of NE, DA, and serotonin. Deanovic *et al.* (32) reported a 40–60% decrease in the release of acetylcholine from the somatosensory cortex 15 min after systemic administration of WR-2721 (200 mg/kg). In addition, we found that simultaneous administration of WR-3689 and caffeine was effective in attenuating the increase in hypothalamic NE and DA content produced by administration of caffeine alone. These studies suggest that WR-3689 can alter neurotransmitter metabolism in the brain, but the mode of action remains to be established.

One explanation for phosphorothioate-induced alterations in catecholamine metabolism is that these agents could produce a general hypoxia (33, 34). If phosphorothioates indeed reduce oxygen tension, the resultant hypoxia could ultimately carry over into the brain. Once the brain becomes hypoxic, neurotransmitter metabolism can be altered (35–37). Another possibility accounting for the phosphorothioate-induced alterations in catecholamine metabolism is the inhibition of dopamine β-hydroxylase (38, 39) by sulfhydryl compounds such as glutathione and cysteamine. In a recent study investigating catecholamine metabolism in the mouse adrenal, we found an accumulation in the content of DA and a depletion in the content of NE and epinephrine 2–4 hr after administration of WR-3689 (40). These results indicate that WR-3689 inhibits dopamine β-hydroxylase. Vujnov *et al.* (41) reported similar decreases in NE in the adrenals and sera of rats 3 hr after WR-2721 administration. Interestingly, once the phosphate group is cleaved from the phosphorothioate, the aminothiol compound resembles cysteamine. In fact, it has been proposed that a small fraction of the administered phosphorothioate can be metabolized to cysteamine by various polyamine, diamine, or monoamine oxidases (42). Unlike phosphorothioates, cysteamine has no problem crossing the BBB (39) and is known to have a number of neuroendocrine effects (43, 44).

The increase in the hypothalamic content of NE and DA by caffeine was dose dependent. Govani *et al.* (22) found similar dose-dependent increases in the content of DA in the rat striatum and nucleus accumbens after administration of 10, 20, 40, and 100 mg/kg of caffeine. However, in the nucleus accumbens, the increase in DA content after injection of 100 mg/kg of caffeine was slightly less than the increase produced by 40 mg/kg, indicating a biphasic effect. Minana and Grisolia (23) administered caffeine to rats by way of the drinking water. At the end of their experiment, NE content in the hypothalamus and in the striatum was more than 300% above control levels, while the DA content was more than 100% above control levels. Corrodi *et al.* (17) found that 50 mg/kg of caffeine administered intraperitoneally slightly increased NE and DA stores in the whole brain of rats. In contrast, these authors reported a slight decrease in the content of NE and DA when 100 mg/kg of caffeine were injected. These results again indicate a biphasic nature of caffeine with the lower doses of caffeine increasing and the higher doses decreasing catecholamine content in the brain. In addition, a relationship between biphasic catecholamine levels and locomotor activity was established by Waldeck (18), who showed that lower doses of caffeine produce dose-dependent increases in locomotor activity, but the higher doses produce no effect or, in some instances, produce hypomotility.

In contrast, a number of studies investigating the effects of caffeine on the content of brain catecholamines report decreases (17) or no changes (16–21). Reasons for these discrepancies include the biphasic nature of caffeine, the time of tissue sampling after caffeine administration, and the use of whole brain preparations rather than discrete brain areas. In some studies, female rats were used without considering the stages of the estrous cycle. This is an important consideration since changes in the reproductive status of female rats are known to affect catecholamine activity (45).

Caffeine can alter catecholamine metabolism in the CNS by at least three modes of action (15). The first is associated with the translocation of calcium. Calcium is an essential ingredient of the secretion-coupling mechanism for the release of catecholamines

as well as other neurotransmitters and neuromodulators (46–48). Caffeine increases mobilization of calcium into the cell, resulting in increased catecholamine release. The second mode of action involves the accumulation of cAMP. The accumulation of cAMP is mediated by caffeine's ability to inhibit cyclic nucleotide phosphodiesterase. In turn, cAMP could increase catecholamine metabolism by stimulating tyrosine hydroxylase (49), the rate-limiting enzyme in catecholamine synthesis. The third mode of action involves blocking receptors for adenosine. Catecholamine release in the CNS can be mediated by specific adenosine receptors (50). Blocking adenosine receptors with caffeine leads to reduced catecholamine release. All three of these modes of action indicate that caffeine stimulates catecholamine metabolism, and this stimulation is in agreement with the results of the present study.

The attenuation of the caffeine-induced catecholamine content when caffeine was administered simultaneously with WR-3689 is intriguing, particularly when WR-3689 *per se* had no effect on the catecholamine levels. It is possible that caffeine alters the BBB via changes in calcium metabolism, permitting WR-3689 to enter the brain and thereby attenuating catecholamine levels. Another possibility is that WR-3689 enters the brain where the BBB is weak or absent. Two such areas are the organum vasculosum of the lamina terminalis, a circumventricular organ located at the tip of the third ventricle, and the area postrema, located immediately rostral to the obex on each side of the fourth ventricle (51). Furthermore, it is known that these two areas of the brain are involved in the regulation of body temperature (52) and in the control of the emetic response (53). It is also known that phosphorothioates alter body temperature (54) and trigger emesis (8).

If WR-3689 enters the brain, it can then interact with caffeine to attenuate catecholamine levels in a number of ways. (i) Phosphorothioates are known to cause a decrease in cytosolic calcium intrusion (55); thus, WR-3689 could reverse caffeine-induced intracellular mobilization of calcium that in turn affects catecholamine release. (ii) Tyrosine hydroxylase, the rate-limiting enzyme in catecholamine synthesis, is dependent upon molecular oxygen. Caffeine can stimulate tyrosine hydroxylase activity, presumably through the action of cAMP (49). If WR-3689 causes hypoxia (33, 34), it could limit the availability of oxygen for this rate-limiting step and hence catecholamine synthesis. (iii) Since phosphorothioates inhibit cAMP formation (56), it is possible that WR-3689 antagonizes the caffeine-induced accumulation of cAMP and, consequently, catecholamine levels. (iv) Caffeine can also stimulate dopamine β-hydroxylase in the hypothalamus (23). This stimulation could then offset the inhibiting effect sulfhydryls have on dopamine β-hydroxylase. (v) Caffeine is known to stimulate alkaline phosphatase (57, 58) that in turn can accelerate the formation of sulfhydryl from phosphorothioates. Although alkaline phosphatase is not detectable in brain, formation of the sulfhydryl from WR-3689 in peripheral blood could facilitate its entry into the brain. These observations could explain why WR-3689, when administered in combination with caffeine, attenuates the increase in hypothalamic catecholamines produced when caffeine is given alone.

The results of this study indicate that WR-3689 attenuates the caffeine-induced increase in hypothalamic concentrations of NE and DA, suggesting that WR-3689 affects catecholamine metabolism in the CNS. WR-3689, *per se*, has no effect on the hypothalamic stores of NE and DA, whereas caffeine alone increases the hypothalamic content of NE and DA in a dose-dependent manner. From these results, it is tempting to speculate that WR-3689-induced alterations in catecholamine metabolism are at least partially responsible for the WR-3689-induced behavioral toxicity.

This work was supported by the Armed Forces Radiobiology Research Institute, Defense Nuclear Agency, under Work Unit 00162. Research was conducted according to the *Guide for the Care and Use of Laboratory Animals* prepared by the Institute of Laboratory Animal Resources, National Research Council. We are greatful to W. A. McLean for technical assistance and to Modeste Greenville for editorial assistance.

1. Giambarresi L, Jacobs AJ. Radioprotectants. In: Conklin JJ, Walker RI, Eds. Military Radiobiology. New York: Academic Press, pp265–301, 1987.
2. Bogo V. Behavioral radioprotection. In: Weiss JF, Simic MG, Eds. Perspectives in Radioprotection. New York: Pergamon Press, pp73–78, 1988.
3. Landauer MR, Davis HD, Dominitz JA, Weiss JF. Comparative behavioral toxicity of four sulfhydryl radioprotective compounds in mice: WR-2721, cysteamine, diethyldithiocarbamate, and n-acetylcysteine. In: Weiss JF, Simic MG, Eds. Perspectives in Radioprotection. New York: Pergamon Press, pp97–100, 1988.
4. Bogo V, Jacobs AJ, Weiss JF. Behavioral toxicity and efficacy of WR-2721 as a radioprotectant. Radiat Res **104**:182–190, 1985.
5. Bogo V, Franz CG, Jacobs AJ, Weiss JF, Young RW. Effects of ethiofos (WR-2721) and radiation on monkey visual discrimination performance. In: Weiss JF, Simic MG, Eds. Perspectives in Radioprotection. New York: Pergamon Press, pp93–95, 1988.
6. Glover D, Fox KR, Weiler C, Kligerman MM, Turrisi A, Glick JH. Clinical trials of WR-2721 prior to alkylating agent chemotherapy and radiotherapy. In: Weiss JF, Simic MG, Eds. Perspectives in Radioprotection. New York: Pergamon Press, pp3–7, 1988.
7. Glover D, Riley L, Carmichael K, Spar B, Glick J, Kligerman MM, Agus ZS, Slatopolsky E, Attie M, Goldfarb S. Hypocalcemia and inhibition of parathyroid hormone secretion after administration of WR-2721 (a radioprotective and chemoprotective agent). N Engl J Med **309**:1137–1141, 1987.
8. Kligerman MM, Glover DJ, Andrew TT, Norfleet AL, Yuhas JM, Coia LR, Simone C, Glick JH, Goodman RL. Toxicity of WR-2721 administered in single and multiple doses. Int J Radiat Oncol Biol Phys **10**:1773–1776, 1984.

9. Walker RI. Requirements of radioprotectors for military and emergency needs. In: Weiss JF, Simic MG, Eds. Perspectives in Radioprotection. New York: Pergamon Press, pp13–20, 1988.
10. Sweeney TR. A Survey of Compounds from the Antiradiation Drug Development Program of the U.S. Army Medical Research and Development Command. Washington, DC: Walter Reed Army Institute of Research, 1979.
11. Brown DQ, Grahm WJ, MacKenzie LJ, Pittock JW, Shaw LM. Can WR-3689 be improved upon? In Weiss JF, Simic MG, Eds. Perspectives in Radioprotection. New York: Pergamon Press, pp157–168, 1988.
12. Landauer MR, Davis HD, Kumar KS, Weiss JF. Behavioral toxicity of selected radioprotectors. Adv Space Res **12**:273–283, 1992.
13. Kumar KS, Weiss JF, McLean WA, Kendrick JM, Landaur MR. Radioprotection by combinations of WR-3689 and caffeine. Abstracts of Papers for the Thirty-Eighth Annual Meeting of the Radiation Research Society, p193, 1990.
14. Lloyd KG, Homyliewicz O. Catecholamines in regulation of motor function. In: Friedhoff AJ, Ed. Catecholamines and Behavior. New York: Plenum Press, Vol **1**: pp41–57, 1975.
15. Rall TW. Central nervous system stimulants (continued), the methylxanthines. In: Gilman AG, Goodman LS, Rall TW, Murad F, Eds. The Pharmacological Basis of Therapeutics (7th ed). New York: Macmillan Publishing, pp589–603, 1985.
16. Berkowitz BA, Tarver JH, Spector S. Release of norepinephrine in the central nervous system by theophylline and caffeine. Eur J Pharmacol **10**:64–71, 1970.
17. Corrodi H, Fuxe K, Jonsson G. Effects of caffeine on central monoamine neurons. J Pharm Pharmacol **24**:155–158, 1972.
18. Waldeck B. Ethanol and caffeine: A complex interaction with respect to locomotor activity and central catecholamines. Psychopharmacologia **36**:209–220, 1974.
19. Waldeck B. On the interaction between caffeine and barbiturates with respect to locomotor activity and brain catecholamines. Acta Pharmacol Toxicol **36**:172–180, 1975.
20. Schlosberg AJ, Fernstrom JD, Kopczynski MC, Cusack BM, Gillis MA. Acute effects of caffeine on neutral amino acids and brain monoamine levels in rats. Life Sci **29**:173–183, 1981.
21. Zielke HR, Zielke CL. Lack of sustained effect on catecholamines or indoles in mouse brain after long term subcutaneous administration of caffeine and theophylline. Life Sci **39**:565–572, 1986.
22. Govani S, Petkov VV, Montefusco O, Missale C, Battaini F, Spano PF, Trabucchi M. Differential effects of caffeine on dihydroxyphenylacetic acid concentrations in various rat brain dopaminergic structures. J Pharm Pharmacol **36**:458–460, 1983.
23. Minana MD, Grisolia S. Caffeine ingestion by rats increases noradrenaline turnover and results in self-biting. J Neurochem **47**:728–732, 1986.
24. Waldeck B. Some effects of caffeine and aminophylline on the turnover of catecholamines in the brain. J Pharm Pharmacol **23**:824–830, 1971.
25. Karaswa T, Furukawa K, Yoshida K, Shimizu M. Effect of theophylline on monoamine metabolism in the rat brain. Eur J Pharmacol **37**:97–104, 1976.
26. Galloway MP, Roth RH. Neuropharmacology of 3-isobutylmethylxanthine: Effects on central noradrenergic systems *in vivo*. J Pharmacol Exp Ther **227**:1–8, 1983.
27. Palazzolo DL, Quadri SK. Reduced variation in retention times of biogenic amines by temperature control in liquid chromatography with electrochemical detection. J Chromatogr **479**:216–219, 1989.
28. Palazzolo DL, Quadri SK. Optimal conditions for long term storage of biogenic amines for subsequent analysis by column chromatography with electrochemical detection. J Chromatogr **518**:258–263, 1990.
29. Rasey JS, Nelson NJ, Mahler P, Anderson K, Krohn KA, Menard T. Radioprotection of normal tissue against gamma rays and cyclotron neutrons with WR-2721: LD_{50} studies and ^{35}S-WR-2721 biodistribution. Radiat Res **97**:598–607, 1984.
30. Rasey JS, Krohn KA, Grunbaum Z, Spence AM, Menard TW, Wade RA. Synthesis, biodistribution, and autoradiography or radiolabeled S-2-(3-methylaminopropylamino)ethylphosphorothioic acid (WR-3689). Radiat Res **106**:366–379, 1986.
31. Dobric S, Milovanovic SR, Tanasijevic D. The effects of gamma-irradiation on the activity of the isolated perfused heart, isolated uterus, and on the amount of monoamines in the brain of the rats pretreated by WR-2721. In: Proceedings of the 30th Anniversary Symposium of Radiation Protection in the Boris Kidric Institute of Nuclear Sciences, Belgrade, pp244–249, 1989.
32. Deanovic ZBM, Isgum V, Geber J. Average evoked potentials and acetylcholine release in the somatosensory cortex of the cat treated with WR-2721. In: Proceedings of the 30th Anniversary Symposium of Radiation Protection in the Boris Kidric Institute of Nuclear Sciences, Belgrade, pp137–144, 1989.
33. Purdie JW, Inhaber ER, Schneider H, Labelle JL. Interaction of cultured mammalian cells with WR-2721 and its thiol, WR-1065: Implications for mechanisms of radioprotection. Int J Radiat Biol **43**:517–527, 1983.
34. Allalunis-Turner MJ, Walden TL, Sawich C. Induction of marrow hypoxia by radioprotective agents. Radiat Res **118**:581–586, 1989.
35. Gibson GE, Pulsinelli W, Blass JP, Duffy TE. Brain dysfunction in mild to moderate hypoxia. Am J Med **70**:1247–1254, 1981.
36. Gordon K, Statman D, Johnston MV, Robinson TE, Becker JB, Silverstein FS. Transient hypoxia alters striatal catecholamine metabolism in immature brain: An *in vivo* microdialysis study. J Neurochem **54**:605–611, 1990.
37. Pastuszko A, Wilson DF, Erecinska M. Neurotransmitter metabolism in rat brain synaptosomes: Effect of anoxia and pH. J Neurochem **38**:1657–1667, 1982.
38. Nagatsu T. Biochemistry of Catecholamines. Baltimore: University Park Press, pp71–73, 1973.
39. Terry LC, Craig R. Cysteamine effects on monoamines, dopamine-β-hydroxylase and the hypothalamic-pituitary axis. Neuroendocrinology **41**:467–475, 1985.
40. Palazzolo DL, McLean WA, Kumar KS. Effects of S-2(3-methylaminopropylamino)ethylphosphorothioic acid (WR-3689) on the content of catecholamines in the mouse adrenals. Proc Soc Neurosci (Abstracts) **18**:1376, 1992.
41. Vujnov S, Simovic M, Cvetkovic M, Savic J. Effects of gammaphos and labetol on adrenaline level in the adrenals, plasma, and urine of rats subjected to irradiation injury. Iugosl Physiol Pharmacol Acta **26**:411–418, 1990.
42. Weiss JF, Kumar KS. Antioxidant mechanisms in radiation injury and radioprotection. In: Chow CK, Ed. Cellular Antioxidant Defense Mechanisms. Boca Raton, FL: CRC Press, Vol **II**: pp163–189, 1988.
43. Cook LL, Bissette G, Dole K, Nemeroff CB. A critical evaluation of cysteamine as a tool to deplete somatostatin in the rat central nervous system. Endocrinology **124**:855–861, 1989.
44. Sagar SM, Millard WJ, Martin JB, Murchison SC. The mechanism of action of cysteamine in depleting prolactin immunoreactivity. Endocrinology **117**:591–600, 1985.
45. Wise PM. Changes in hypothalamic catecholamines associated with aging and reproductive functions. In: Ben-Jonathan N, Bahr JM, Weiner RI, Eds. Catecholamines as Hormone Regulators. New York: Raven Press, pp51–62, 1985.
46. Douglas WW, Poisner AM. Stimulus-secretion coupling in a neurosecretory organ: The role of calcium in the release of vasopressin from the neurohypophysis. J Physiol **172**:1–18, 1964.
47. Foreman MM, Porter JC. Prolactin augmentation of dopamine and norepinephrine release from superfused medial basal hypothalamic fragments. Endocrinology **108**:800–804, 1981.

48. Hartter DE, Ramirez VD. The effects of ions, metabolic inhibitors, and colchicine on luteinizing hormone-releasing hormone release from superfused rat hypothalami. Endocrinology **107**:375–382, 1980.
49. Porter JC, Aguila-Mansilla N, Ramin SM, Kozlowski GP, Kedzierski W. Tyrosine hydroxylase expression in hypothalamic cells: Analysis of the roles of adenosine 3′,5′-monophosphate- and Ca^{2+}/calmodulin-dependent protein kinases in the action of pituitary cytotropic factor. Endocrinology **129**:2477–2485, 1991.
50. Ebstein RP, Daly JW. Release of norepinephrine and dopamine from brain vesicular preparations: Effects of adenosine analogues. Cell Mol Neurobiol **2**:193–204, 1982.
51. Carpenter MB, Sutin J. Human Neuroanatomy (8th ed). Baltimore: Williams & Wilkins, 1983.
52. Gale CC. Neuroendocrine aspects of thermoregulation. Annu Rev Physiol **35**:391–430, 1973.
53. Carpenter DO. Neural mechanisms of emesis. Can J Physiol Pharmacol **68**:230–236, 1990.
54. Kandasamy SB, Kumar KS, Hunt WA, Weiss JF. Opposite effects of WR-2721 and WR-1065 on radiation-induced hypothermia: Possible correlation with oxygen uptake. Radiat Res **114**:240–247, 1988.
55. Polla BS, Donati Y, Kondo M, Tochon-Danguy HJ, Bonjour JP. Protection from cellular oxidative injury and calcium intrusion by N-(2-mercaptoethyl)-1,3-propanediamine, WR-1065. Biochem Pharmacol **40**:1469–1475, 1990.
56. Weaver ME, Morrissey J, McConkey C, Goldfarb S, Slatopolsky E, Martin K. WR-2721 inhibits parathyroid adenylate cyclase. Am J Physiol **252**:E197–E201, 1987.
57. Nakamoto T, Joseph F Jr, Yazdani M, Hartman AD. Effects of different levels of caffeine supplemented to the maternal diet on the brains of newborn rats and their dams. Toxicol Lett **44**:167–185, 1988.
58. Nakamoto T, Joseph F Jr. Interaction between caffeine and zinc on brain in newborn rats. Biol Neonate **60**:118–126, 1991.

INT. J. RADIAT. BIOL., 1993, VOL. 63, NO. 6, 693-701

Membranes as sensitive targets in thymocyte apoptosis

N. RAMAKRISHNAN*†, D. E. McCLAIN‡ and G. N. CATRAVAS†

(Received 4 November 1992; revision received 8 February 1993; accepted 11 February 1993)

Abstract. The role of cellular membranes in thymocyte apoptosis has been examined. Trolox, a water soluble analogue of vitamin E and inhibitor of membrane damage, inhibits DNA fragmentation in thymocytes exposed to γ-radiation. Trolox is most effective in inhibiting DNA fragmentation when added to cells within 30 min post-irradiation. Exposure to trolox only during irradiation did not prevent DNA fragmentation, suggesting that it does not work by scavenging free radicals generated during radiation exposure. Incubation of the irradiated cell suspension with trolox for 2 h post-irradiation was sufficient to prevent DNA fragmentation measured at 24 h in irradiated cells. This suggests that trolox irreversibly inhibits a cellular lesion required for apoptosis. The induction of DNA fragmentation appears to be related to a concurrent, pronounced flow of Ca^{2+} into the cell. At 3 h post-irradiation the amount of Ca^{2+} in irradiated thymocytes was more than twice that of unirradiated thymocytes. Membrane damage has been shown to affect the transport of Ca^{2+}. Trolox treatment completely blocked the radiation-induced influx of Ca^{2+} into the thymocytes. These results suggest that membrane damage is a critical lesion that is involved in DNA fragmentation in thymocyte apoptosis.

1. Introduction

Thymocytes are among the most radiation sensitive cells in the body. At clinically relevant doses of radiation they die by a process termed interphase death or apoptosis (Maruyama and Feola 1987, Sellins and Cohen 1987). Apoptosis can also be induced by other physical agents, including hyperthermia (Sellins and Cohen 1991, Harmon *et al.* 1991), UV irradiation (Martin and Cotter 1991, Servoma and Rytoma 1990), and the photodynamic action of phthalocyanines (Agarwal *et al.* 1991). Agents such as cytotoxic T-cells (Martz and Howell 1989), antibodies against CD3 (Smith *et al.* 1989) and other molecules of the cell membrane (Trauth *et al.* 1989), or glucocorticoids (Wyllie 1980) induce apoptosis in target cells by receptor-mediated processes. Apoptosis is distinguishable from the more common necrotic death, which is characterized by a generalized breakdown of cellular structure and function. Apoptotic death is, on the other hand, a physiological response to stimuli that has also been called cellular suicide or programmed cell death (Kerr *et al.* 1972).

Even though several morphological and biochemical changes have been described in apoptosis, it is not clear which biological systems or molecules participate in the process, or how their damage results in cell death. The most characteristic biochemical event during apoptosis is fragmentation of nuclear DNA into oligonucleosomal subunits that precedes cell death (Ramakrishnan and Catravas 1992a, Cohen and Duke 1984, Smith *et al.* 1989, Bellomo *et al.* 1992). The fragmentation of nuclear DNA during apoptosis appears to be due to activation of a Ca^{2+}-dependent nuclear endonuclease that is constitutively present in an inactive form in thymocyte nuclei (Nikonova *et al.* 1982, Cohen and Duke 1984, Kaminskas and Li 1989, Ramakrishan and Catravas 1992a). The process by which this enzyme becomes activated is unknown, though there is an increase in intracellular Ca^{2+} concentration during apoptosis (McConkey *et al.* 1988, 1989a, 1990, Story *et al.* 1992). The integrity of the plasma membrane plays an important role in maintaining the Ca^{2+} homeostasis in the cell (Lucy 1972, Pascoe and Reed 1989).

An essential role for the lymphocyte plasma membrane in the development of apoptosis has been proposed (Konings 1981, Ashwell *et al.* 1986, Sungurov and Sharlaeva 1988). In irradiated thymocytes the onset of nuclear DNA fragmentation is preceded by changes in the structure and function of cellular membranes (Zherbin and Chukhlovin 1984, Yamada *et al.* 1969, Chandra and Stefani 1981, Sungurov and Sharlaeva 1988). The permeability of the plasma membrane and cell volume increases following γ-irradiation of lymphocytes, which may be mediated by an oxygen-dependent free-radical chain reaction (Ashwell *et al.* 1986). Lymphocyte survival following γ-irradiation is inversely dose-rate dependent, and may be due to radiation-induced damage to the plasma membrane of the cell (Kon-

*Author for correspondence.
†Office of Chair of Science, ‡Radiation Biochemistry Department, Armed Forces Radiobiology Research Institute, 8901 Wisconsin Avenue, Bethesda, MD 20889-5603, USA.

ings 1981). The expression of surface IgG on B cells is highly radiosensitive and involves activation of protein kinase C (Ojeda *et al.* 1991). Recently, it has been reported that protein kinase C is activated during apoptosis induced by γ-irradiation (Ojeda *et al.* 1992) and glucocorticoids (Ojeda *et al.* 1990). This activation of protein kinase C may be related to increases in diacylglycerol, one of the earliest signal-induced breakdown products of membrane-bound inositol phospholipid.

In this study we used trolox to investigate the involvement of membranes in DNA fragmentation in thymocytes exposed to γ-radiation. Trolox is a water-soluble analogue of vitamin E that penetrates biomembranes rapidly (Doba *et al.* 1985, Castle and Perkins 1986). It is a powerful inhibitor of membrane damage and protects mammalian cells from oxidative damage both *in vivo* (Casini *et al.* 1985, Mickle *et al.* 1989) and *in vitro* (Wu *et al.* 1990). Our results show that exposing thymocytes to trolox after irradiation blocks DNA fragmentation. The radiation-induced influx of extracellular Ca^{2+} is also inhibited in trolox-treated cells.

2. Materials and methods

2.1. *Thymocyte isolation*

CD2F1 male mice (6–7 weeks old) were killed with CO_2 and their thymuses removed and placed in ice-cold culture medium [RPMI 1640 medium supplemented with 25 mM HEPES buffer, 2 mM L-glutamine, 55 μM 2-mercaptoethanol, 100 U/ml penicillin, 100 μg/ml streptomycin, 0·25 μg/ml amphotericin B, all from GIBCO/BRL (Grand Island, NY, USA) and 10% heat-inactivated foetal calf serum (HyClone Laboratories, Logan, UT, USA)]. Single-cell suspensions were prepared by pressing the organs through wire mesh screens followed by passage through a 25-gauge needle. The cells were washed once and resuspended in medium. Viable cells were determined by their ability to exclude trypan blue (Warters 1992).

2.2. *Irradiation*

Thymocytes suspended in medium (2×10^6/ml) were exposed to 1·5–6·0 Gy ^{60}Co γ-radiation at a nominal dose rate of 1 Gy/min using the AFRRI cobalt facility.

2.3. *Trolox treatment*

Immediately after irradiation, cells were centrifuged at 200*g* for 10 min, resuspended in fresh medium at 2×10^6 cells/ml, and incubated with trolox (Hoffman–LaRoche, Nutley, NJ, USA) at 37°C under an atmosphere of 5% CO_2 in air. It was necessary to prepare stock concentrations of trolox (100 mM) in 1 M $NaHCO_3$ because of its poor solubility in water above 1·8 mM (Wu *et al.* 1990). The pH of the stock was adjusted to 7·0 with 1 N HCl, and the stock was diluted to working concentrations with medium.

Dexamethazone was dissolved in a minimal volume of ethanol and diluted to the desired concentration with culture medium. Thymocytes were incubated with dexamethazone with or without trolox as described above. A similar volume of ethanol was added to controls.

2.4. *DNA fragmentation assay*

DNA fragmentation was assayed as previously described (Ramakrishnan and Catravas 1992a). At selected times cells were harvested by centrifugation at 200*g* for 10 min. The cells were lysed with 0·2 ml ice-cold hypotonic 10 mM Tris-HCl, pH 7·5, containing 1 mM EDTA and 0·2% Triton X-100 (lysis buffer) and centrifuged at 13 000*g* for 20 min to separate intact from fragmented DNA. The pellet was then sonicated for 10 s in 0·2 ml lysis buffer. DNA in the pellet and supernatant fractions was determined by an automated fluorometric method using Hoechst 33258 fluorochrome (Calbiochem-Behring, La Jolla, CA, USA) (Brunk *et al.* 1979, Cesarone *et al.* 1979), modified for our studies. The method utilized the Technicon Autoanalyzer II components (Technicon Instruments Corp., Tarrytown, NY, USA), including an autosampler fitted with a 40-place sample tray, a single-speed proportioning pump, and a fluoronephelometer. All tubes were flow-rated Tygon tubing (Fisher Scientific, Pittsburg, PA, USA). The sampler cam permitted the analysis of 40 samples/h with a 1 min running buffer wash between 30-s sample draws. The fluorescence signal was directed to a Hewlett-Packard 3390A integrator (Downer's Grove, IL, USA), which automatically identified and quantitated sample peaks.

The concentration of DNA was determined with computer software that compared the sample peak height value with a standard curve of peak heights of known concentrations of calf thymus DNA. The fluorometric autoanalysis of DNA is more sensitive

and reproducible than the diphenylamine method. Sample concentrations of 1–20 μg/ml were easily analysed with the system. Increased sensitivity can be obtained by increasing the volume of the sample draw and/or adjusting the sensitivity of the fluorone-phelometer and integrator. Measurements were unaffected by the presence of cell homogenates or reagents in the sample.

The percentage of DNA fragmentation refers to the ratio of DNA in the 13 000 *g* supernatant to the total DNA in the pellet and 13 000 *g* supernatant.

2.5. *DNA electrophoresis*

Thymocytes were lysed in lysis buffer and incubated with proteinase K (50 μg/ml at 37°C for 30–45 min). The DNA was sequentially extracted with equal volumes of phenol/chloroform/isoamyl alcohol (25:24:1). The aqueous phase was precipitated overnight at −20°C in 100% ethanol. DNA was collected by centrifugation at 13 000 *g* for 20 min, air dried, and resuspended in 10 mM Tris, 1 mM EDTA, pH 7·8. Horizontal electrophoresis of DNA was performed for 2 h at 100 V in a 0·75% agarose gel with 90 mM Tris, 90 mM boric acid, and 2 mM EDTA, pH 8·0 as running buffer (Ramakrishnan and Catravas 1992a).

2.6. *Calcium measurements*

Ca^{2+} uptake studies were performed by a method modified from McClain *et al.* (1984). Thymocytes (1×10^7/ml) were incubated at 37°C for 30 min prior to radiation exposure in medium containing 10 μC $^{45}Ca^{2+}$/ml ($^{45}CaCl_2$, 28·6 mC/mg, Dupont/NEN, Wilmington, DE, USA). This preincubation time was sufficient to equilibrate Ca^{2+} stores in the thymocytes with the isotope (unpublished observations). After irradiation the cell suspension was returned to 37°C and incubated with gentle mixing. At selected times post-irradiation aliquots of the cell suspension (50 μl, 5×10^5 cells) were removed and layered over 150 μl of a silicone oil mixture [Versilube F50, General Electric, Waterford, NY, USA with 8% (v/v) light mineral oil (Fisher Scientific)] in a 0·6 ml micro-centrifuge tube. The sample was centrifuged at 13 500 *g* in a microfuge for 45 s to pellet the cells through the oil, separating them from the radioactive medium. The aqueous and oil layers were carefully aspirated, and the cell pellet was resuspended in Hanks' Balanced Salt Solution (GIBCO/BRL) containing 1% Triton X-100. The samples were transferred to 7-ml scintillation vials. The precision of replicates was greatly improved by also adding to each vial the pipet tip used to transfer the sample and the bottom 75–100 μl volume of the micro-centrifuge tube (cut with a Micro Tube Cutter, Thomas Scientific, Swedesboro, NJ, USA). Ecoscint A biodegradable scintillation solution (7 ml) (National Diagnostics, Manville, NJ, USA) was added to each scintillation vial, the vial contents vigorously shaken, and the radioactivity in the samples counted on a scintillation counter (LS5801, Beckman Instruments, Fullerton, CA, USA).

The amount of Ca^{2+} associated with the cells was calculated from the cpm in the cell pellet divided by the specific activity of $^{45}Ca^{2+}$ in the incubation medium. The specific activity was calculated by dividing the cpm in 10 μl of the radioactive cell suspension by the Ca^{2+} concentration in the incubation medium (0·42 mM). The quantity of Ca^{2+} associated with the cell pellet was normalized to that in 1×10^6 cells.

3. Results

The effect of trolox on DNA fragmentation in thymocytes exposed to increasing doses of γ-radiation is shown in Figure 1a and b. There was no DNA fragmentation in irradiated thymocytes immediately after irradiation (6 Gy data; Figure 1a). DNA fragmentation began in irradiated thymocytes 2–3 h following irradiation and increased with time. This fragmentation was completely blocked by trolox following the post-irradiation incubation. There was a 10–20% background DNA fragmentation in unirradiated thymocytes not treated with trolox following an 8-h incubation at 37°C (Figure 1a and b). Incubation of unirradiated thymocytes with trolox reduced even the background fragmentation to negligible levels. Exposure of the cells to trolox did not alter significantly the viability of the cells. After an 8-h incubation with 10 mM trolox at 37°C under an atmosphere of 5% CO_2, 85 ± 3% (mean ± sem, $n = 3$) of the thymocytes retained the ability to exclude trypan blue. This compared with a value of 90 ± 3% ($n = 3$) for cells incubated under the same conditions without trolox.

Electrophoretic analysis of DNA isolated from thymocytes irradiated with 3 Gy showed a typical 'ladder' pattern of DNA fragments that were multiples of 200 base pairs (lane 4, Figure 2). The DNA isolated from irradiated thymocytes following trolox treatment showed no fragmentation (lane 5). The DNA of unirradiated thymocytes contained a small degree of fragmentation (lane 2), and there were no fragments in the DNA isolated from unirradiated trolox-treated thymocytes (lane 3). The results indi-

cate that the fragmentation of nuclear DNA into oligonucleosomal subunits, the most important biochemical event in apoptosis, can be inhibited by trolox.

Figure 3 shows the effect of different concentrations of trolox on DNA fragmentation in thymocytes

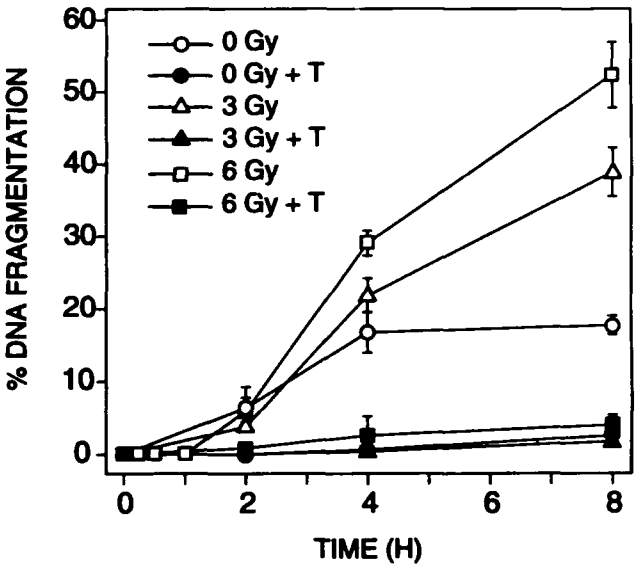

(a)

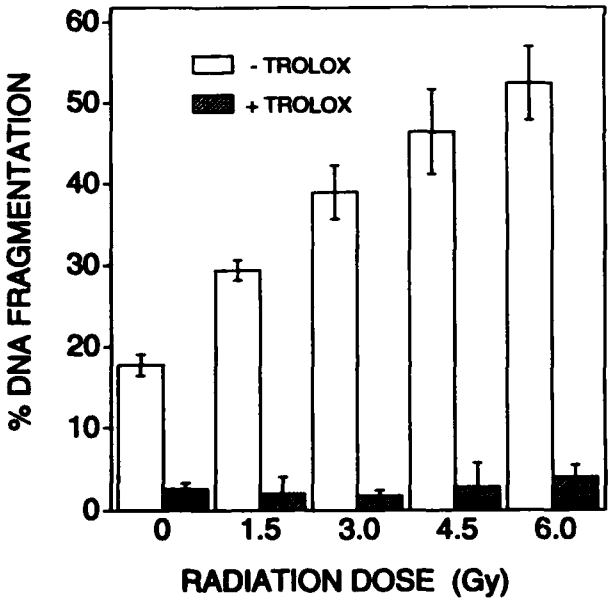

(b)

Figure 1. DNA fragmentation in irradiated thymocytes and inhibition by trolox. (a), at different post-irradiation times; (b), at 8 h after increasing doses of γ-irradiation. Thymocytes (2×10^6 cells/ml) were irradiated at a dose rate of 1 Gy/min. After irradiation cells were incubated in fresh medium with or without 10 mM trolox at 37°C under an atmosphere of 5% CO_2 in air. At indicated times DNA fragmentation was determined as described in §2. The results are mean ± SE from three independent experiments ($n = 6$). T, trolox.

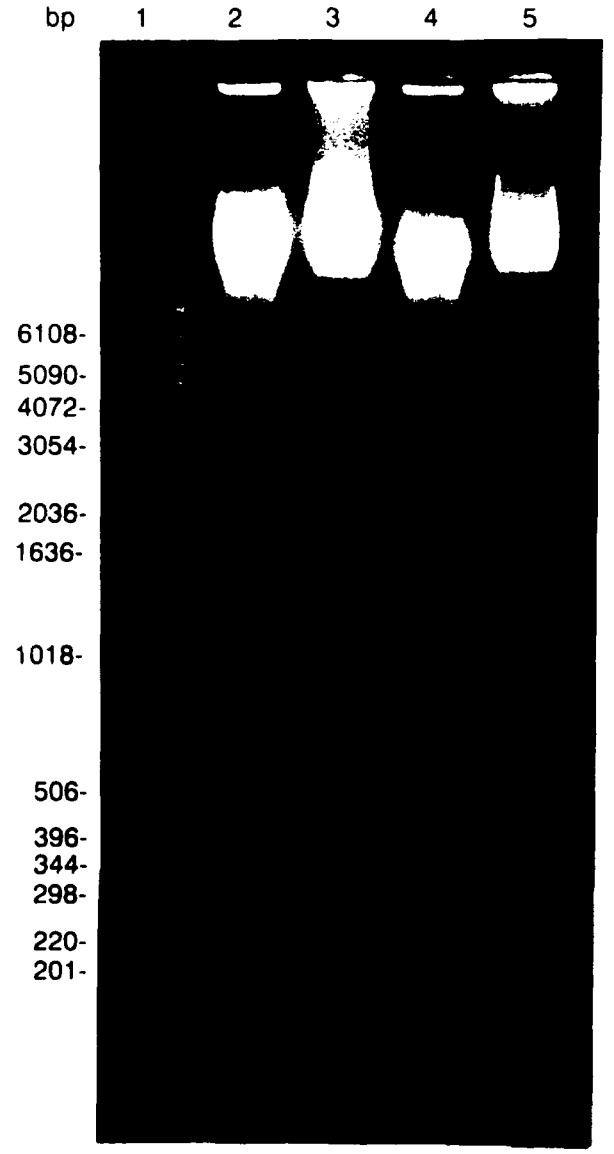

Figure 2. Trolox inhibits DNA fragmentation. DNA was isolated from unirradiated (0 Gy) and irradiated (3 Gy) thymocytes after 6-h incubation with or without 10 mM trolox and analysed by agarose gel electrophoresis. Lane 1, standard 1 kb DNA ladder; lane 2, 0 Gy; lane 3, 0 Gy + trolox; lane 4, 3 Gy; and lane 5, 3 Gy + trolox.

exposed to 6 Gy. The inhibition of fragmentation by trolox depended on its concentration in the incubation medium. Because DNA fragmentation was completely blocked by 10 mM trolox we used this concentration in all subsequent studies.

In the studies above, trolox was present in the medium during the entire post-irradiation incubation period. It was possible, however, that the effeciveness of trolox required it to be present only at a certain stage during the sequence of steps leading to DNA fragmentation. We therefore performed a series of experiments to determine how long trolox must

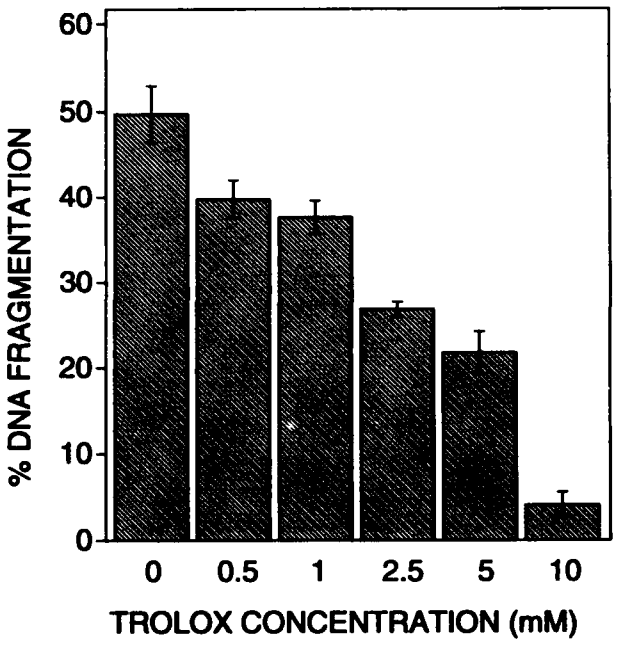

Figure 3. Inhibition of DNA fragmentation depends on concentration of trolox. Irradiated thymocytes (6 Gy) were incubated in fresh medium with different concentrations of trolox as described in Figure 1. DNA fragmentation was determined 8 h after irradiation. The results are mean ± SE from three independent experiments ($n=6$).

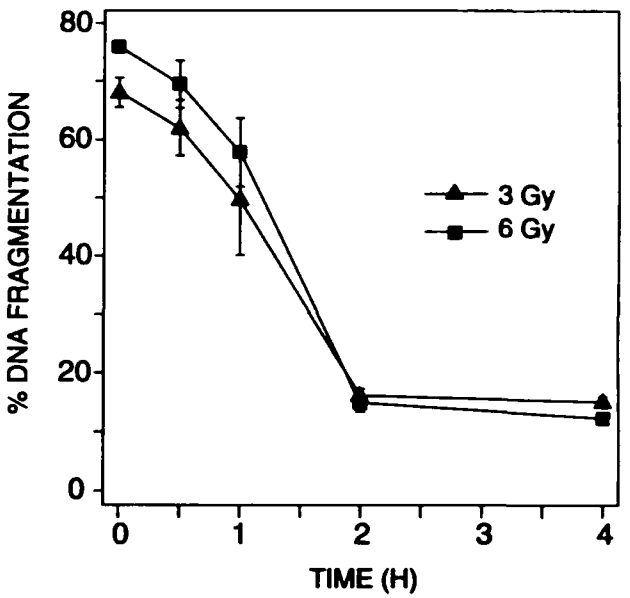

Figure 4. Inhibition of DNA fragmentation depends on the duration of trolox treatment. Irradiated thymocytes (3 and 6 Gy) were incubated in fresh medium with 10 mM trolox for different periods of time. At indicated times thymocytes were removed from the medium by centrifugation. The cells were resuspended in trolox-free medium and incubated under the conditions described in Figure 1. DNA fragmentation was determined 24 h after irradiation. The results are mean ± SE from three independent experiments ($n=6$).

be present after irradiation and how soon after irradiation it must be added to inhibit DNA fragmentation.

Figure 4 shows the results of experiments in which irradiated thymocytes were incubated with trolox for different lengths of time. At selected times (0·5–4 h) cells were removed from the medium containing trolox by centrifugation and incubated in fresh medium without trolox at 37°C in air containing 5% CO_2. DNA fragmentation was then determined 24 h after irradiation. As shown in Figure 4 the DNA fragmentation in thymocytes irradiated at 3 and 6 Gy was 68 and 76%, respectively. The extent of DNA fragmentation decreased as the incubation time with trolox increased, reaching a minimum after a 2-h incubation. DNA fragmentation in irradiated thymocytes after a 2-h incubation with trolox was 15%, the same level measured in unirradiated thymocytes treated the same way with trolox. These data indicate that a 2-h incubation with trolox is sufficient to block the DNA fragmentation measured at 24 h and that once the trolox-sensitive step is inhibited, fragmentation fails to occur even after trolox is removed.

To identify how early trolox must be present to block DNA fragmentation after irradiation, we added trolox to thymocytes during or at different times following irradiation (6 Gy), and determined the extent of DNA fragmentation 8-h post-irradiation. The results shown in Figure 5 indicate that trolox does not inhibit DNA fragmentation when present only during irradiation. The addition of trolox within 30 min after irradiation was sufficient to inhibit almost completely the DNA fragmentation. Adding trolox 1 h after irradiation resulted in about 15% of the DNA becoming fragmented. Trolox added 2 or 4 h after irradiation resulted in 20 or 33% DNA fragmentation, respectively. Therefore, trolox completely inhibits DNA fragmentation only when added within 30 min after radiation exposure, suggesting that there is a critical event in the process of apoptosis within the first 30 min after irradiation that is sensitive to trolox.

We performed experiments to determine whether DNA fragmentation was correlated with changes in Ca^{2+} uptake into irradiated thymocytes. The amount of Ca^{2+} associated with irradiated thymocytes remained the same as unirradiated controls until 2 h post-irradiation (Figure 6). At 3 h the amount of Ca^{2+} associated with irradiated thymocytes was more than, twice that of unirradiated

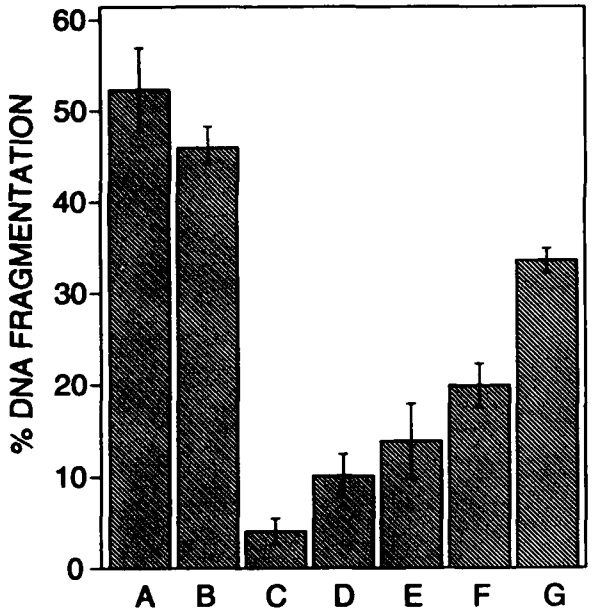

Figure 5. Inhibition of DNA fragmentation depends on timing of trolox treatment. Thymocytes were exposed to 6 Gy γ-radiation and incubated under the conditions described in Figure 1. In one set, thymocytes were irradiated in the presence of trolox. Immediately after irradiation the medium containing the trolox was removed by centrifugation and the incubation continued in trolox-free medium. The other sets were irradiated in medium without trolox; trolox (10 mM) was then added at the indicated times after irradiation and the incubation continued. DNA fragmentation was determined 8 h after irradiation. The results are mean ± SE from three independent experiments ($n=6$). 6 Gy (bar A); trolox present during irradiation, then removed (bar B); trolox added to irradiated thymocytes at 0 min (bar C); 30 min (bar D); 1 h (bar E); 2 h (bar F); or 4 h (bar G) after irradiation.

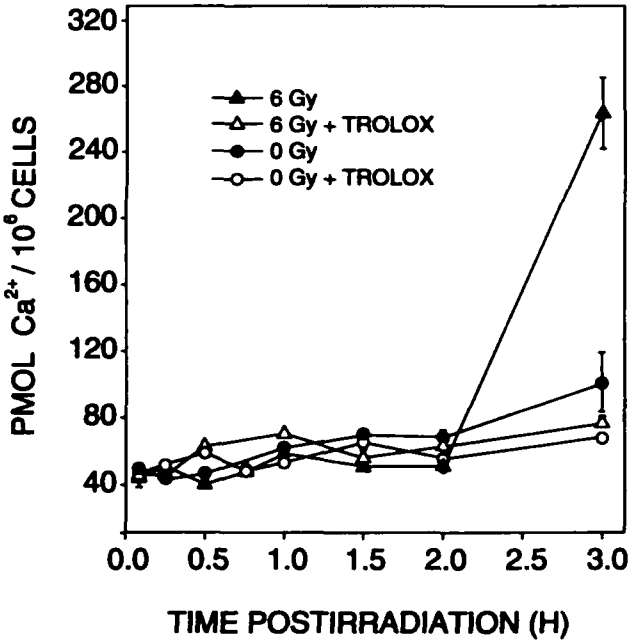

Figure 6. Trolox inhibits Ca^{2+} influx in irradiated thymocytes. Thymocytes (2×10^7 cells/ml) were incubated at 37°C in medium containing $^{45}Ca^{2+}$ (10 μC/ml) for 30 min before irradiation. Immediately after irradiation (6 Gy) trolox (10 mM) or buffer was added and the incubation continued. At selected times aliquots of the suspension were removed, the cells separated from the medium by centrifugation through oil, and radioactivity in the cell pellet determined by scintillation counting. Data represent the mean ± SE of two independent experiments ($n=8$).

thymocytes (261 ± 18 versus 101 ± 20 pmol/10^6 cells). The induction of DNA fragmentation and influx of Ca^{2+} appear concurrent (2–3 h post-irradiation; compare Figures 1a and 6). Interestingly, trolox completely inhibited the influx of Ca^{2+} in irradiated thymocytes.

We also studied the effect of trolox on DNA fragmentation following glucocorticoid treatment to determine whether the events blocked by trolox were specific for apoptosis stimulated by radiation. The results shown in Figure 7 indicate that trolox also inhibited DNA fragmentation induced in thymocytes by dexamethazone (compare lanes 4 and 5).

4. Discussion

Our findings demonstrate that trolox protects thymocytes from DNA fragmentation induced by γ-irradiation. DNA fragmentation was not inhibited if trolox was present only during irradiation (Figure 5), which suggests that the effectiveness of trolox in these experiments is not a result of its scavenging of free radicals generated during irradiation. On the other hand, trolox was very effective in inhibiting DNA fragmentation if added to the cells during the first 30 min after irradiation (Figure 5). The longer the addition of trolox was delayed, the less the level of protection observed, which suggests trolox inhibits an early step in a process that leads to an influx of Ca^{2+} and DNA fragmentation 2–3 h post-irradiation (Figures 1a and 6) (Ramakrishnan and Catravas 1992a, Story *et al.* 1992). Trolox need not be present continuously to exert its effect. Removing it from the irradiated cell suspension 2 h post-irradiation led to no greater degree of DNA fragmentation observed at 24 h than that measured in unirradiated controls (Figure 4). These results also suggest that the events responsible for DNA fragmentation begin soon after irradiation. Once these early steps are blocked the succeeding steps will not occur.

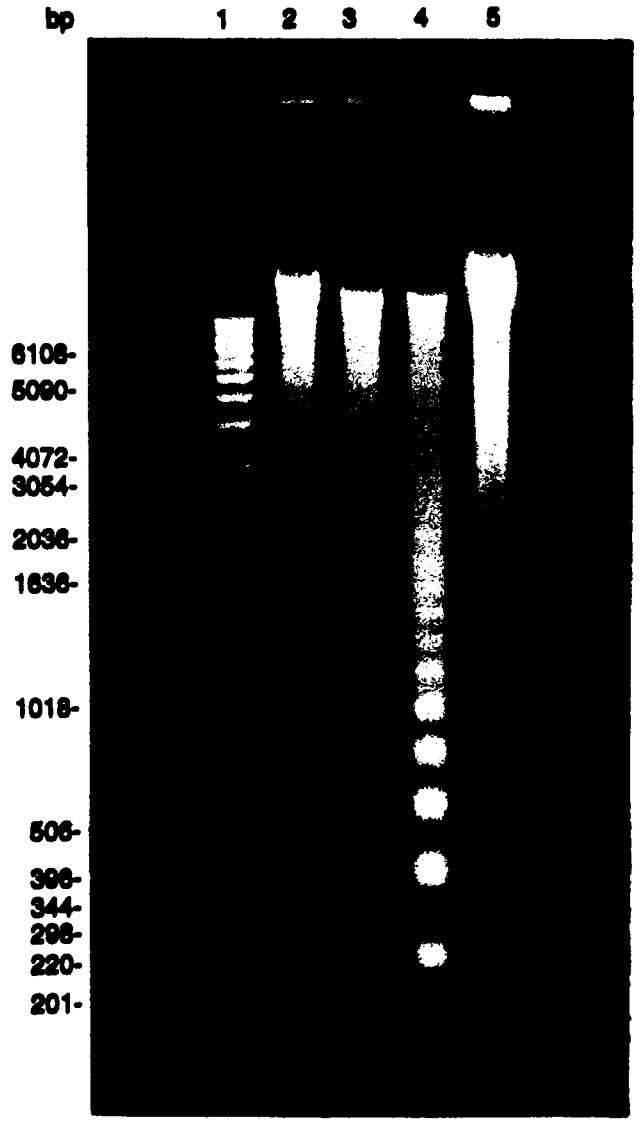

Figure 7. Trolox inhibits dexamethazone-induced DNA fragmentation. DNA was isolated from untreated and dexamethazone-treated (50 nM) thymocytes after 6 h incubation with or without 10 mM trolox and analysed by agarose gel electrophoresis. Lane 1, standard 1 kb DNA ladder; lane 2, control; lane 3, control + trolox; lane 4, 50 nM dexamethazone; and lane 5, dexamethazone + trolox.

Because trolox has been shown to be an inhibitor of membrane damage (Liu *et al.* 1990, Casini *et al.* 1985, Doba *et al.* 1985, Mickle *et al.* 1989, Barclay *et al.* 1984, Burton and Ingold 1985), it seems likely that trolox protects thymocytes by inhibiting structural and/or functional membrane changes responsible for triggering apoptosis. This interpretation is supported by our earlier studies with another lipophilic membrane-protecting antioxidant, dihydrolipoic acid, which also protects thymocytes from radiation-induced DNA fragmentation (Ramakrishnan and Catravas 1992b). It is not surprising that events within membranes play a central role in radiation-induced apoptosis. Membrane damage has been reported in mammalian cells at radiation doses as low as 0·5 Gy (Parasassi *et al.* 1991). Human lymphocytes exhibit morphological changes in the plasma membrane within 15 min after irradiation with 0·5–1·5 Gy (Chandra and Stefani 1981, Stefani *et al.* 1977). Furthermore, changes in the structure and function of cellular membranes in irradiated thymocytes have been shown to occur much earlier than DNA fragmentation (Zherbin and Chukhlovin 1984, Yamada *et al.* 1969, Chandra and Stefani 1981, Sungurov and Sharlaeva 1988).

Our initial hypothesis of the mechanism of action of trolox was that it acted as an antioxidant to block lipid peroxidation and other membrane oxidations induced by radiation. However, our observation that trolox is also a potent inhibitor of glucocorticoid-induced DNA fragmentation (Figure 7) suggests that such a hypothesis might be too narrow to explain the trolox inhibition. Glucocorticoid-stimulated apoptosis is not known to involve changes in the membrane like those induced by radiation. However, little is known of the specific reactions that occur in the membrane during glucocorticoid stimulation. They may well involve changes in the oxidation state of reactants, which the antioxidant trolox could interfer with. The glucocorticoid experiments do not contradict the basic notion that trolox interfers with a membrane-related event early in the process of apoptosis. Apoptosis stimulated by glucocorticoids is a receptor-mediated process (Wyllie 1980). Glucocorticoids have been shown to impair membrane-related transport functions; cellular transport of amino acids, glucose, and nucleosides have been shown to be inhibited in thymocytes within 60 min after glucocorticoid treatment (Munck 1968, Makman *et al.* 1968, 1971).

Although it is not yet clear what membrane functions trolox protects to prevent the DNA degradation induced by radiation, our results strongly suggest trolox blocks some aspect of calcium metabolism associated with apoptosis. Many studies have shown that a critical event in apoptosis is an increase in cytosolic Ca^{2+} due to an internal mobilization of intracellular Ca^{2+} and an influx of extracellular Ca^{2+} (McConkey *et al.* 1989b, Story *et al.* 1992). Three hours post-irradiation, the amount of Ca^{2+} in irradiated thymocytes was more than twice that of those not irradiated (Figure 6). The fact that trolox blocked the influx of extracellular Ca^{2+} in irradiated thymocytes (Figure 6) suggests that trolox inhibits a change in membrane function that is

responsible for calcium mobilization during apoptosis. It may be that trolox protects calcium translocating mechanisms in the membrane that are otherwise altered by radiation. Indeed, it has been shown that vitamin E, from which trolox is derived, protects calcium translocases that are impaired during membrane damage (Ananieva *et al.* 1984).

In summary, this study supports the hypothesis that early events in apoptosis stimulated by physical agents or receptor-mediated processes occur at the membrane level. Trolox, an inhibitor of membrane damage, protects thymocytes from apoptosis. The critical lesion(s) blocked by trolox occur soon after stimulation. Once the lesion is prevented, trolox can be removed and apoptosis will not proceed. Experiments are currently in progress to identify the specific membrane events modulated by trolox to prevent apoptosis.

Acknowledgements

Trolox was kindly provided by Hoffman–La Roche. We thank W. Wolfe for his excellent technical assistance. The assistance of the Veterinary Sciences Department, Radiation Sources Department, and Information Services Department is also appreciated. This work was performed while Dr. Ramakrishnan held a National Research Council-AFRRI Associateship, and the research was supported by the Armed Forces Radiobiology Research Institute, Defense Nuclear Agency. Research was conducted according to the principles enunciated in the Guide for the Care and Use of Laboratory Animals prepared by the Institute of Laboratory Animal Resources, National Research Council.

References

AGARWAL, M. L., CLAY, M. E., HARVEY, E. J., EVANS, H. H., ANTUNEZ, A. R. and OLEINICK, N. L., 1991, Photodynamic therapy induces rapid cell death in L5178Y mouse lymphoma cells. *Cancer Research*, **51**, 5993–5996.

ANANIEVA, L. K., IVANOV, I. I., TAVIDZE, L. V. and KAGAN, V. E., 1984, Mechanism of sarcoplasmic reticulum Ca^{2+}-ATPase stabilization by α-tocopherol against thermodenaturation, activated by fatty acids. *Biokhimiya*, **49**, 421–426.

ASHWELL, J. D., SCHWARTZ, R. H., MITCHELL, J. B. and RUSSO, A., 1986, Effect of gamma radiation on resting B lymphocytes. *Journal of Immunology*, **136**, 3649–3656.

BARCLAY, L. R. C., LOCKE, S. J., MACNEIL, J. M. and VAN KESSEL, J., 1984, Autooxidation of micelles and model membranes. Quantitative kinetic measurements can be made by using either water-soluble or lipid-soluble chain-breaking antioxidants. *Journal of the American Chemical Society*, **106**, 2479–2481.

BELLOMO, G., PEROTTI, M., TADDEI, F., MIRABELLI, F., FINARDI, G., NICOTERA, P. and ORRENIUS, S., 1992, Tumor necrosis factor α induces apoptosis in mammary adenocarcinoma cells by an increase in intracellular free Ca^{2+} concentration and DNA fragmentation. *Cancer Research*, **52**, 1342–1346.

BRUNK, C. F., JONES, K. C. and JAMES, T. W., 1979, Assay for nanogram quantities of DNA in cellular homogenates. *Analytical Biochemistry*, **92**, 497–502.

BURTON, G. W. and INGOLD, K. U., 1985, Autoxidation of biological molecules. 1. The antioxidant activity of vitamin E and related chain-breaking phenolic antioxidants *in vitro*. *Journal of the American Chemical Society*, **103**, 6472–6477.

CASINI, A. F., POMPELLA, A. and COMPORTI, M., 1985, Liver glutathione depletion induced by bromobenzene, iodobenzene, and diethylmaleate poisoning and its relation to lipid peroxidation and necrosis. *American Journal of Pathology*, **118**, 225–274.

CASTLE, L. and PERKINS, M. J., 1986, Inhibition kinetics of chain-breaking phenolic antioxidants in SDS micelles. Evidence that intermicellar diffusion rates may be rate-limiting for hydrophobic inhibitors such as alpha-tocopherol. *Journal of The American Chemical Society*, **108**, 6381–6382.

CESARONE, C. F., BOLOGNESI, C. and SANTI, L., 1979, Improved microfluorometric DNA determination in biological material using 33258 Hoechst. *Analytical Biochemistry*, **100**, 188–192.

CHANDRA, S. and STEFANI, S., 1981, Plasma membrane as a sensitive target in radiation-induced cell injury and death: an ultrastructural study. *International Journal of Radiation Biology*, **40**, 305–311.

COHEN, J. J. and DUKE, R. C., 1984, Glucocorticoid activation of a calcium-dependent endonuclease in thymocyte nuclei leads to cell death. *Journal of Immunology*, **132**, 38–42.

DOBA, T., BURTON, G. W. and INGOLD, K. U., 1985, Antioxidant and co-antioxidant activity of vitamin C. The effect of vitamin C, either alone or in the presence of vitamin E or a water soluble vitamin E analogue, upon the peroxidation of aqueous multilamellar phospholipid liposomes. *Biochimica Biophysica Acta*, **835**, 298–303.

HARMON, B. V., TAKANO, Y. S., WINTERFORD, C. M. and GOBE, G. C., 1991, The role of apoptosis in the response of cells and tumours to mild hyperthermia. *International Journal of Radiation Biology*, **59**, 489–501.

KAMINSKAS, E. and LI, J. C., 1989, DNA fragmentation in permeabilized cells and nuclei: the role of ($Ca^{2+}Mg^{2+}$)-dependent endonuclease. *Biochemical Journal*, **261**, 17–21.

KERR, J. F. R., WYLLIE, A. H. and CURRIE, A. R., 1972, Apoptosis: a basic biological phenomenon with wide ranging implications in tissue kinetics. *British Journal of Cancer*, **26**, 239–257.

KONINGS, A. W. T., 1981, Dose-rate effects on lymphocyte survival. *Journal of Radiation Research*, **22**, 282–285.

LUCY, J. A., 1972, Functional and structural aspects of biological membranes: a suggested structural role for vitamin E in the control of membrane permeability and stability. *Annals of the New York Academy of Sciences*, **203**, 4–11.

MARMAN, M. H., DVORKIN, B. and WHITE, A., 1968, Influence of cortisol on the utilization of precursors of nucleic acids

and protein by lymphoid cells *in vitro*. *Journal of Biological Chemistry*, **243**, 1485–1497.

MAKMAN, M. H., DVORKIN, B. and WHITE, A., 1971, Evidence for induction by cortisol *in vitro* of a protein inhibitor of transport and phosphorylation processes in rat thymocytes. *Proceedings of the National Academy of Sciences, USA*, **68**, 1269–1273.

MARTIN, S. J. and COTTER, T. G., 1991, Ultraviolet B irradiation of human leukaemia HL-60 cells *in vitro* induces apoptosis. *International Journal Radiation Biology*, **59**, 1001–1016.

MARTZ, E. and HOWELL, D. M., 1989, CTL: virus control cells first and cytolytic cells second? DNA fragmentation, apoptosis and the prelytic halt hypothesis. *Immunology Today*, **10**, 79–85.

MARUYAMA, Y. and FEOLA, J. M., 1987, Relative radiosensitivities of the thymus, spleen and lymphohemopoietic systems. *Advances in Radiation Biology*, **12**, 1–82.

MCCLAIN, D. E., DONLON, M. A., HILL, T. A. and CATRAVAS, G. N., 1984, Early kinetics of Ca^{2+} fluxes and histamine release in rat mast cells stimulated with compound 48/80. *Agents and Actions*, **15**, 279–284.

MCCONKEY, D. J., HARTZELL, P., DUDDY, S. K., HAKANSSON, H. and ORRENIUS, S., 1988, 2,3,7,8-Tetrachlorodibenzo-*p*-dioxin kills immature thymocytes by Ca^{2+}-mediated endonuclease activation. *Science*, **242**, 256–259.

MCCONKEY, D. J., HARTZELL, P., NICOTERA, P. and ORRENIUS, S., 1989a, Calcium activated DNA fragmentation kills immature thymocytes. *FASEB Journal*, **3**, 1843–1849.

MCCONKEY, D. J., NICOTERA, P., HARTZELL, P., BELLOMO, G., WYLLIE, A. H. and ORRENIUS, S., 1989b, Glucocorticoids activate a suicide process in thymocytes through an elevation of cytosolic Ca^{2+} concentration. *Archives of Biochemistry and Biophysics*, **269**, 365–370.

MCCONKEY, D. J., CHOW, S. C., ORRENIUS, S. and JONDAL, M., 1990, NK cell-induced cytotoxicity is dependent on a Ca^{2+} increase in the target. *FASEB Journal*, **4**, 2661–2664.

MICKLE, D. A. G., LI, R. K., WEISEL, R. D., BIRNBAUM, P. L., WU, T. W., JACKOWSKI, G., MADONIK, M. M., BURTON, G. and INGOLD, U., 1989, Myocardial salvage with trolox and ascorbic acid for an acute evolving infarction. *Annals of Thoracic Surgery*, **47**, 553–557.

MUNCK, A., 1968, Metabolic site and time course of cortisol action on glucose uptake, lactic acid output, and glucose 6-phosphate levels of rat thymus cells *in vitro*. *Journal of Biological Chemistry*, **243**, 1039–1042.

NIKONOVA, L. V., NELLIPOVICH, P. A. and UMANSKY, S. R., 1982, The involvement of nuclear nucleases in rat thymocyte DNA fragmentation after γ-irradiation. *Biochimica Biophysica Acta*, **699**, 281–285.

OJEDA, F., ANDRADE, J., MALDONADO, C., GUARDA, M. I. and FOLCH, H., 1991, Radiation-induced surface IgG modulation: protein kinase C involvement. *International Journal of Radiation Biology*, **59**, 53–58.

OJEDA, F. GUARDA, M. I., MALDONADO, C. and FOLCH, H., 1990, Protein kinase-C involvement in thymocyte apoptosis induced by hydrocortisone. *Cellular Immunology*, **125**, 535–539.

OJEDA, F., GUARDA, M. I., MALDONADO, C. and FOLCH, H. and DIEHL, H., 1992, Role of protein kinase C in thymocyte apoptosis induced by irradiation. *International Journal of Radiation Biology*, **61**, 663–667.

PARASASSI, T., SAPORA, O., GIUSTI, A. M., DE STASIO, G. and RAVAGNAN, G., 1991, Alterations in erythrocyte membrane lipids induced by low doses of ionizing radiation as revealed by 1,6-diphenyl-1,3,5-hexatriene fluorescence lifetime. *International Journal of Radiation Biology*, **59**, 59–69.

PASCOE, G. A. and REED, D. J., 1989, Cell calcium, vitamin E, and the thiol redox system in cytotoxicity. *Free Radicals in Biology and Medicine*, **6**, 209–224.

RAMAKRISHNAN, N. and CATRAVAS, G. N., 1992a, *N*-(2-mercaptoethyl)-1,3-propanediamine (WR-1065) protects thymocytes from programmed cell death. *Journal of Immunology*, **148**, 1817–1821.

RAMAKRISHNAN, N. and CATRAVAS, G. N., 1992b, Protection of thymocytes from radiation-induced interphase death by dihydrolipoic acid and WR-1065. In: *Eicosanoids and Other Bioactive Lipids in Cancer, Inflammation and Radiation Injury*. Edited by S. Nigam, L. J. Marnett, K. V. Hohn and T. L. Walden, Jr., (Boston, Kluwer Academic pp. 349–352).

SELLINS, K. S. AND COHEN, J. J., 1987, Gene induction by γ-irradiation leads to DNA fragmentation in lymphocytes. *Journal of Immunology*, **139**, 3199–3206.

SELLINS, K. S. and COHEN, J. J., 1991, Hyperthermia induces apoptosis in thymocytes. *Radiation Research*, **126**, 88–95.

SERVOMA, K. and RYTOMA, T., 1990, UV light and ionizing radiation cause programmed death of rat chloroleukaemia cells by inducing retropositions of a mobile DNA element (LIRn). *International Journal of Radiation Bilogy*, **57**, 331–343.

SMITH, C. A., WILLIAMS, G. T., KINGSTON, R., JENKINSON, E. J. and OWEN, J. J. T., 1989, Antibodies to CD3/T-cell receptor complex induce death by apoptosis in immature T cells in thymic cultures. *Nature*, **337**, 181–184.

STEFANI, S., CHANDRA, S. and TONAKI, H., 1977, Ultrastructural events in the cytoplasmic death of lethally-irradiated human lymphocytes. *International Journal of Radiation Biology*, **31**, 215–225.

STORY, M. D., STEPHENS, L. C., TOMASOVIC, S. P. and MEYN, R. E., 1992, A role for calcium in regulating appotosis in rat thymocytes irradiated *in vitro*. *International Journal of Radiation Biology*, **61**, 243–251.

SUNGUROV, A. YU. and SHARLAEVA, T. M., 1988, Thymocyte membrane changes and modifications of interphase death. *International Journal of Radiation Biology*, **53**, 501–506.

TRAUGHT, B. C., KLAS, C. H., PETERS, D. M., MATZKU, S., MOLLER, P., FALK, W., DEBATIN, K. M. and KRAMER, P. H., 1989, Monoclonal antibody mediated tumor regression by induction of apoptosis. *Science*, **245**, 301–305.

WARTERS, R. L., 1992, Radiation-induced apoptosis in murine T-cell hybridoma. *Cancer Research*, **52**, 883–890.

WU, T. W., HASHIMOTO, N., WU, J., CAREY, D., LI, R. K., MICKLE, D. A. G. and WEISEL, R. D., 1990, The cytoprotective effect of trolox demonstrated with three types of human cells. *Canadian Journal of Biochemistry and Cell Biology*, **68**, 1189–1194.

WYLLIE, A. H., 1980, Glucocorticoid induced thymocyte apoptosis is associated with endogenous endonuclease activation. *Nature (London)*, **324**, 55–56.

YAMADA, T., OHYAMA, H., KUMATORI, T. and MINAKAMI, S., 1969, Changes in glycolysis of rat thymocytes after a whole-body X-irradiation. *International Journal of Radiation Biology*, **45**, 179–183.

ZHERBIN, E. A. and CHUKHLOVIN, A. B., 1984, Possible association of membrane and nuclear changes in γ-irradiated rat thymocytes. *International Journal of Radiation Biology*, **45**, 179–183.

DOES THE TOPOLOGY OF CLOSED SUPERCOILED DNA AFFECT ITS RADIATION SENSITIVITY?

C.E. Swenberg, J.M. Speicher, and J.H. Miller*

Radiation Biochemistry Department
Armed Forces Radiobiology Research Institute
8901 Wisconsin Ave, Bethesda, MD 20889-5145
*Biology and Chemistry Department
Pacific Northwest Laboratory, Richland, WA 99352

ABSTRACT

Several families of negatively supercoiled topoisomers of the plasmid pIBI30 were ^{60}Co γ-irradiated and assayed for the induction of strand scission by agarose gel electrophoresis. Form-I DNA for all topoisomers decreased exponentially with increasing dose. The radiation sensitivity ($1/D_{37}$) was dependent on the average linking difference (ΔL) associated with a given supercoiled family. For $|\Delta L| < 2.5$ the radiation sensitivity of DNA decreased with increasing $|\Delta L|$, whereas for $|\Delta L| > 2.5$ enhanced radiation sensitivity was observed with increasing $|\Delta L|$. These results are in agreement with data reported by Miller, *et al.* (1991) also for pIBI30 (250kV X-irradiated), but are inconsistent with experiments by Milligan, *et al.* (1992) for ^{137}Cs γ-irradiated pUC18. Our results are suggestive of several mechanisms that could be operative in explaining the dependence of DNA radiation sensitivity on topology.

INTRODUCTION

Plasmid DNA is a useful model system for investigating the initial radiation damage in the absence of repair processes due to the ease of quantifying strand scission by agarose gel electrophoresis. In this paper we investigate the dependence of ^{60}Co γ-radiation sensitivity on the conformational state of DNA. It is almost an axiom of radiation research that smaller target volumes are less sensitive to ionizing radiation. We present experimental evidence that disputes the validity of this axiom in some circumstances. Our data strongly suggest that the organization of DNA in small domains can have pronounced effects on its radiation sensitivity.

It is well known that covalently closed duplex DNA is topologically constrained and can assume a large number of topologically inequivalent conformations. These different DNA conformational states can be classified by their linking number (Cozzarelli, Boles, and White, 1990). A more useful quantity, the linking difference (ΔL) denotes the difference between linking numbers of a given topoisomer and fully relaxed plasmid DNA. Native plasmids all have $\Delta L < 0$, a condition corresponding to more base pairs per turn than predicted by the Watson-Crick model. To address whether standard target theory (Fowler, 1964) might be inapplicable for small domain sizes, *i.e.* whether DNA's topology alters its radiation sensitivity, we have prepared supercoiled families of pIBI30 and have measured their response to ^{60}Co γ-irradiation. Our results strongly suggest that DNA's conformational state affects its radiation

Biological Effects and Physics of Solar and Galactic Cosmic Radiation, Part A, Edited by C.E. Swenberg *et al.*, Plenum Press, New York, 1993

response. For DNA in superhelical states an increase in $|\Delta L|$ corresponds to a decrease in target size as is indicated by an increase in electrophoretic mobility. In our studies for DNA characterized by low linking difference ($|\Delta L| < 2.5$) the response was that expected on the basis of standard target theory. However, for smaller, more compact DNA corresponding to larger negative linking differences ($|\Delta L| > 2.5$), the radiation sensitivity (defined as the negative of the slope of the semi-logarithmic plot of the fraction of Form-I DNA as a function of dose) was found to increase with increase in $|\Delta L|$. Several possible competing processes responsible for the enhanced sensitivity of DNA to radiation-induced strand scission at high $|\Delta L|$ values are suggested. Our results compare favorably with data on plasmid pIBI30 reported for 250kV X-rays by Miller and co-workers (1991), but are not in accord with recent results for ^{137}Cs γ-irradiated pUC18 by Milligan, *et al.* (1992).

EXPERIMENTAL METHODS

Protocol for preparation of supercoiled families (topoisomers) of pIBI30

Plasmid pIBI30 was isolated from Escherichia coli by alkaline lysis (Ausubel, *et al.* , 1989). Eukaryotic topoisomerase-I (topo-I) was purchased from Bethesda Research Laboratory (BRL) and was prepared for assay following the recommendations of the supplier. A relaxation protocol was modified from the published procedure of Singleton and Wells (1982). In our method 30 to 50μg of plasmid were relaxed with 30 units of enzyme in the presence of 1.4, 6.4, 9.7, 12, or 16.4 μmol dm^{-3} ethidium bromide at 37° C for four hours in a total volume of 150μl per reaction tube. Native plasmid was subjected to the same manipulations by combining it in a reaction mixture containing all ingredients with the exception of topo-I and ethidium bromide. Since topoisomers were desired in quantity and in order to maximize use of the enzyme, a typical preparation involved twelve reaction tubes (six for each of two topoisomers). The individual tubes were combined to a single tube following incubation and prior to extraction.

Rigorous adherence to recommended standard DNA clean-up protocols (Sambrook, Fritsch, and Maniatis 1989, and Davis, Dibner, and Battey 1986) was found necessary to avoid contamination of sample with chemical substances and to insure removal of residual proteins and introduced enzymes. Fig. 1 depicts an admittedly exaggerated illustration of the absorption spectra of improperly prepared DNA. Topoisomer reaction volumes were extracted once (always with equal volume) with buffer saturated phenol (BRL, catalog number 5513UA) and once with phenol/chloroform/isoamyl alcohol (proportions: 25::24::1) removing the aqueous phase to a fresh tube following each extraction. The resulting volume was subjected to three extractions with water saturated ethyl ether with careful removal of the organic layer to waste. Following each extraction a brief centrifugation (5000 rpm for 1 to 5 min) aided in phase separation. Finally, resulting volumes were incubated for ≈ 10 min at 65° C with constant flow of N_2 gas to purge residual ether from the system.

Ethanol precipitation of topoisomer preparations was adapted from standard protocols. Approximately 200μl of topoisomer solution was combined with 200μl of deionized water (Millipore, Milli-Q water system) to dilute solution salts below the level of co-precipitation with DNA. To this was added 44μl of 3 mol dm^{-3} sodium acetate (pH 5.2) and the volume thoroughly mixed by vortexing before addition of chilled 95% ethanol to a total volume of ≈ 1.5ml. The tubes were again vortexed and chilled on dry ice for ≈ 20 min. Centrifugation in a microcentrifuge at 4° C for 10 min pelleted the DNA. The pellets were carefully rinsed in 0.5ml of chilled 70% ethanol. Centrifugation at 4° C for 4 min prepared the samples for lyophilization (approximately one hour). The DNA was dissolved in a small volume of 50 mmol dm^{-3} potassium phosphate buffer (pH 7.2) and stored at 4° C for a minimum of 24 hours. If the lyophilization step of the topoisomer preparation involved multiple tubes, they were combined to a single tube using a vigorous wash- through method which took advantage of the innate stability (resistance to shearing) of plasmid (supercoiled) DNA. Topoisomer preparations were

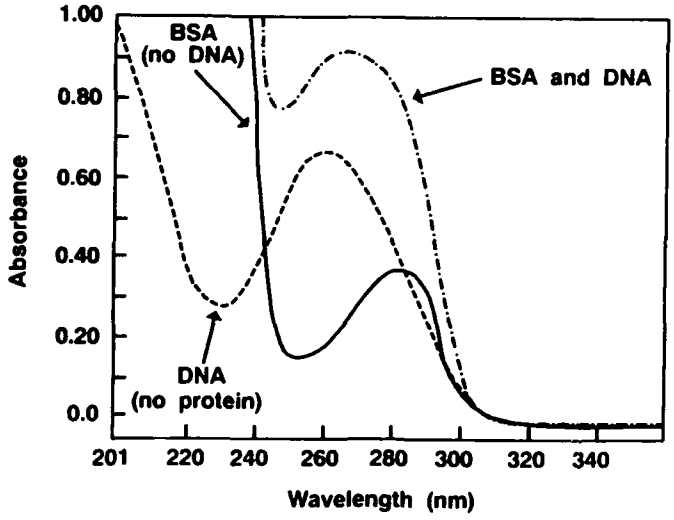

Figure 1. Spectrophotometric scans of solutions of plasmid DNA (pIBI30), protein (Bovine Serum Albumen), and mixed protein/DNA.

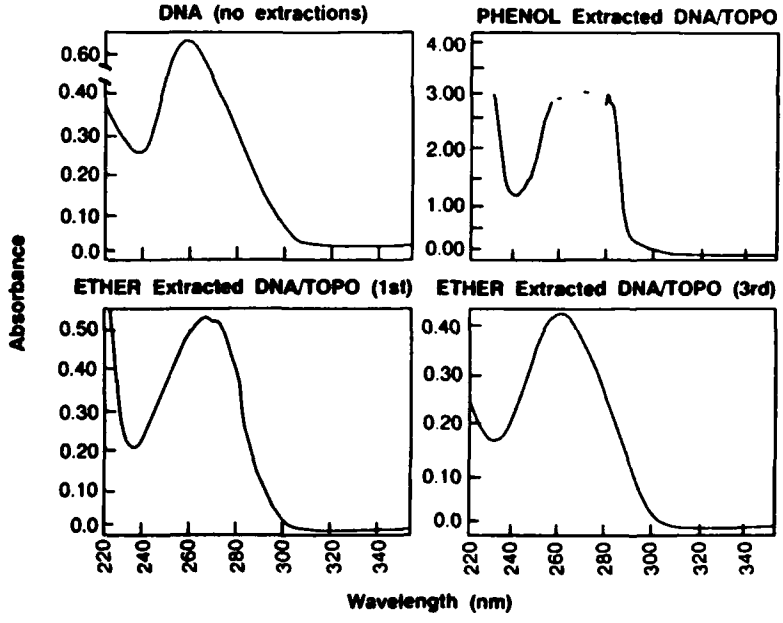

Figure 2. Spectrophotometric scans of solutions of untreated pIBI30 (DNA, one panel), and topoisomerase-I treated pIBI30 (DNA/TOPO) showing decreased levels of contaminants at stages of the purification protocol (see text for details).

brought to a final concentration of ≈ 0.2μg/μl following a careful dilution protocol. DNA concentration was determined by scanning sample solutions at 260nm on a Hewlett Packard 8450A diode array spectrophotometer. DNA purity was determined by monitoring the shape of the curve of a broad-spectrum scan (220 to 350nm) of the DNA in solution (see Fig. 2) and by monitoring the absorption ratio A_{260}::A_{280} of the DNA. DNA was certified as RNA-free and double-checked for absolute concentration by monitoring fluorescence of the topoisomers in the presence of Hoechst 33258 with a dedicated fluorometer (Hoefer Scientific Instruments, model TKO-100). The purified supercoiled families of pIBI30 utilized are shown in Fig. 3.

Figure 3. Electrophoretic *signature* of supercoiled families (topoisomers) of pIBI30. Native plasmid was relaxed with topoisomerase-I in the presence of (A) 0.0, (B) 12.0, (C) 9.7, (D) 6.4, (E) 16.4, and (F) 1.4 μmol dm^{-3} ethidium bromide (see text). Electrophoretic conditions: 7 x 10 cm gel, 1.6% agarose in TBE buffer (89 mmol dm^{-3} Tris, 89 mmol dm^{-3} boric acid, 2.5 mmol dm^{-3} EDTA, pH 8.0, not incorporating ethidium bromide) run at constant voltage (75 Volts) for several hours at room temperature.

Link number analysis of supercoiled families

Aliquots containing ≈ 0.75μg of the purified supercoiled families of pIBI30 were applied to agarose gels (horizontal) for link number analysis. Each topoisomer was characterized by an average linking difference, $|\Delta L|$, defined by the equation:

$$|\Delta L| = \Sigma |L_i| (x_i (\Sigma x_i)^{-1}) \qquad (1)$$

where the sum extends over all individual bands associated with a given topoisomer (A to F, see Fig. 3), L_i is the link difference assigned to an individual band i, and x_i denotes a measurement of area for the corresponding band. Our results indicate that $|\Delta L|$ is 13, 3.74, 2.74, 0.96, 5.92, and 0.75 for A through F of Fig. 3. The absolute magnitude of $|\Delta L|$ for pIBI30 upon isolation from *E. coli* was taken arbitrarily to be 13. This assumption does not qualitatively affect conclusions which may be inferred from the data. Assigning maximum $|\Delta L|$ of 13 corresponds to a reasonable (lower limit) value of 225 base pairs per supercoil.

Analysis of irradiated supercoiled families of pIBI30

Supercoiled families (0.2μg/μl) were exposed to ^{60}Co γ-irradiation at room temperature. The dose rate was ≈ 10 Gy min^{-1}. Dosimetry was performed using a calibrated tissue-equivalent ionization chamber (calibration traceable to N.I.S.T.) and following the AAPM TG21 protocol (American Association of Physicists in Medicine, Task Group 21, Radiation Therapy Committee,

1983). Irradiated topoisomers were stored at 4° C for at least two weeks prior to assay in tightly capped eppendorf tubes which were further protected from desiccation by enclosure within sealed 50ml conical centrifuge tubes. DNA was adversely affected by storage, but the effect stabilized after approximately 14 days (data not shown). Irradiated samples were prepared just prior to analysis by dilution with potassium phosphate buffer (50 mmol dm^{-3}) and bromophenol blue/glycerol tracking dye solution to a concentration of 0.075μg/5μl. 5μl of this preparation were applied to each of several lanes such that the entire spectrum of experimental treatments (radiation doses) including control (no radiation) were represented at least twice on each of two lane-sets on a single gel. Also included on the gel were marker bands composed of native pIBI30 delineating the extremes of the linear response region - separately determined (data not shown).

Agarose gels (1.6%, 15 x 20cm, in TBE buffer {89 mmol dm^{-3} Tris, 89 mmol dm^{-3} boric acid, 2.5 mmol dm^{-3} EDTA}, pH 8.0) incorporating ethidium bromide (0.5μg/ml) were run at constant voltage (75 Volts) for two hours at room temperature. Electrophoresis resolved samples into three distinct bands with the nicked circular band widely separated from the rapidly migrating supercoiled band. The band corresponding to linearized plasmid (Form-III) migrated slower than Form-I, but faster than Form-II. Following electrophoresis, gels were photographed using Polaroid 665 positive/negative film with a Polaroid MP-4 camera. The photographic negatives were analyzed with a microdensitometer (Molecular Dynamics model 300B). Densitometric analysis yielded measurements of band densities. A log/lin plot of the supercoiled (Form-I) band densities (normalized to control) versus dose provided a means for determining the D_{37} dose according to the equation:

$$\text{Form-I}(D) = d(\exp(-D/D_{37})) \qquad (2)$$

where d is the intercept, D is dose, and $1/D_{37}$ is an estimate of the sensitivity of the supercoiled family to strand scission. This relationship is illustrated in Fig. 4 for two supercoiled families of pIBI30 (family A, native plasmid, and family C).

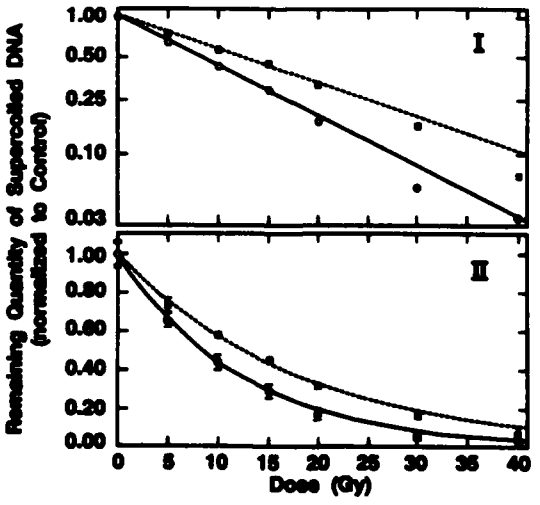

Figure 4. Loss of supercoiled pIBI30 DNA (Form-I) with increasing dose of ^{60}Co γ-irradiation. Figure curves (both panels) show the least squares fit of the data (according to equation (2)). Data represented as closed symbols were near or below the threshold of reliable detection and were not used for least squares curve-fitting. Circles represent native pIBI30 (A from Fig. 3); squares denote supercoiled family C. Panel I shows a log/linear plot of the data. Panel II shows the same data ± one standard deviation in a linear/linear format.

Correction factors for supercoiled families of pIBI30

It is well known that the binding of the intercalator ethidium bromide to DNA depends on the conformational state of DNA (Morgan, *et al.* , 1979). Correction factors for interpreting ethidium bromide/DNA uv-excitation intensities for topoisomers of pUC18 are reported in the literature (Milligan, Arnold, and Ward, 1992). We have also determined correction factors for topoisomers prepared from plasmid pIBI30 in our lab (Fig. 3). Linearized pIBI30 (L-pIBI30) was prepared, purified and brought to concentrations of 0.04 and 0.03μg/5μl. Five supercoiled families and native pIBI30 were also prepared, purified and concentrated similarly. Finally, topoisomer/L-pIBI30 mixtures were prepared which contained 0.08 and 0.06μg/5μl (combined DNA species). Agarose gels were prepared containing 20 lanes to provide four lanes each for topoisomers, topoisomer/L-pIBI30 mixtures, and L-pIBI30 - all of a uniform concentration (0.04, or 0.03μg/5μl), and 3 lanes of a (0.01μg/5μl) reference L-pIBI30 standard; 5μl of sample were applied to a lane. This experimental protocol facilitated the determination of correction factors when supercoiled families and L-pIBI30 were combined and when they were separated but adjacent to one another.

Analysis was by agarose gel electrophoresis and microdensitometry following the protocols already detailed for irradiated samples with the exception that densitometric analysis yielded density values for each of the distinct bands for Form-I, Form-II, and Form-III pIBI30. Correction factors, (CF), corresponding to weaker binding of ethidium to supercoiled DNA relative to the open-circular, or linear conformations, were determined using the formula:

$$CF = (L - NC)/SC \qquad (3)$$

where L, NC, and SC denote the fluorescence intensities of linear, nicked circular, and supercoiled pIBI30 DNA. The average correction factors for the supercoiled families of pIBI30 are shown in Fig. 5. Included, also, are correction factors reported by Milligan, *et al.* (1992) for pUC18 investigated under conditions similar to ours.

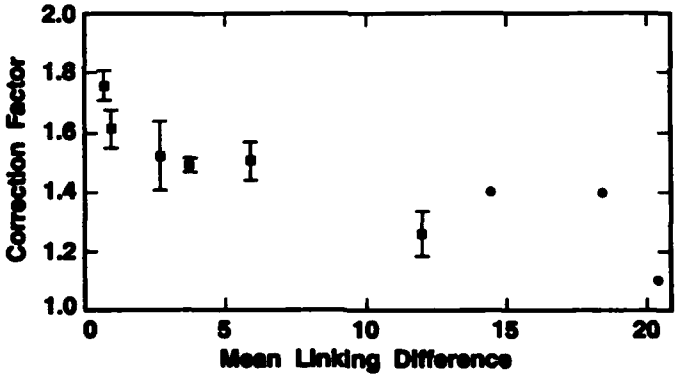

Figure 5. Correction factors versus mean linking difference for pIBI30 (squares) and pUC18 (circles). DNA quantities applied to agarose gels were 0.04μg for linearized and supercoiled families of pIBI30. Supercoiled and linearized pIBI30 were assayed independently in adjacent lanes (this figure) and combined in a single lane (data not shown). Error bars for pIBI30 indicate one standard deviation. pUC18 data are from Milligan, Arnold, and Ward (1992).

When we undertook the investigation of correction factors for topoisomers of pIBI30 we were uncertain of their value in the interpretation of our data. We remain uncertain although we note that, clearly, there are differences for CF's for supercoiled families as shown in Fig. 5. However, we note that the value of CF for a topoisomer would not be expected to remain unchanged over a dose response curve and, in fact, for each dose a separate determination of CF would seem to be required. G(SSB) values reported by Milligan, *et al.* (1992) and sensitivity(Gy^{-1}) values reported in this work and in the work of Miller, *et al.* (1991) are derived from $1/D_{37}$ values which are themselves derived from the slopes of plots like fig. 4 (top). It would seem to us that application of CF values as a data filter would serve only to shift the data framework without altering the slope of the response curve or the value of $1/D_{37}$. Therefore, we decided, albeit arbitrarily, to ignore CF values in the interpretation of our data.

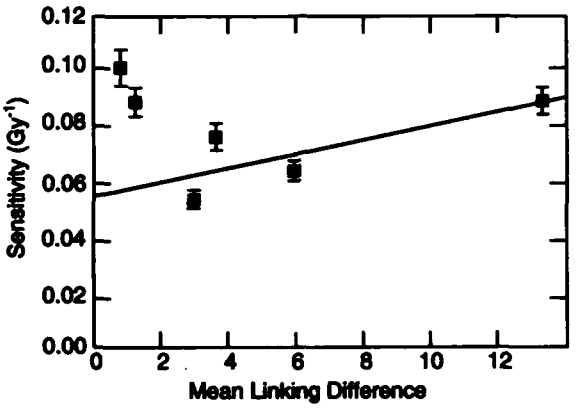

Figure 6. The sensitivity of topoisomers of pIBI30 to the induction of single strand scission (SSB) by ^{60}Co γ-radiation. The data points were obtained by a least squares fit of the survival of Form-I DNA versus dose, *i.e.* from plots like those shown in Fig. 4.

RESULTS

Our data, as evident from Fig. 4, suggest that the degree of superhelicity of topoisomers of pIBI30 influences their sensitivity to ionizing radiation. In Fig. 6 we plot the sensitivity of topoisomers of pIBI30 to the induction of single strand scission (SSB) by ^{60}Co γ-radiation. The data points were obtained by a least squares fit of the survival of Form-I DNA versus dose from plots like those shown in Fig. 4. Results shown in Fig. 6 agree with data reported by Miller and co-workers (1991) for 250 kV X-rays. Both studies report an approximate linear relationship of radiation sensitivity as a function of linking difference (for $|\Delta L| > 2.5$). We attribute the difference between plot intercept values primarily to differences in buffer systems. Miller, *et al.* (1991) used a Tris buffer which is known to have a radioprotective effect, while we employed a potassium-phosphate buffer offering little in the way of protection from ionizing radiation.

For small values of $|\Delta L|$ (*i.e.* values < 2.5) the sensitivity to ionizing radiation appears to decrease with an increase in $|\Delta L|$. It is only this portion of our data that follows standard radiation target theory. To estimate the G-value for single strand scission, G(SSB), we note that at the D_{37} dose there is an average of one SSB per plasmid (*i.e.* the concentration of SSB at D = D_{37} is equal to the concentration of plasmid molecules), hence

$$G(SSB) = [DNA]/(D_{37}Gy^{-1})(\rho/kg\ dm^{-3}) \qquad (4)$$

where ρ is the density of the solution (taken to be unity) and [DNA] is DNA concentration/μmol dm^{-3}. Milligan, *et al.* (1992) found G(SSB) to be insensitive to superhelical density for pUC18 (2686 base pairs) with a value of about $4x10^{-4}$ μmol J^{-1}. By contrast our results for pIBI30 (2926 bp) show a dependence of G(SSB) on superhelical density (data derived from Fig. 6, but not shown). For families A and C of Fig. 3 we find G(SSB) to be $8.8x10^{-3}$, and $6.0x10^{-3}$ μmol J^{-1} respectively.

DISCUSSION

Under our experimental conditions (sparsely ionizing radiation, low DNA concentration, and a solvent with only modest, at best, scavenging capacity) attack by reactive species produced in the aqueous environment of the macromolecule is a much more likely pathway for DNA damage than direct ionization. The compact tertiary structure of supercoiled DNA, which is evident from electron micrographs (Stryer, 1981) illustrated in Fig. 7, should make it less sensitive to this indirect mode of radiation damage than relaxed closed-circular DNA which has a more extended conformation. This protective effect of supercoiling can be understood by considering the volume of solvent within which products of water radiolysis (mainly OH radicals) have a finite probability of reaching DNA before they are scavenged by small-molecule solutes. For the relaxed conformation of DNA (A of Fig. 7) this volume is roughly approximated by a tube surrounding the double helix with a radius equal to the average diffusion distance of OH radicals. For supercoiled DNA (B of Fig. 7) the separation between duplexes in an interwound branch may be less than the OH diffusion length. In this case the target volume per nucleotide is smaller than it is in the relaxed state and a greater portion of the absorbed dose is lost in the production of radical species that are scavenged before they can react with DNA.

The tendency of negative supercoiling to produce strand separation may also reduce the sensitivity of supercoiled DNA to radiation-induced strand scission relative to the relaxed state. This protective mechanism follows from the shielded base hypothesis (Ward, 1975, Ward and

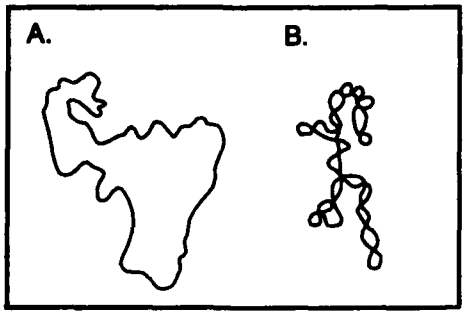

Figure 7. Electron micrograph of mitocondria plasmid DNA illustrating the difference between fully relaxed and supercoiled conformational states.

Kuo, 1978) which asserts that the yield of radiation-induced base damage is limited by the solvent accessibility of sites for OH radical addition in the standard B-DNA double helix. Strand separation increases the accessiblilty of these sites which increases the probability that OH radical attack on DNA leads to modified bases rather than backbone cleavage.

If the above considerations of target volume and solvent accessibility are valid and our observations of an increase in the sensitivity of plasmid DNA to radiation-induced strand breaks with negative superhelicity for both X- and γ-radiation are not due to an experimental artifact, then the physiological levels of negative supercoiling (superhelical densities of the order of -0.05) must affect DNA interactions leading to strand breaks in ways that more than compensate for the protective effects of compactness and single-strandedness. One possible mechanism by which this might occur is through a change in the energetics of the β-phosphate elimination pathway (Beesk, *et al.* , 1979) that follows hydrogen abstraction from the C4' position of sugar moieties. Even though in duplex B-DNA, hydrogens on sugar moieties are about 10 times more accessibile to solvent than base aromatic carbon atoms (Ward, 1985), not more than 20% of the OH radicals reaching DNA react with sugars (Schulte-Frohlinde, 1988). This suggests that OH addition to the double bonds of DNA bases is energetically favored in relaxed DNA over abstraction of hydrogen from ribose. However, in supercoiled DNA hydrogen abstraction from sugar opens a channel (backbone cleavage) to a much lower energy state of the molecule than can be achieved by base modifications resulting from OH addition to double bonds. This may provide a thermodynamic driving force that makes strand scission more competitive with base damage as the elastic energy stored in supercoiled DNA increases.

Exceptions to the general rule that base damage does not lead to strand scission have been found for the single-stranded homopolymers poly(U) and poly(dA) (Adinarayana, *et al.* , 1988). In these systems base radicals resulting from OH addition are able to abstract hydrogen from sugar moieties. Thus far, this process has not been detected in double-stranded DNA, where the more rigid tertiary structure probably makes it more difficult for carbon-centered base radicals to get close enough to sugar moieties to allow hydrogen abstraction. Evidence for the importance of strand flexibility in base-to-sugar radical transfer is seen from the salt dependence of the lifetime of peroxyl radicals in poly(U) (Schulte-Frohlinde, *et al.* , 1986) and the higher yield of strand breaks in poly(dA) relative to poly(A) (Adinarayana, *et al.* , 1988). In the latter case differences in sugar pucker and base stacking make poly(A) a more rigid polymer (Evans and Sarma, 1976). Although the single-stranded characteristics that negative supercoiling confers to duplex DNA probably increase OH addition to bases at the expense of hydrogen abstraction from sugar, a significant fraction of the primary base damage may be converted to strand breaks by base-to-sugar radical transfer. The preference for strand separation in regions of low GC content and the observed decay of base radicals to strand breaks in poly(dA) support this mechanism of sensitization by negative supercoiling.

Our data suggest that DNA response to ionizing radiation can be a strong function of its conformational state in addition to its intrinsic base pair composition. For these reasons the lack of a dependence of pUC18 radiation sensitivity on superhelical density (Milligan, *et al.* , 1992) and our data on plasmid pIBI30 showing just such a relationship, in fact, might have been expected. An understanding of the consequences of other variables (not investigated) including plasmid size and base composition, temperature, DNA and scavenger concentrations, and ionic environment might elucidate the reasons for the apparent discrepancies between our results and those of Milligan and co-workers (1992).

We have recently shown (unpublished data, see also Holwitt, Koda, and Swenberg, 1990) that the radioprotectants WR-1065 [N-(2-mercaptoethyl)-1,3-diaminopropane] and its disulfide, WR-33278, modulate the relaxation of supercoiled pIBI30 DNA by calf thymus topoisomerase-I.

Topoisomerase-I is a ubiquitous eukaryotic enzyme that relaxes supercoiled DNA by single-strand cleavage and re-ligation (Maxwell and Gellert, 1986, D'Arpa and Liu, 1989). Most mechanisms of radioprotection proposed for WR-1065 have focused on its scavenging properties (Philip, 1980, Durand, 1983). Because supercoiled domains exist in both prokaryotic and eukaryotic cells, the results reported here and the observed stimulation of topo-I induced unwinding of supercoiled DNA (Holwitt, Koda, and Swenberg, 1990) suggest that the WR compounds may confer some protection to the genome by decreasing the superhelicity of DNA. The data that we report in this paper leads us to believe that a decrease in DNA supercoiling should result in a decrease in DNA damage. If this is the case, then the critical DNA damage sites would correspond to chromosomal regions where the superhelicity is large. Alternately, a decrease in superhelicity may change the functional properties of DNA. This mechanism suggests changes in metabolic processes, a virtually unexplored field although there have been reports that WR-1065 enhances DNA repair (Lowenstein, *et al.* , 1989, Riklas, *et al.* , 1988, Swenberg, 1989). The actual process responsible for DNA's radiation sensitivity to increase when confined to very small domains, and the molecular mechanism underlying the stimulation of eukaryotic type I topoisomerase by WR-1065 and WR-33278 are not known.

REFERENCES

Adinarayana, M., Bothe, E., and Schulte-Frohlinde, D., 1988, Hydroxyl radical-induced strand break formation in single-stranded polynucleotides and single-stranded DNA in aqueous solutions as measured by light scattering and conductivity, Int. J. Radiat. Biol., 54, 723-737.

American Association of Physicists in Medicine, Task Group 21, Radiation Therapy Committee, 1983. A protocol for the determination of absorbed dose from high-energy photon and electron beams, Med. Phys., 10, 741-771.

Ausubel, F.M., Brent, R., Kingston, R.E., Moore, D.D., Seidman, J.G., Smith, J.A., and Strabl, K., 1989, Current Protocols in Molecular Biology, (Wiley Interscience), 1.71-1.74.

Beesk, F., Dizdaroglu, M., Schulte-Frohlinde, D., and von Sonntag, C., 1979, Radiation-induced DNA strand breaks in deoxygenated aqueous solutions. The formation of altered sugar and end groups, Int. J. Radiat. Biol., 36, 565-576.

Cozzarelli, N.R., Boles, T.C., and White, J.H., 1990, Primer on the topology and geometry of DNA supercoiling, in DNA topology and its biological effects, N.R. Cozzarelli, and J.C. Wang, eds., (Cold Spring Harbor Laboratory Press), 139-184.

Davis, L.G., Dibner, M.D., Battey, J.F., 1986. Basic Methods in Molecular Biology, (Elsevier Science Publishing Co. Inc.).

D'Arpa, P., and Liu, L.F., 1989, Topoisomerase-targeting antitumor drugs, Biochem. Biophys. Acta, 989, 163-177.

Durand, R.E., 1983, Radioprotection by WR-2721 *in vitro* at low oxygen tensions. Implications for its mechanism of action, Br. J. Cancer, 47, 387-392.

Evans, F.E., and Sarma, R.H., 1976, Nucleotide rigidity, Nature, 263, 567-572.

Fowler, J.F., 1964, Differences in survival curve shape for formal multi-target and multi-hit models, Phys. Med. Biol., 9, 177-188.

Holwitt, E.A., Koda, E., and Swenberg, C.E., 1990, Enahncement of topoisomerase-I mediated unwinding of supercoiled DNA by the radioprotector WR-33278, Radiat. Res., 124, 107-109.

Lowenstein, E., Gleeson, J.L., Hecht, E., Factor, R., Goldfischer, C., Cajigas, A., and Steinberg, J.J., 1989, Excision repair is enhanced by WR2721 radioprotection, in Terrestrial Space Radiation and Its Biological Effects, eds., P.D. McCormack, C.E. Swenberg, and H. Bucker, (Plenum Press, New York), 697-714.

Maxwell, A., and Gellert, M., 1986, Mechanistic aspects of DNA topoisomerase, Adv. Protein Chem., 38, 69-86.

Miller, J.H., Nelson, J.M., Ye, M., Swenberg, C.E., Speicher, J.M., and Benham, C.J., 1991, Negative supercoiling increases the sensitivity of plasmid DNA to single-strand break induction by X-rays, Int. J. Radiat. Biol., 59, 941-949.

Milligan, J.R., Arnold, A.D., Ward, J.F., 1992. The effect of superhelical density on single strand break yield for gamma irradiated plasmid DNA, Rad. Res., 132, 69-73.

Morgan, A.R., Lee, J.S., Pulleyblank, D.E., Murray, N.L., and Evans, D.H., 1979, Ethidium fluorescence assays. Part I. Physiochemical studies, Nucleic Acids Res., 7, 547-569.

Phillips, T.L., 1980, Rationale for initial trials and future development of radioprotectants, Cancer Clin. Trials, 3, 165-173.

Riklas, E., Kob, R., Green, M., Prager, R., Marko, R., and Mintsberg, M., 1988, Increased radioprotection attained by DNA repair enhancement, Pharmacol. Ther., 39, 311-322.

Schulte-Frohlinde, D., Behrens, G., Onal, A., 1986, Lifetime of peroxyl radicals in poly(U), poly(A), and single- and double-stranded DNA and their reaction with thiols, Int. J. Radiat. Biol., 50, 103-110.

Schulte-Frohlinde, D., 1988, The effect of oxygen on the OH radical-induced strand break formation in vitro and in vivo, Basic Life Sci., 49, 403-417.

Sambrook, J., Fritsch, E.F., Maniatis, T., 1989, Molecular Cloning: A Laboratory Manual, 2nd edition, (Cold Spring Harbor Laboratory Press).

Singleton, C.K., and Wells, R.D.,1982, The facile generation of covalently closed circular DNAs with defined negative superhelical densities, Anal. Biochem., 122, 253-257.

Stryler, L., 1981, Biochemistry, 2nd edition, (W.H. Freeman, San Francisco), 574.

Swenberg, C.E., 1989, DNA and radioprotection, in Terrestrial Space Radiation and Its Biological Effects, eds., P.D. McCormack, C.E. Swenberg, and H. Bucker, (Plenum Press, New York), 675-695.

Ward, J.F., 1975, Molecular mechanisms of radiation-induced damage to nucleic acids, Advances in Radiation Biology, J.T. Lett and H. Adler, eds., (Academic Press, New York), vol. 5, 181-239.

Ward, J.F., and Kuo, I., 1978, Radiation damage to DNA in aqueous solution: a comparison of the response of the single-stranded form with that of the double-stranded form, Radiat. Res., 75, 278-285.

Ward, J.F., 1985, Biochemistry of DNA lesions, Radiat. Res., 104, S103-S111.

Radiotherapy and Oncology, 23 (1992) 160–169

RADION 00944

Survival after total body irradiation: Effects of irradiation of exteriorized small intestine

H. M. Vriesendorp[1,2], R. M. Vigneulle[1], G. Kitto[1], T. Pelky[1], P. Taylor[1,*] and J. Smith[1]

[1]*Armed Forces Radiobiology Research Institute, Bethesda, MD 20889 5145 U.S.A., and* [2]*Johns Hopkins Oncology Center, Baltimore, MD 21205, U.S.A.*

(Received 14 March 1991, revision received 5 August 1991, accepted 5 November 1991)

Key words: Radiosensitivity small intestine; Crypt stem cell; Abdominal irradiation; Morphometric intestinal histology

Summary

Rats receiving lethal irradiation to their exteriorized small intestine with pulsed 18 MVp bremsstrahlung radiation live about 4 days longer than rats receiving a dose of total-body irradiation (TBI) causing intestinal death. The LD_{50} for intestinal irradiation is approximately 6 Gy higher than the LD_{50} for intestinal death after TBI. Survival time after exteriorized intestinal irradiation can be decreased, by adding abdominal irradiation. Adding thoracic or pelvic irradiation does not alter survival time. Shielding of large intestine improves survival after irradiation of the rest of the abdomen while the small intestine is also shielded. The kinetics of histological changes in small intestinal tissues implicate the release of humoral factors after irradiation of the abdomen. Radiation injury develops faster in the first (proximal) 40 cm of the small intestine and is expressed predominantly as shortening in villus height. In the last (distal) 40 cm of the small intestine, the most pronounced radiation effect is a decrease in the number of crypts per millimeter. Irradiation (20 Gy) of the proximal small intestine causes 92% mortality (median survival 10 days). Irradiation (20 Gy) of the distal small intestine causes 27% mortality (median survival > 30 days). In addition to depletion of crypt stem cells in the small intestine, other issues (humoral factors, irradiated subsection of the small intestine and shielding of the large intestine) appear to influence radiation-induced intestinal mortality.

Introduction

In the past, the crypt stem cell of the small intestine has been identified as the critical target for radiation injury of the intestine [2,7,9,26]. In experiments with well-defined moderately homogeneous total-body irradiation (TBI), shielding of short pieces of small intestine improves survival after TBI [1,14,18,22]. The increase in survival time is directly correlated to the length of intestine shielded, and shielding the ileum (distal small intestine) is more effective than shielding the duodenum (proximal small intestine) [22]. The interpretation offered for these results is that the number of crypt stem cells that survive radiation in the small intestine is not the sole determinant of radiation morbidity or mortality. Additional factors appear to modify the intestinal radiation response. The present experiments in rats were designed to test the possibility that (1) humoral substances released by irradiated parts of the body can modify radiation-induced intestinal mortality and (2) different parts of the small intestinal tract have different radiation sensitivities. For these purposes, isolated loops of small intestine with or without other parts of the body received single, high-dose radiation, while the rest of the animal was shielded.

Material and methods

Animals

Specific pathogen free Sprague-Dawley rats 6–8 weeks old and weighing 250–350 g were quarantined on arrival and screened for the absence of disease and *Pseudo-*

Address for correspondence: H. M. Vriesendorp, University of Texas, MD Anderson Cancer Center, Box 97, 1515 Holcombe Boulevard, Houston, TX 77030, U.S.A.

* *Present address:* Department of Radiation Medicine, Georgetown University Hospital, Washington, DC 20007, U.S.A.

monas spp. before being released. They were maintained in an AAALAC-accredited facility, caged in pairs with filter covers, and provided commercial rat food pellets and acidified tap water (pH 2.5) *ad libitum*. Animal holding rooms were maintained at 21 ± 2 °C with 50 ± 10% relative humidity using at least 10 air changes per hour of 100% conditioned fresh air. They were on a 12 h light/dark full-spectrum light cycle with no twilight. Lights were on between 7:00 a.m. and 7:00 p.m.

Surgery and anesthesia

General anesthesia was maintained during surgical procedures using ketamine hydrochloride (50 mg/kg) in combination with xylazine hydrochloride (10 mg/kg) given intramuscularly and supplemented as needed. Aseptic procedures were used. A midline abdominal incision was made and the portion of the small intestine to be shielded or irradiated was exteriorized. Hemorrhage was not normally a problem in this surgical procedure; however, if it occurred, 4-0 chromic gut suture material was used to ligate bleeding vessels. The animal was irradiated as described below. After irradiation, the small intestine was repositioned in the abdominal cavity and the abdominal wall was closed using single interrupted 4-0 monofilament nylon sutures. The skin was closed with clamps. Anesthesia was maintained for the entire time (approximately 40 min). Pedal reflexes were monitored to assure maintenance of adequate anesthesia depth. Animals were allowed to regain consciousness in individual cages after completion of the irradiation exposure and surgical closure.

Irradiation

A linear accelerator was operated at 18 MVp, 60 pulses/sec, 4 μsec pulse width, and a nominal dose rate of 10 Gy/min. A bremsstrahlung beam was generated by impinging 18 MeV electrons onto a 4-mm thick water-cooled tantalum target. The average photon energy was 6 MeV. The target to skin distance was 325 cm. The dose per pulse was determined before irradiation of each group of animals. The restraint device allowed for shielding of the exteriorized portion of the small intestine or shielding of different parts of the body with slabs of lead during irradiation. Lead slabs 0.5, 1.0, 2.0, 3.0, or 10.0 cm thick were used. Figure 1 shows the physical setup. The exteriorized intestine was contained in a 30-ml glass beaker filled with Ringer's lactate at a temperature of 37 °C. Every radiation exposure was monitored by two ionization chambers in the field that were calibrated to the midline dose in an acrylic rat or intestinal phantom for each irradiation day. The actual dose delivered was ±3% of the prescribed dose.

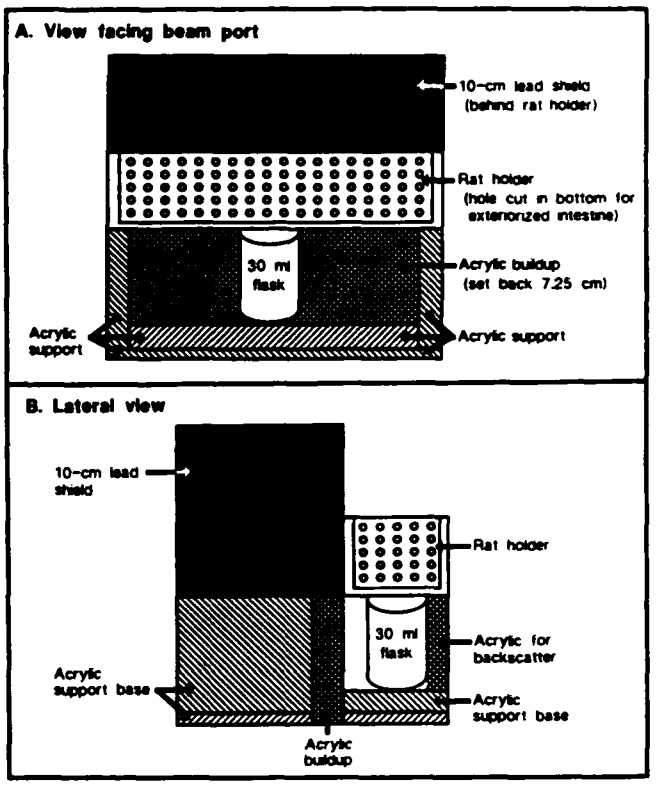

Fig. 1. Physical set up for exposure of small intestine to 18 MeV linear accelerator.

Dose measurements were made with ionization chambers and thermoluminescent dosimeters (TLDs) placed in an acrylic rat or intestinal phantom. Ionization chambers were used to determine the dose rate according to the protocol established by Task Group 21 of the American Association of Physicists in Medicine [19]. The TLDs were used to determine dose uniformity and the effectiveness of the shielding. Single doses between 15 and 60 Gy were used. Doses higher than 60 Gy were not used because of the logistics of working with animal tissue radioactivity induced by neutron activation [27] and the higher doses delivered to the shielded areas. Experiments of a maximum of 12 rats were planned per day and always performed during the same time of day. All animals were irradiated between 10:00 a.m. and 3:00 p.m.

In addition to the exteriorized small intestine, three different 5 × 5 cm fields, were irradiated: (1) the thorax, which included heart, mediastinum, and lungs; (2) the abdomen, which included liver, gall bladder, spleen, stomach, kidney, adrenal gland, pancreas, and colon; and (3) the pelvis, which includes bladder, rectum, and testes. The irradiated exteriorized small intestine consisted of the entire 80 cm of small intestine that can be exteriorized or the (proximal) first 40 cm,

the middle 40 cm or the last (distal) 40 cm of the small intestine.

Animal care after irradiation

Rats remained in individual cages after irradiation. They were evaluated for appetite, hydration, health status, and diarrhea twice a day during the normal work week and once daily during the weekends. Moribund animals and animals that had completed the experiment (>30 days after irradiation) were killed by CO_2 inhalation. Approximately 15% of the animals were killed before day 30 when they were considered moribund. The other 85% was found dead on inspection rounds or killed at the completion of the experiments.

Morphometric analysis

Computer-assisted morphometric studies [Bioquant System IV; R&M Biometrics, Inc., Nashville, TN (1985)] were performed on tissues obtained from animals killed at predetermined days. The small intestine samples were taken at 20, 40, and 60 cm of an average 80-cm total length. The samples at 20 cm (proximal) and 60 cm (distal) were selected for complete histological and statistical analysis. The tissues were fixed in 10% buffered formalin. Transverse sections were embedded in paraffin. Five-micron sections were cut, placed on glass slides, and stained with hematoxylin and eosin. At least five slides per animal were analyzed for each sample. Tissues of three or more animals were used for each parameter evaluated: the intestinal circumference, crypts per millimeter, villus height, and the number of cells per crypt-villus length. A crypt containing only necrotic cells (crypt abscess) was not counted. The base of the villus was determined by comparing several adjacent villi and drawing a line through the estimated bases of several villi. Villus height and villus-crypt length were measured in millimeters from the tip to the base of the villus and the muscularis mucosa, respectively. Tissues taken from the proximal and distal small intestines from four experimental groups were analyzed: (1) rats receiving 20 Gy irradiation to 80 cm of exteriorized small intestine, (2) rats receiving 20 Gy of abdominal irradiation while 80 cm of exteriorized small intestine were shielded, (3) rats receiving 20 Gy irradiation to the abdomen and the 80 cm of exteriorized small intestine, and (4) rats receiving anesthesia, surgery, and sham-irradiation.

Statistics

LD_{50} values were determined by probit analysis (Fig. 2). Differences in means of survival times or morphometric parameters between two experimental groups or between an experimental group and a control group were analyzed for statistical significance by the Student's *t*-test (Fig. 2 and Table IV). Nonparametric tests (Mann-Whitney rank test) were used for determining differences between experimental groups with survival times not normally distributed (Figs. 2,3 and 4). For Fig. 5, a linear-regression, analysis was performed. In the analysis of Fig. 6A,B, *t*-tests and an analysis of variance (ANOVA) was performed.

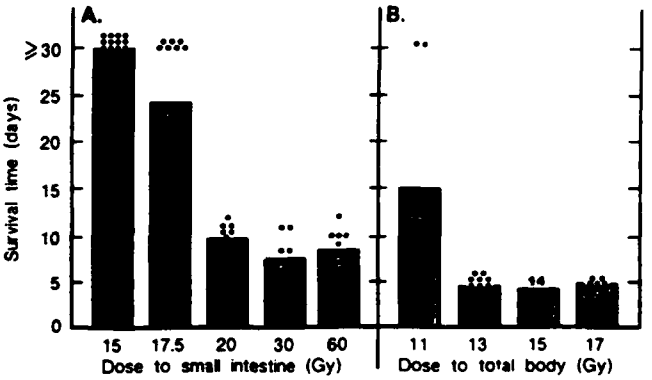

Fig. 2. Influence of small intestinal irradiation or TBI on survival. Survival times of individual animals are shown by closed circles. Bar height indicates mean survival time. Experiments are terminated after day 30.

Results

Dosimetry

Tables I and II summarize the TLD studies. The isolated intestinal loop received a moderately homogeneous radiation dose; the ratio between the maximum

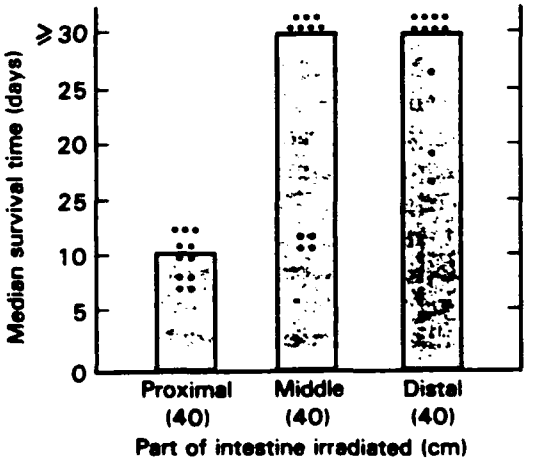

Fig. 3. Influence of partial small intestinal irradiation with 20 Gy on survival. Survival times of individual animals are shown by closed circles. Bar height indicates median survival time. Experiments are terminated after day 30.

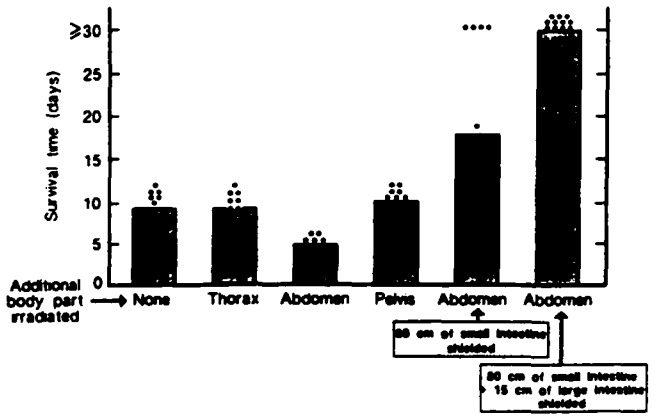

Fig. 4. Survival after a 20 Gy dose of radiation to exteriorized small intestine and irradiation of additional body parts. Survival times of individual animals are shown by closed circles. Bar height indicates mean survival time. Experiments are terminated after day 30.

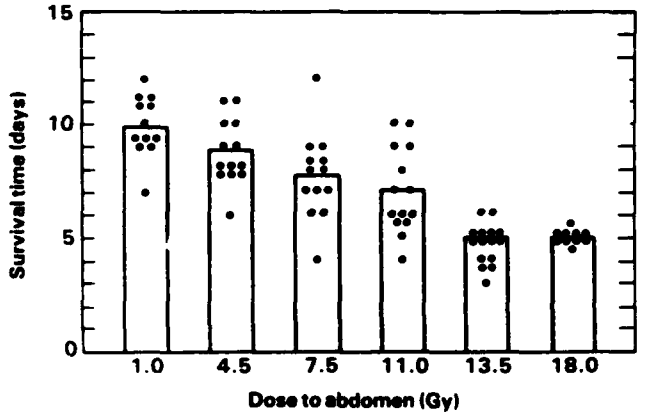

Fig. 5. Influence of the radiation dose received by the abdomen on survival after 20 Gy radiation to exteriorized small intestine. Survival time of individual animals is shown by closed circles. Bar height indicates mean survival time. Experiments are terminated after day 30.

and minimum measured dose was 1.11 (105:95; Table I, last column). The shielding of the rat's body was effective, as 7% or less of the central-axis open-field dose was measured in the shielded rat phantom. Adding an abdominal field of 5 x 5 cm contiguous to the irradiation field of the exteriorized intestinal loop resulted in an abdominal dose of approximately 90% of the intestinal dose. Shielding appeared to be effective in this array as well. Eight percent or less of the open-field dose was measured behind the shield. Highest doses were found close to the block edges.

Irradiation of exteriorized small intestine

The maximum length of small intestine that can be exteriorized in the rat is approximately 80 cm. The stomach and the first 5–8 cm of the small intestine, the latter due to its retroperitoneal location, cannot be

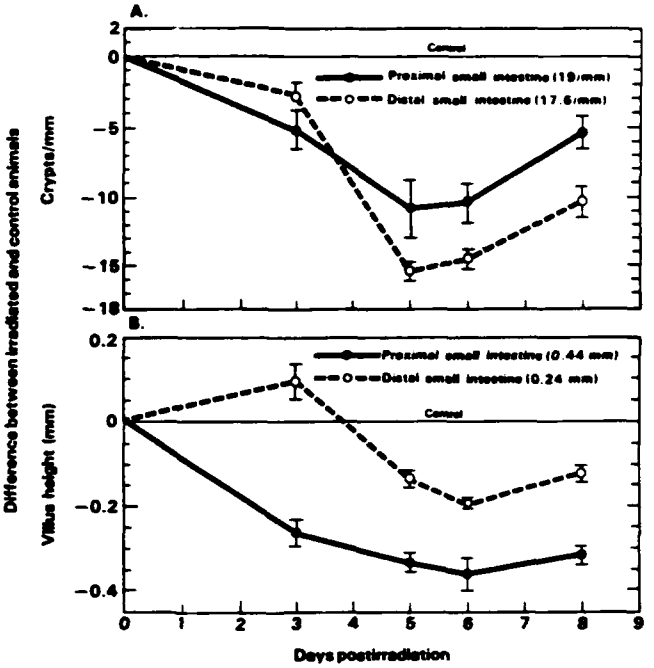

Fig. 6. Changes in the number of crypts/mm (A) and villus height (B) after intestinal irradiation. Mean values with standard error bars are given of the daily mean minus the normal mean (day 0). Day 0 values of control animals are given in parentheses.

exteriorized without irreversibly disturbing the normal anatomy. Figure 2, panel A summarizes the effect of radiation on 80 cm of exteriorized small intestine. For comparison, Fig. 2, panel B also shows results obtained in a previous study of TBI using the same rat model [22]. Irradiating the isolated small intestine caused morbidity (watery diarrhea and lethargy) and mortality at higher radiation doses and at a later time than after TBI.

The $LD_{50/30}$ and 95% confidence limits after exteriorized intestinal irradiation were 17.9 Gy (17.1–19.5). The $LD_{50/6}$ and 95% confidence limits after TBI were 12.3 Gy (12.0–12.9). The $LD_{50/30}$ and 95% confidence limits after TBI (using all the data given in reference 22) were 9.9 Gy (9.0–10.5). Probit analysis for the $LD_{50/6}$ data is of limited value due to 0% or 100% responses for most data. Just averaging the difference between the highest dose leading to a bone marrow syndrome (11 Gy) and the lowest dose leading to an intestinal syndrome (13 Gy) gives a $LD_{50/6}$ of 12 Gy (instead of 12.3 Gy with probit analysis).

The mean survival time after high dose intestinal irradiation was 8.5 days and the mean survival time for the intestinal syndrome after TBI is 5 days. This difference is statistically significant ($p < 0.01$). Thus, the LD_{50} was approximately 5.5 Gy higher for irradiation of the exteriorized small intestine and survival time was approximately 3–4 days longer than after TBI.

TABLE I

Dosimeters in rat phantom and intestinal loop phantom.[a]

Thermoluminescent dosimeter placement	Rat body[b] (shielded)		Intestinal loop[c] (irradiated)	
	Location	Dose (%)	Location	Dose (%)
Top → bottom midline field	0.8[d]	4		
	1.8[d]	4		
	2.5[d]	4		
	3.2[d]	5		
	4.1[d]	7	0.1[d]	98
			Central axis (2.5)[d]	100
			4.6[d]	105
Left → right mid-level phantom	1[e] (nose)	6		
	3[e]	5	0.3[e]	105
	5[e]	5	0.8[e]	100
	7.5[e] (mid)	5	1.5[e]	100
	9[e]	5	2.1[e]	104
	11[e]	5	2.6[e]	102
	13[e]	5		
	15[e] (tail)	5		
Entry → exit mid-level phantom	0.8[f]	4	0.3[f]	100
	1.8[f]	4	0.9[f]	101
	2.5[f]	5	1.5[f]	100
	3.2[f]	5	2.1[f]	97
	4.1[f]	6	2.6[f]	95

[a] Radiation set up as in Fig. 1. Doses in percent of central intestinal dose.
[b] Acrylic cylinder (nose end tapered), diameter 5.0 cm, height 16.0 cm.
[b] Acrylic flat end cylinder, diameter 3.0 cm, height 5.0 cm in glass flask.
[d] Centimeters from top of midline field.
[e] Centimeters from left of phantom.
[f] Centimeters from entry of phantom.

The survival time of animals receiving 20 Gy to their small intestine was longer than the survival of animals receiving 30 Gy ($p < 0.01$). The difference between the 20 and 60 Gy group did not reach statistical significance, presumably due to the limited number of animals tested. In contrast, survival times of rats given TBI of 13, 15, 17, 20, or 30 Gy were not significantly different. Data for the 20-Gy and 30-Gy TBI groups are not shown in Fig. 2. Results in Fig. 3 indicate that the most sensitive part of the small intestine was the proximal 20–40 cm of the small intestine. After 20 Gy the median survival time was 10 days. Irradiation of the middle 40 cm or distal 40 cm with 20 Gy caused mortality significantly later in some animals ($p < 0.001$). However, most of the animals receiving 20 Gy to the middle or distal 40 cm of the small intestine survived longer than 30 days.

Irradiation of small intestine and other body compartments

Different body compartments were irradiated in addition to the whole 80 cm of small intestine. Figure 4 summarizes these results. Thoracic irradiation (5 ×

TABLE II

Dosimetry in rat phantom for irradiating rat abdomen.[a]

Thermoluminescent dosimetry placement	Location (cm)	Dose[b]
Abdomen Top → bottom Midline (open field)	Top	**87**
	Bottom	**90**
Abdomen Left → right at midplane Phantom (Open field from 8.0–13.0 cm)	1 (nose)	5
	3	4
	5	5
	7	8
	9	**90**
	11	**85**
	13	27
	15 (tail)	6
Abdomen Entry → exit Midline (open field)	Entrance	**87**
	Exit	**85**

[a] Dosimetry performed in a 5 × 5 cm field with thermoluminescent dosimeters. Radiation set up as in Fig. 1. Phantom same as used in Table I.
[b] Dose in percent of dose of exteriorized small bowel simultaneously irradiated in extension of 5 × 5 cm abdominal field. Rest of body shielded with 10 cm of lead. Open field values in bold print.

TABLE III

Small intestinal circumference in millimeter ± SE* after irradiation to abdomen or small intestine.

Experimental group	Proximal small intestine	Distal small intestine
1 Control day 0	9.00 ± 0.01	9.50 ± 0.02
2 Abdominal irradiation (20 Gy) small intestine shielded day 5	16.50 ± 0.10	27.50 ± 0.10
3 Small intestine irradiation (20 Gy) body shielded day 5	11.50 ± 0.05	14.00 ± 0.05

* Three animals per entry, 15 observations; differences between group 1 and 2 are different with a p value of <0.001 in a t-test for proximal as well as distal small intestine.

5 cm field, 20 Gy) or pelvic irradiation (5 × 5 cm field, 20 Gy) did not change survival time after small intestinal irradiation. However, abdominal irradiation (5 × 5 cm field, 20 Gy) reduced survival time from approximately 10 days to 5 days and made it similar to survival times after 15 or 20 Gy of TBI. Death before day 10 after irradiation was observed in animals receiving TBI, intestinal irradiation, or partial body irradiation in addition to irradiation of the exteriorized small intestine. Two days preceding the day of death, all irradiated animals showed watery-thin diarrhea and lethargy. Irradiation with 20 Gy of the abdominal field alone with 80 cm of the small intestine exteriorized and shielded caused late mortality (> 10 days) in some animals. Their cause of death could not be determined. When, in addition to 80 cm of small intestine, 15 cm of proximal large intestine were exteriorized and shielded and the rest of the abdomen received 20 Gy, all animals survived ⩾ 30 days. Irradiation (20 Gy) of the exteriorized large intestine alone did not induce any mortality within 30 days after radiation. Shielding of the large intestine, while the small intestine and the rest of the abdomen received 20 Gy, did not influence the survival time of rats, when compared to animals without large intestinal shielding (data not shown). In separate experiments, the amount of radiation received by the abdomen in the 5 × 5 cm field was decreased by placing lead slabs 0.5, 1.0, 2.0, 3.0, or 10.0 cm thick in the field. The exteriorized small intestine always received 20 Gy. Figure 5 summarizes the results and shows that the mean survival time correlated inversely with the dose given to the abdomen. By regression analysis a correlation coefficient of -0.94 is found with a p value of <0.01.

Morphometrics of shielded intestine

The circumference of the shielded small intestine increased after a 20 Gy dose of abdominal radiation. Five days after irradiation, the increase was more pronounced in the distal than in the proximal part of the small intestine (Table III). In the villi of the proximal small intestine, shrinkage was observed (decrease in villus length with increasing numbers of cells per millimeter in comparison to controls), while in the villi of the distal small intestine, elongation and an increased number of cells were observed (concentration of cells per millimeter was same as in control, see Table IV). Smaller differences in the same direction as noted in Tables III and IV were seen on postirradiation days 3, 6 and 8. The day of the largest difference (day 5) was selected for presentation.

Morphometrics of irradiated intestine

Direct irradiation of the exteriorized small intestine caused different histological abnormalities in the proximal and the distal small intestine. In the proximal region, a larger decrease in villus length was observed while, in the distal region, the decrease in the number of crypts per millimeter was more pronounced. This

TABLE IV

Villus height (mm) and cells per villus-crypt after irradiation to abdomen or small intestine.*

Experimental crypt group	Villus height		Cells per villus	
	Proximal intestine	Distal intestine	Proximal intestine	Distal intestine
1 Control day 0	0.44 (0.03)	0.24 (0.01)	58.4 (3.2)	33.6 (1.6)
2 Abdominal irradiation (20 Gy) small intestine shielded day 5	0.15 (0.02)	0.34 (0.04)	25.6 (1.6)	68.8 (4.8)
3 Small intestine irradiation (20 Gy) body shielded day 5	0.13 (0.02)	0.11 (0.02)	16.8 (3.2)	11.2 (2.4)

* Three animals per entry, 15 observations, standard error between brackets. Differences between group 1 and 2 are significant in a t-test at a p value of <0.001, except for cells per villus crypt in the distal intestine, where p value is <0.01.

TABLE V

Paradox between effects of irradiation and shielding.*

Experimental protocol	Mean survival time (days)	
	Proximal intestine	Distal intestine
20 Gy radiation to exteriorized small intestine with rest of body shielded	10	>30
15 Gy TBI and intestinal shielding	6	7

* See text for explanation.

decrease of crypts per mm in the distal region started later than the decrease in villus length in the proximal region; although, for both (crypts per millimeter and villus length) the maximum decrease was found day 5–6 postirradiation. Plotted in Fig. 6A,B are daily means minus the normal mean (day 0) plus and minus one standard error. For villus height (Fig. 6B), normalized distal values were higher than those for normalized proximal values for all time periods ($p < 0.001$). For normalized crypt values (Fig. 6A), there was no significant difference between the distal and proximal values on day 3. *P* values for the differences on the remaining days (5, 6, 8) were respectively. 0.0186, 0.0069, and 0.001 and indicated significantly less crypts/mm in the distal small intestines on those days.

A 2-way ANOVA was run to determine any significant interaction in Fig. 6A,B. Significance was found in both cases ($p < 0.001$) indicating that distal and proximal values behave differently across time. From Fig. 6A it appears that the difference occurs between days 3 and 5; distal values fall (from normal) faster than proximal values do. From Fig. 6B it appears that the difference occurs between day 0 and 3, in that *proximal* values fall from normal faster than distal values.

To determine what significant changes occur across time for both normalized proximal and distal values, a 1-way ANOVA was run for values on days 3, 5, 6, and 8. In most cases, significant ($p < 0.01$) changes were found. Days 5 and 6 were the exception. No significant changes were found in values for these days.

Discussion

For experiments with TBI as well as with smaller field irradiation, such as isolated loops of the small intestine, well-defined dosimetry is a prerequisite. The results in Tables I and II indicate that the planned doses were received in a moderately homogeneous manner [19]. Therefore, the observed difference in LD_{50} and survival time between TBI and small intestinal irradiation (Fig. 2) are real biological differences and not due to differences in absorbed dose in the intestines under the two different radiation setups. No clinical differences were observed between animals dying after TBI or after small intestines irradiation, indicating that the cause of death was the same in both groups. i.e. fluid and electrolyte loss [6]. Reabsorption of electrolytes and fluid from the irradiated small intestine by the (nonirradiated) colon might play a role in extending survival in animals subjected to small intestinal irradiation. The animals in the last column of Fig. 4 (irradiated abdomen; shielded large intestine) probably provide an example of prolonged survival due to reabsorption of fluids and electrolytes in the large intestine [21]. Previously, other investigators have irradiated exteriorized small intestines of rats using higher doses of radiation and shorter length of intestines (2.5 cm) than used in the present study [12]. Late deaths (between 20 and 100 days after radiation) were observed and proven to be due to radiation-induced intestinal obstruction. This mode of death was not observed in our study due to the indicated differences in experimental design between the studies. Twenty Gy to exteriorized large intestine did not induce mortality within 30 days after irradiation. Shielding of the large intestine did not change the survival time observed after small intestinal plus abdominal irradiation. Reabsorption of fluids in the large intestine appears to be only one of the mechanisms that prolongs survival after small intestinal or abdominal irradiation.

The difference in survival time after small intestinal irradiation or TBI can be attributed to the influence of structure(s) distinct from the small intestine that are only irradiated in the TBI procedure. Blood or lymph vessels feeding or draining the small intestine are irradiated in both cases and cannot explain the difference observed. Larger vessels (aorta, vena cava, and thoracic duct) are only irradiated during TBI. Radiation effects on large vessels are not expected to influence mortality due to intestinal toxicity occurring 5 to 10 days after radiation. By exclusion of other explanations, the release of humoral substances in the irradiated tissues (other than the small intestine) remain as a more probable explanation of the observed results. Such substances would travel to and influence events in the small intestines outside the irradiated field. After abdominal irradiation, the changes in intestinal circumference of the nonirradiated small intestine suggest the release of a humoral factor that decreases muscular tone of the small intestine (see Table III). The results shown in Table IV suggest the presence of humoral factor(s) with different effects on the proliferation of cells in the

nonirradiated proximal and distal small intestine. The influence of dietary factors on intestinal histology after irradiation was excluded by comparison of experimental animals to surgery/anesthesia controls. Eating habits of control and experimental animals receiving intestinal or abdominal irradiation were similar up to day 6 post-irradiation.

Shielding experiments (Fig. 4) exclude bone marrow as the source of the suggested humoral substances that influence mortality from radiation damage to the small intestine. Animals with most of their bone marrow irradiated (pelvis, thorax or both, the latter data not shown) did not die earlier than animals receiving exteriorized small intestinal irradiation only. Tissues other than bone marrow as sources for humoral factors remain to be considered. Radiation itself might change secretion patterns in surviving cells directly. More likely, initial release of humoral factors after radiation is caused by cell death. Due to the short time period after abdominal irradiation in which effects are observed (<6 days), cells would have to die quickly after irradiation if they are to be the source of humoral factors. Rapid death occurs in high-turnover self-renewal systems or in other specific tissues by the mechanism of apoptosis ("interphase") death. This would implicate lymphocytes, spermatogonia, large intestinal cells, and some types of exocrine cells as potential sources of humoral factors [9,15,16,17]. Testes were included in the pelvic field; irradiating them did not appear to influence survival. Splenic lymphocytes, exocrine glands (like the pancreas and gall bladder) and the stomach were included in the abdominal irradiation field and might be the source of the suggested factors. Studies of irradiated dogs with surgically changed and separated flows of bile, pancreatic secretions, and "intrinsic" intestinal secretions indicated that secretions of the irradiated pancreas can decrease survival time and increase histological changes in the intestinal mucosa after abdominal irradiation [8,11].

An interesting paradox was revealed between proximal and distal small intestine. Early mortality was found only after irradiation of the proximal small intestine (Fig. 3). However, as shown earlier, shielding the *distal* small intestine prolonged survival more effectively [22]. In Table V, the paradoxical sets of observations are summarized. Radiation of the proximal small intestine causes death earlier. Histologically predominantly a "villus" response is observed (Fig. 6B). After irradiation of the distal small intestine (histologically predominantly a "crypt" response; Fig. 6A), mortality occurs later or not at all. A decrease in villus function (absorption) in the normal small intestines would cause rapid functional deficits and mortality, whereas decreases in crypt function (secretion, cell production) in the distal small intestines remain compatible with survival if sufficient villus function remains. The effectiveness of shielding the distal small intestine as evidenced in a preceding paper [7] can be explained by assuming humoral factors from the shielded distal small intestine that influence regeneration in the irradiated proximal small intestine. Such "trophic" factor(s) would have to travel through the bloodstream to affect the proximal small intestine and would be different from the humoral factors released by the irradiated abdomen postulated in this communication. The shielded proximal small intestine could release substances into either the intestinal lumen or the bloodstream that influence the irradiated distal small intestine, but, if so, they would affect the prevention or delay of radiation mortality less significantly. The sites of origin, mode of transportation, and target sites for humoral factors postulated in this communication appear to be similar to suggestions made on totally different data sets summarized in a recent review of intestinal physiology [4]. The reviewed studies explored the adaptation of the small intestine to surgical resection and food diversions and indicated trophic luminal factors coming from the proximal intestine and trophic systemic factors from the distal small intestine.

The crypt stem cell assay as described by Withers and Elkind utilizes the jejunum [26]. Figure 6A indicates that this assay will indicate an "average" radiation damage if taken as representing the radiation response of the whole small intestine. Less damage is seen in proximal crypts (duodenal), more damage in distal crypts (in the ileum). Overall results and in particular the survival times observed in our study (Fig. 3) indicate that the crypt stem cell assay in the jejunum cannot predict morbidity or mortality after intestinal irradiation.

Wheldon and Michalowski postulated that radiation distinguishes between so-called Hierarchial (H) self-renewal systems and Flexible (F) self-renewal systems by the latency period of expression of radiation damage [25]. H-systems would have a fixed latency period independent of radiation dose that is equivalent to the stem cell transit time (the time it takes a stem cell to produce end cells). F-systems would show an inverse relationship between latency period and radiation dose. The small intestines were considered a H-system, with a latency period of 5 days, determined by the time it takes a crypt stem cell to reach the villus tip [2,5]. Results given in Fig. 2 indicate that their proposed discriminatory test for H/F systems identifies the small intestine as an H-system after TBI but as an F-system after small intestinal irradiation. It appears that the proposed use

of radiation to discriminate between H- and F-systems excludes the influence of humoral factors (such as hormones, growth factors, or toxins) on latency periods and cannot be applied to circumstances where those effects can be observed.

Recently, in studies using small rodents delayed deaths were observed after radiation doses that are considered to cause an intestinal syndrome. The investigators changed the previous definition of this endpoint (death occurring up to 6 days after TBI [13]) to death occurring up to 10 days after TBI [10,20]. This definition change was justified by claiming that in specific pathogen free animals the intestinal syndrome can be delayed [10,20]. However, rats in the present study were also specific pathogen-free and died from intestinal damage 5 days after high-dose TBI. Other studies with germ-free mice and totally decontaminated dogs showed that intestinal mortality is delayed only by 1–2 days (not 5 days) and that an increase in LD_{50} of approximately 1.5 Gy is observed [5,9,23]. The extension of the endpoint for intestinal lethality to day 10 after irradiation causes an overlap between intestinal syndrome (death after TBI before day 10) and bone marrow syndrome (death between day 6 and 30 after TBI) lethality; this adjustment can be justified if one could demonstrate experimentally that irradiation of a large volume of bone marrow enhances intestinal toxicity and mortality (not found in this communication; see Fig. 4) or that transplanting bone marrow cells after irradiation prevents or delays death from intestinal radiation toxicity. In fact, this was not observed in several investigations using different species [21,24]. In one of the more recent studies the authors claimed a beneficial influence of bone marrow transplantation on radiation-induced intestinal mortality. However, dosimetric control in the study was insufficient, bone marrow and intestinal mortality could not be separated out appropriately and bone marrow transplantation could only have relieved mortality in animals that were destined to die from bone marrow aplasia [20]. In the other study using a 10-day endpoint of intestinal death sufficient detail to support uniformity of dose distribution was not given [10]. Indeed, the radiation quality and treatment distances reported in both communications produce nonuniform radiation distributions in small rodents [28]. The dosimetry preformed in our study indicates that over or under doses to different compartments in the body can change survival patterns after intestinal radiation. Therefore, we conclude, like others before us [13,21] that with at least a moderately uniform dose distribution and an endpoint selection in laboratory animals based on absorbed dose in the appropriate compartment of the body, no evidence exists for a significant influence of the bone marrow syndrome on the intestinal syndrome.

The implications of the described research are important for clinical management of certain types of radiation accidents, e.g. irradiation to the abdomen. For accurate prognostication, the doses received by the proximal small intestine, the distal small intestine, and the abdomen must be determined separately. This will probably require biological dosimetry given that intestinal organs are distributed diffusely in the abdomen. Presently, the enzyme diamine oxidase (DAO) is a prime candidate for assaying the absorbed dose using intestinal biopsies. However, it would not be suitable for defining doses received by other abdominal organs from which biopsies cannot be taken easily and/or contain very little DAO [3]. In retrospect, the differences observed in response of the proximal and distal small intestine to radiation are not surprising, as their tissues do differ in various other aspects, e.g. morphology, function, and neuroendocrine factors. Further studies are required to explore the mechanisms of radiation damage to different parts of the small intestine, as the radiation-induced intestinal syndrome appears to be more complicated than previously appreciated. New applications of the information obtained will not be limited to radiation protection or radiation oncology, but will also be useful in studies of intestinal physiology and pathology.

Acknowledgments

This research was supported by the Armed Forces Radiobiology Research Institute, Defense Nuclear Agency, under work unit 107. The opinions and assertions contained herein are those of the authors; no endorsement by the Defense Nuclear Agency has been given or should be inferred. The experiments reported herein were conducted according to the principles set forth in the "Guide for the Care and Use of Laboratory Animals", Institute of Animal Resources, National Research Council, DHEW Publications No. (NIH)78-2.

References

1 Bond, V. P., Swift, M. N., Allen, A. C. and Fishler, M. C. Sensitivity of abdomen of rat to x-irradiation. Am. J. Physiol. 164: 323–330, 1956.

2 Bond, V. P., Fliedner, T. M. and Archambeau, J. O. Mammalian Radiation Lethality, a Disturbance in Cellular Kinetics, pp. 231–275, Academic Press, New York, 1965.

3 DeBell, R. M., Ledney, G. D. and Snyder, S. L. Quantification of gut injury with Diamine Oxidase activity: development of a fission neutron RBE and measurements with combined injury in mouse models. Radiat. Res. 112: 508–516, 1987.

4 Dowling, R. H. Update on intestinal adaptation. Triangle Sandoz J. Med. Sci., 27: 149–164, 1988.

5 Fry, R. J. M., Reiskin, A. B., Kisieleski, W., Sallese, A. and Staffeldt, E. Radiation effects and cell renewal in rodent intestine. In: Comparative Cellular and Species Radiosensitivity, pp. 255–270. Editors: V. P. Bond and T. Sugahara. Igaku Shoin, Tokyo, 1969.

6 Geraci, J. P., Dunston, S. G., Jackson, K. L., Mariano, M. S., Holeski, C. and Eaton, D. L. Bile loss in the acute intestinal radiation syndrome in rats. Radiat. Res. 109: 47–57, 1987.

7 Hendry, J. H., Potten, C. S. and Roberts, N. P. The gastrointestinal syndrome and mucosal clonogenic cells. Relationships between target cells sensitivities. LD_{50} and cell survival and their modification by antibiotics. Radiat. Res. 96: 100–112, 1983.

8 Hiatt, N., Morgenstern, L. and Warner, N. E. Prolongation of post irradiation survival by diversion of intestinal content. Radiat. Res. 35: 301–310, 1968.

9 Maisin, J., Maisin, J. R. and Dunjic, A. The gastrointestinal tract. In: Pathology of Irradiation, pp. 296–344. Editor: C. C. Berdjis, Williams & Wilkins Co., Baltimore, 1971.

10 Mason, K. A., Withers, H. R. and Davis, C. A. Dose dependent latency of fatal gastrointestinal and bone marrow syndromes. Int. J. Radiat. Biol. 55: 1–5, 1989.

11 Morgenstern L. and Hiatt, N. Injurious effects of pancreatic secretions on post radiation enteropathy. Gastroenterology 53: 923–929, 1967.

12 Osborne, J. W., Prasad, K. N. and Zimmerman, J. R. Changes in rat intestine after X irradiation of exteriorized short segments of ileum. Radiat. Res. 43: 131–142, 1970.

13 Quastler, H. Studies on roentgen death in mice. I. Survival time and dosage. Am. J. Roentgenol. 54: 449–456, 1945.

14 Quastler, H., Lanzl, E. F., Keller, M. E. and Osborne, J. W. Acute intestinal death. Studies on roentgen death in mice. III. Am. J. Physiol. 164: 546–556, 1951.

15 Sommers, S. C. Effect of ionizing radiation upon endocrine glands. In: Pathology of Irradiation. pp. 408. Editor: C. C. Berdgis, Williams & Wilkins Co., Baltimore, 1971.

16 Stephens, L. C., King, G. K., Peters, L. J., Ang, K. K., Schultheiss, T. E. and Jardine, J. H. Acute and late radiation injury in rhesus monkey parotid glands. Evidence of interphase cell death. Am. J. Pathol. 124: 469–478, 1980.

17 Sucui, D. Cellular death by apoptosis in some radiosensitive and radioresistant mammalian tissue. J. Theor. Biol. 105: 391–401, 1983.

18 Swift, M. N. and Taketa, S. T. Modification of acute intestinal radiation syndrome through shielding. Am. J. Physiol. 185, 85–91, 1956.

19 Task Group 21. Radiation Therapy Committee, AAPM. A protocol for the determination of absorbed dose from high-energy photon and electron beams. Med. Phys. 10: 741–771, 1983.

20 Terry, N. H. A. and Travis, E. L. The influence of bone marrow depletion on intestinal radiation damage. Int. J. Radiat. Oncol. Biol. Phys. 17: 569–574, 1989.

21 Van Bekkum, D. W. and de Vries, M. J. Radiation Chimeras. Logos Academic Press, London, 1967.

22 Vigneulle, R. M., Vriesendorp, H. M., Taylor, P., Burns, W. and Pelkey, T. Survival after total body irradiation. I. Effects of partial small bowel shielding. Radiat. Res. 119: 313–324, 1989.

23 Vriesendorp, H. M., Heidt, P. and Zurcher, C. Gastrointestinal decontamination of dogs treated with total body irradiation and bone marrow transplantation. Exp. Hematol. 9: 904–916, 1981.

24 Vriesendorp, H. M., Klapwijk, W. M., Heidt, P. J., Hogeweg, B., Zurcher, C. and Van Bekkum, D. W. Factors controlling the engraftment of transplanted dog bone marrow cells. Tissue Antigens 20: 63–75, 1982.

25 Wheldon, T. E. and Michalowski, A. S. Alternate models for the proliferative structure of normal tissues and their response to irradiation. Br. J. Cancer 53, Suppl. VII: 382–385, 1986.

26 Withers, H. R. and Elkind, M. M. Radiosensitivity and fractionation response of crypt cells of mouse jejunum. Radiat. Res. 38: 598–613, 1969.

27 Wilensick, R. M., Almond, P. R., Oliver, G. D. and DeAlmeida, C. E. Measurements of fast neutrons produced by high energy x-ray beams of medical electron accelerators. Phys. Med. Biol. 18: 396–401, 1973.

28 Zoetelief, J., Hennen, L. A. and Broerse, J. J. Some practical aspects of dosimetry and dose specifications for whole body irradiation. In: Response of Different Species to Total Body Irradiation, pp. 3–28. Editors: J. J. Broerse and T. J. MacVittie. Martinus Nijhoff Publishers, Boston, 1984.

DISTRIBUTION LIST

DEPARTMENT OF DEFENSE

ARMED FORCES INSTITUTE OF PATHOLOGY
ATTN: RADIOLOGIC PATHOLOGY DEPARTMENT

ARMED FORCES RADIOBIOLOGY RESEARCH INSTITUTE
ATTN: PUBLICATIONS DIVISION
ATTN: LIBRARY

ARMY/AIR FORCE JOINT MEDICAL LIBRARY
ATTN: DASG-AAFJML

ASSISTANT TO SECRETARY OF DEFENSE
ATTN: AE
ATTN: HA(IA)

DEFENSE NUCLEAR AGENCY
ATTN: TITL
ATTN: DDIR
ATTN: RARP
ATTN: MID

DEFENSE TECHNICAL INFORMATION CENTER
ATTN: DTIC-DDAC
ATTN: DTIC-FDAC

FIELD COMMAND DEFENSE NUCLEAR AGENCY
ATTN: FCFS

INTERSERVICE NUCLEAR WEAPONS SCHOOL
ATTN: TCHTS/RH

LAWRENCE LIVERMORE NATIONAL LABORATORY
ATTN: LIBRARY

UNDER SECRETARY OF DEFENSE (ACQUISITION)
ATTN: OUSD(A)/R&AT

UNIFORMED SERVICES UNIVERSITY OF THE HEALTH SCIENCES
ATTN: LIBRARY

DEPARTMENT OF THE ARMY

AMEDD CENTER AND SCHOOL
ATTN: HSMC-FCM

HARRY DIAMOND LABORATORIES
ATTN: SLCHD-NW
ATTN: SLCSM-SE

LETTERMAN ARMY INSTITUTE OF RESEARCH
ATTN: SGRD-ULY-OH

SURGEON GENERAL OF THE ARMY
ATTN: MEDDH-N

U.S. ARMY AEROMEDICAL RESEARCH LABORATORY
ATTN: SCIENTIFIC INFORMATION CENTER

U.S. ARMY CHEMICAL RESEARCH, DEVELOPMENT, AND ENGINEERING CENTER
ATTN: SMCCR-RST

U.S. ARMY INSTITUTE OF SURGICAL RESEARCH
ATTN: DIRECTOR OF RESEARCH

U.S. ARMY MEDICAL RESEARCH INSTITUTE OF CHEMICAL DEFENSE
ATTN: SGRD-UV-R

U.S. ARMY NUCLEAR AND CHEMICAL AGENCY
ATTN: MONA-NU

U.S. ARMY RESEARCH INSTITUTE OF ENVIRONMENTAL MEDICINE
ATTN: SGRD-UE-RPP

U.S. ARMY RESEARCH OFFICE
ATTN: BIOLOGICAL SCIENCES PROGRAM

WALTER REED ARMY INSTITUTE OF RESEARCH
ATTN: DIVISION OF EXPERIMENTAL THERAPEUTICS

DEPARTMENT OF THE NAVY

NAVAL AEROSPACE MEDICAL RESEARCH LABORATORY
ATTN: COMMANDING OFFICER

NAVAL MEDICAL COMMAND
ATTN: MEDCOM-21

NAVAL MEDICAL RESEARCH AND DEVELOPMENT COMMAND
ATTN: CODE 40C

NAVAL MEDICAL RESEARCH INSTITUTE
ATTN: LIBRARY

NAVAL RESEARCH LABORATORY
ATTN: LIBRARY

OFFICE OF NAVAL RESEARCH
ATTN: BIOLOGICAL SCIENCES DIVISION

SURGEON GENERAL OF THE NAVY
ATTN: MEDICAL RESEARCH AND DEVELOPMENT

DEPARTMENT OF THE AIR FORCE

BOLLING AIR FORCE BASE
ATTN: AFOSR

BROOKS AIR FORCE BASE
ATTN: AL/OEBSC
ATTN: USAFSAM/RZ
ATTN: OEHL/RZ
ATTN: AL/DEBL

OFFICE OF AEROSPACE STUDIES
ATTN: OAS/XRS

SURGEON GENERAL OF THE AIR FORCE
ATTN: HQ USAF/SGPT
ATTN: HQ USAF/SGES

U.S. AIR FORCE ACADEMY
ATTN: HQ USAFA/DFBL

OTHER FEDERAL GOVERNMENT

ARGONNE NATIONAL LABORATORY
ATTN: ACQUISITIONS

BROOKHAVEN NATIONAL LABORATORY
ATTN: RESEARCH LIBRARY, REPORTS SECTION

CENTER FOR DEVICES AND RADIOLOGICAL HEALTH
ATTN: HFZ-110

GOVERNMENT PRINTING OFFICE
ATTN: DEPOSITORY RECEIVING SECTION
ATTN: CONSIGNED BRANCH

LIBRARY OF CONGRESS
ATTN: UNIT X

LOS ALAMOS NATIONAL LABORATORY
ATTN: REPORT LIBRARY/P364

NATIONAL AERONAUTICS AND SPACE ADMINISTRATION
ATTN: RADLAB

NATIONAL AERONAUTICS AND SPACE ADMINISTRATION
GODDARD SPACE FLIGHT CENTER
ATTN: LIBRARY

NATIONAL CANCER INSTITUTE
ATTN: RADIATION RESEARCH PROGRAM

NATIONAL DEFENSE UNIVERSITY
ATTN: LIBRARY

NATIONAL LIBRARY OF MEDICINE
ATTN: OPI

U.S. ATOMIC ENERGY COMMISSION
ATTN: BETHESDA TECHNICAL LIBRARY

U.S. DEPARTMENT OF ENERGY
ATTN: LIBRARY

U.S. FOOD AND DRUG ADMINISTRATION
ATTN: WINCHESTER ENGINEERING AND ANALYTICAL CENTER

U.S. NUCLEAR REGULATORY COMMISSION
ATTN: LIBRARY

RESEARCH AND OTHER ORGANIZATIONS

BRITISH LIBRARY (SERIAL ACQUISITIONS)
ATTN: DOCUMENT SUPPLY CENTRE

CENTRE DE RECHERCHES DU SERVICE DE SANTE DES ARMEES
ATTN: DIRECTOR

INHALATION TOXICOLOGY RESEARCH INSTITUTE
ATTN: LIBRARY

INSTITUTE OF RADIOBIOLOGY, ARMED FORCES MEDICAL ACADEMY
ATTN: DIRECTOR

KAMAN SCIENCES CORPORATION
ATTN: DASIAC

NBC DEFENSE RESEARCH AND DEVELOPMENT CENTER OF THE FEDERAL ARMED FORCES
ATTN: WWDBW ABC-SCHUTZ

NCTR-ASSOCIATED UNIVERSITIES
ATTN: EXECUTIVE DIRECTOR

RUTGERS UNIVERSITY
ATTN: LIBRARY OF SCIENCE AND MEDICINE

UNIVERSITY OF CALIFORNIA
ATTN: LABORATORY FOR ENERGY-RELATED HEALTH RESEARCH
ATTN: LAWRENCE BERKELEY LABORATORY

UNIVERSITY OF CINCINNATI
ATTN: UNIVERSITY HOSPITAL, RADIOISOTOPE LABORATORY

XAVIER UNIVERSITY OF LOUISIANA
ATTN: COLLEGE OF PHARMACY